Marine Composites

Webb Institute
Senior Elective

Failure Modes

Eric Greene, Naval Architect
EGAssoc@aol.com
410.703.3025 (cell)
http://ericgreeneassociates.com/webbinstitute.html

Bending Stresses in Panels

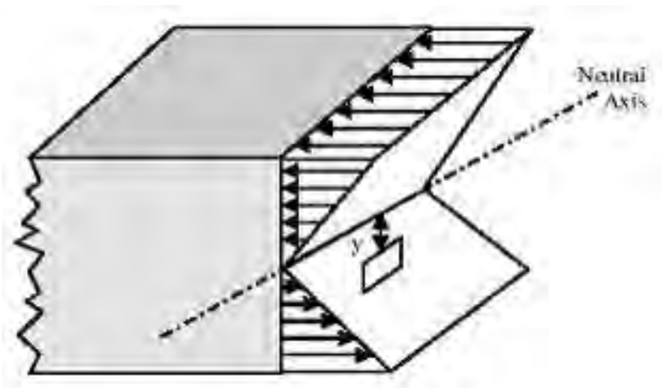

Maximum In-Plane Stress in Beams Subject to Bending

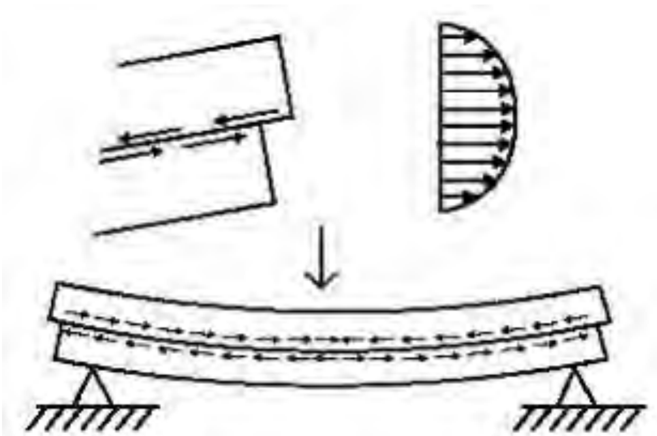

Maximum Shear Stress in Beams Subject to Bending

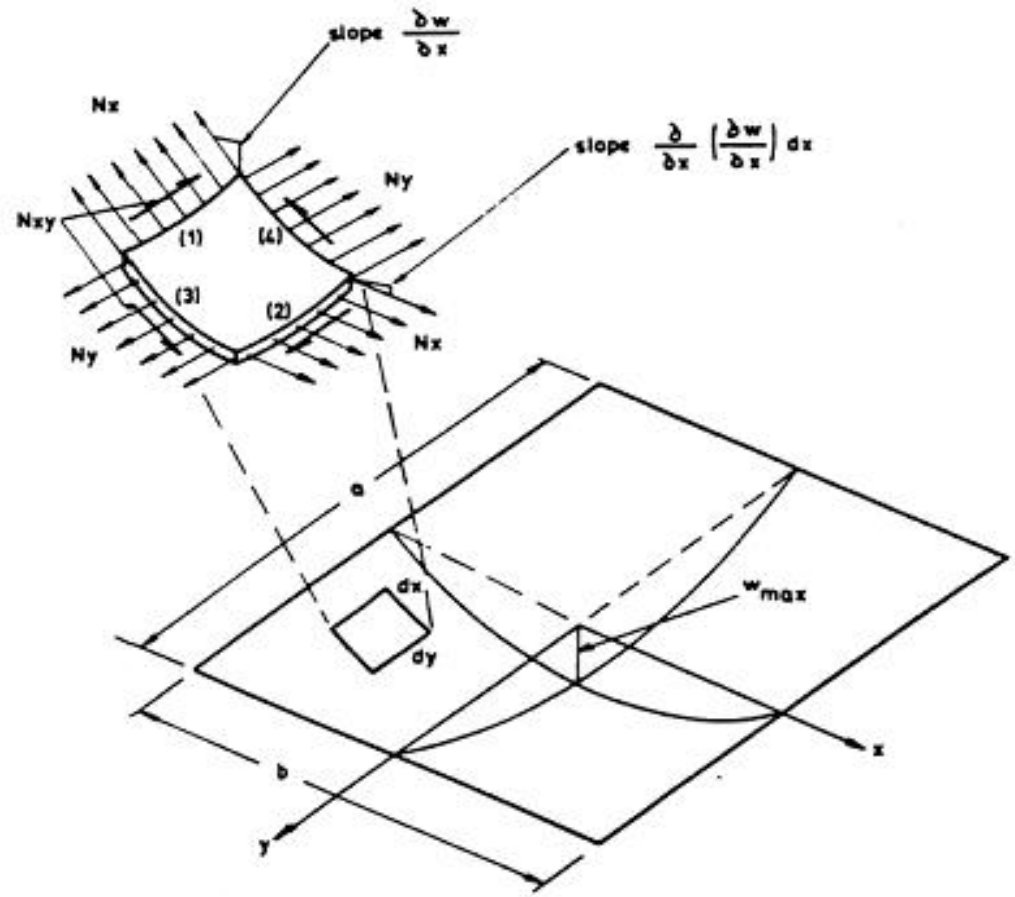

Stresses and Deflections due to Membrane Effects

Transversely-Stiffened Panels in Compression

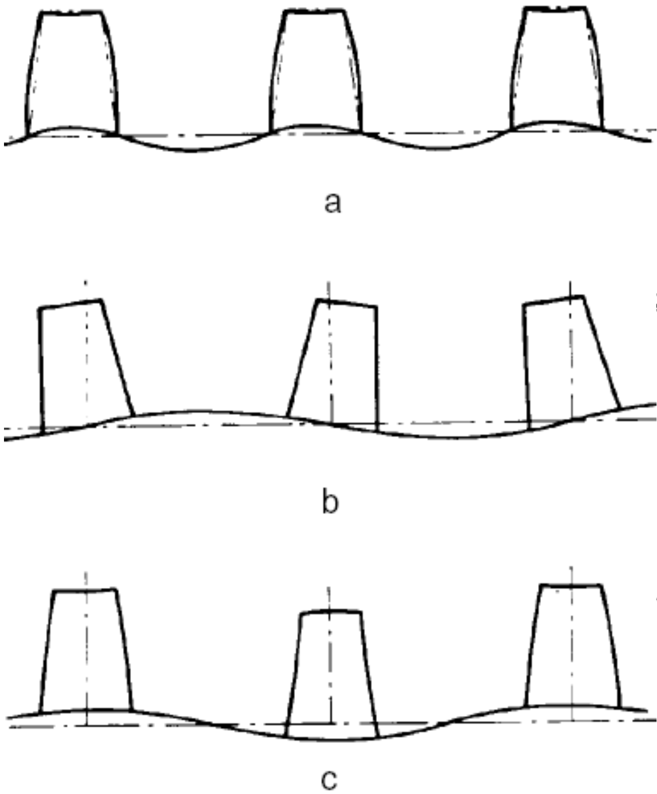

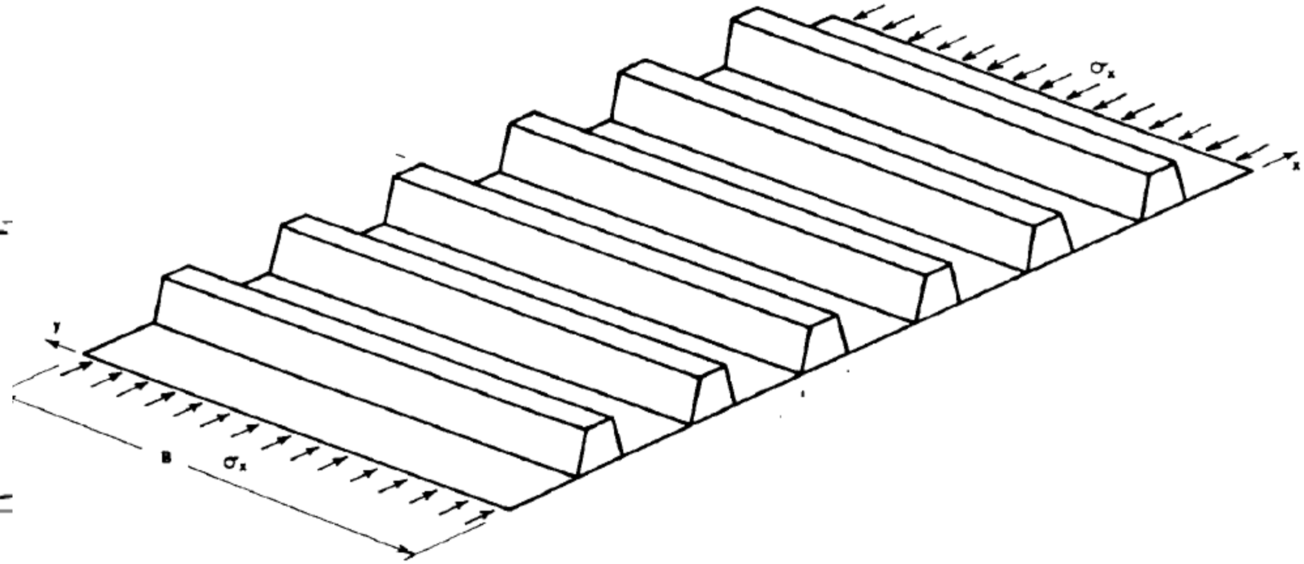

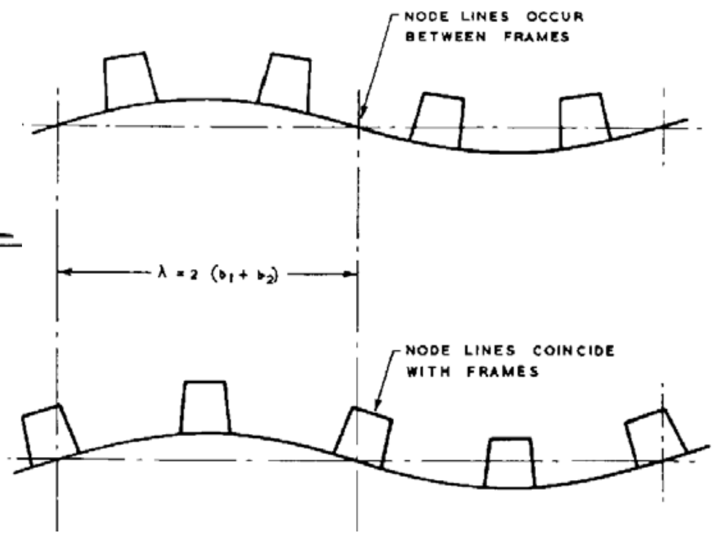

Transversely Stiffened Panel (above) and Buckling Modes (below) [Smith, *Buckling Problems in the Design of Fiberglass Reinforced Plastic Ships*]

First Ply Failure based on Critical Strain

$$\varepsilon_{crit} = \frac{\sigma_{ai}}{E_{ai}\left[\,\left|\bar{y} - y_i\right| + \tfrac{1}{2} t_i\right]}$$

where:

σ_{ai} = strength of ply under consideration
= σ_t for a ply in the outer skin
= σ_c for a ply in the inner skin

E_{ai} = modulus of ply under consideration
= E_t for a ply in the outer skin
= E_c for a ply in the inner skin

$\bar{y}$ = distance from the bottom of the panel to the neutral axis

y_i = distance from the bottom of the panel to the ply under consideration

t_i = thickness of ply under consideration

σ_t = tensile strength of the ply being considered

σ_c = compressive strength of the ply being considered

E_t = tensile stiffness of the ply being considered

E_c = compressive stiffness of the ply being considered

First Ply Failure Based on First Play Critical Strain Limits from the *ABS Guide for Building and Classing High-Speed Craft*

eric greene associates

Micro-buckling

Schematics of micro-buckling

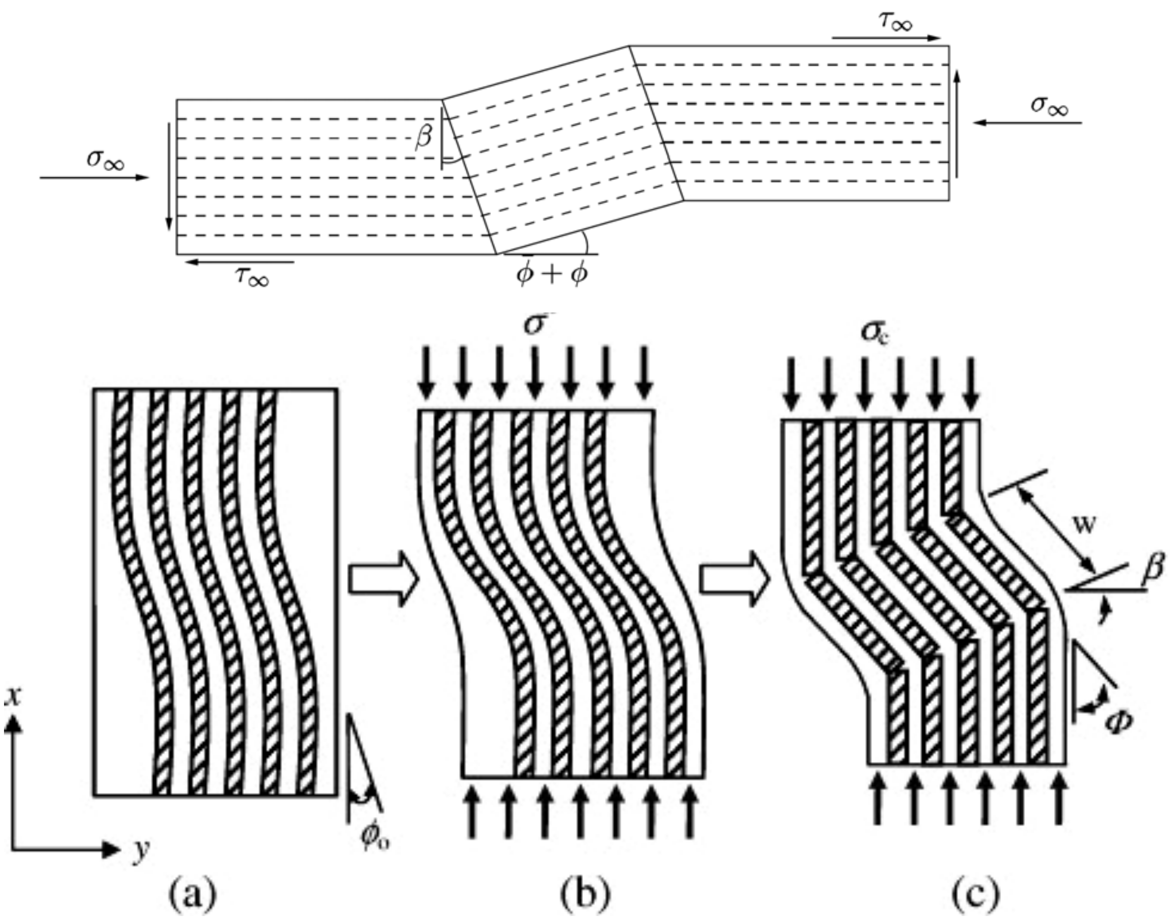

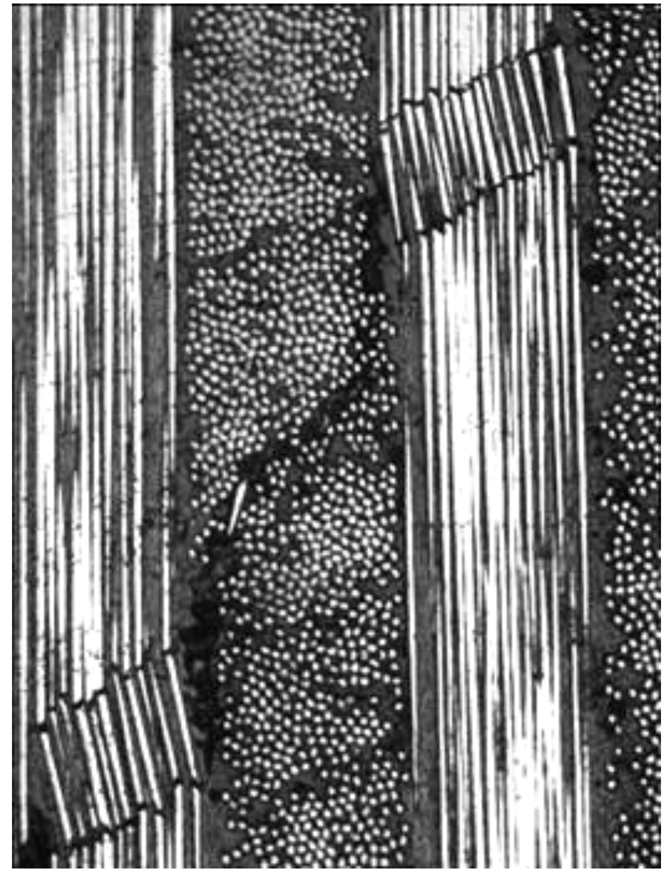

The schematic diagram showing the formation of kinking failure mode and its geometry: (a) in-plane buckling of 0° fibers with an initial fiber misalignment φ_o, (b) deformation of 0° fibers via fiber microbuckling mechanism when it is loaded in compression σ∞ and (c) fibres kinking phenomena causing catastrophic fracture of the UD laminate. The kink band geometry: w = kink band width, β = boundary orientation and $\varphi = \varphi_o + \gamma$ = inclination angle. [A. Jumahata, C. Soutisa, F.R. Jonesb, and A. Hodzica, “Fracture mechanisms and failure analysis of carbon fiber/toughened epoxy composites subjected to compressive loading,” Composite Structures, Jan 2010.

Fatigue

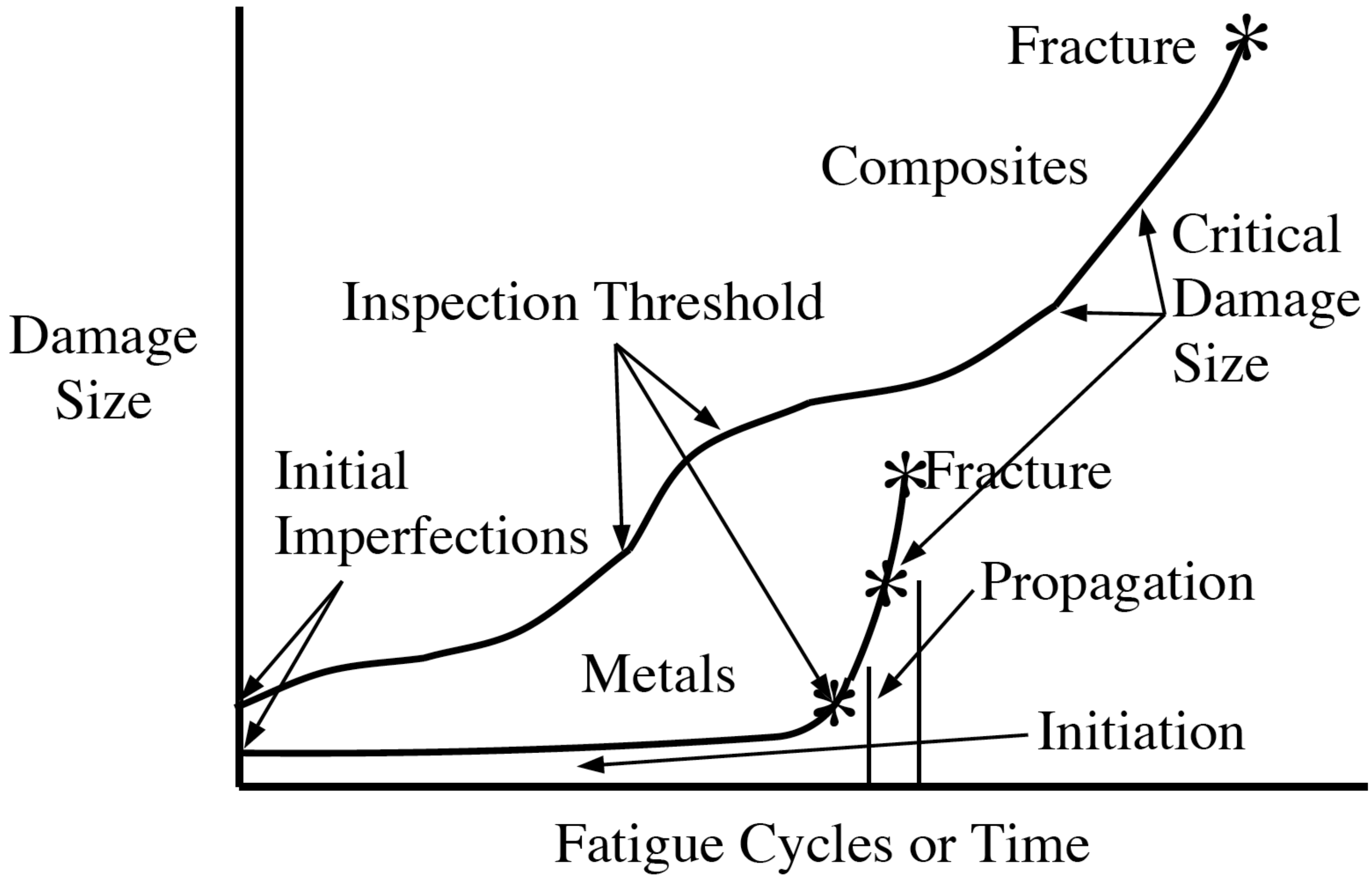
Fracture
Composites
Critical
Damage
Size
Inspection Threshold
Damage
Size
Initial
Imperfections
Fracture
Propagation
Metals
Initiation
Fatigue Cycles or Time

S-N Curves for Composite Laminates

Composite & Metal S-N Curves

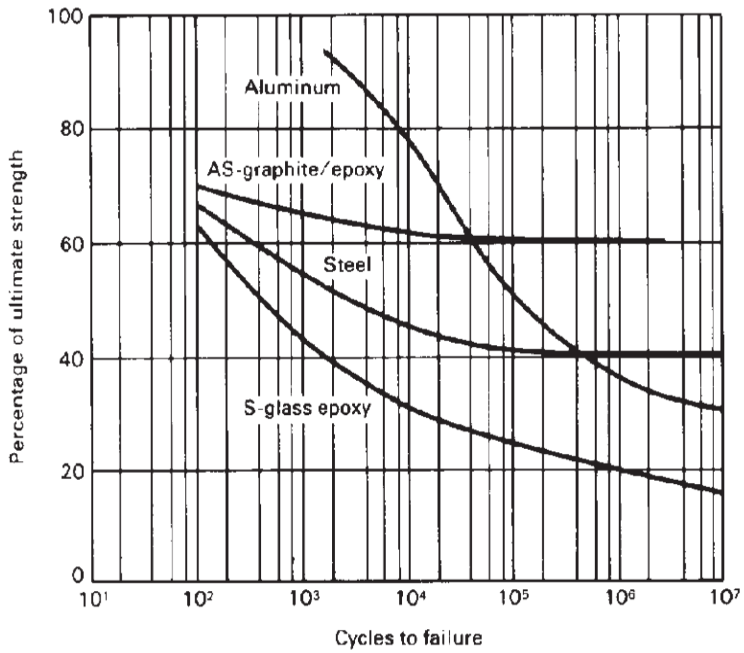

Comparison of Fatigue Strengths of Graphite/Epoxy, Steel, Fiberglass/Epoxy and Aluminum [Hercules]

Stiffness S-N Curves

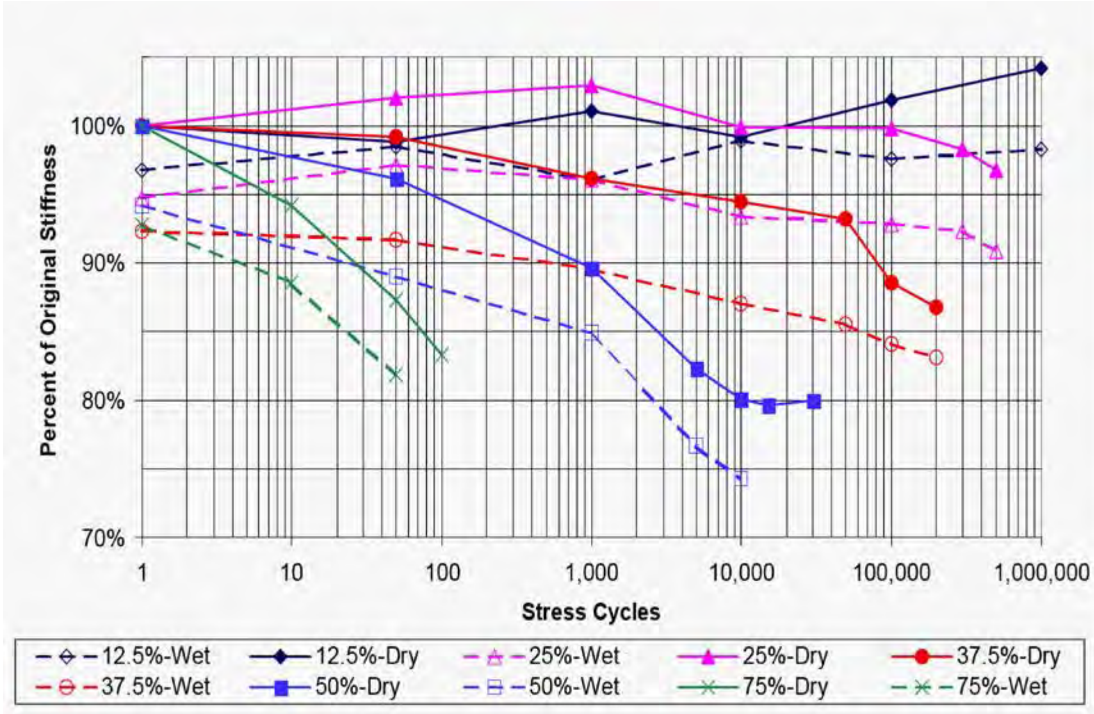

Stiffness S-N Curve for J/24 Sailboat Sandwich Laminate from Paul Miller's "*Fatigue Prediction Verification of Fiberglass Hulls*"

S-N Curves Comparing Material Systems

Fiber Architecture Comparison S-N Curves

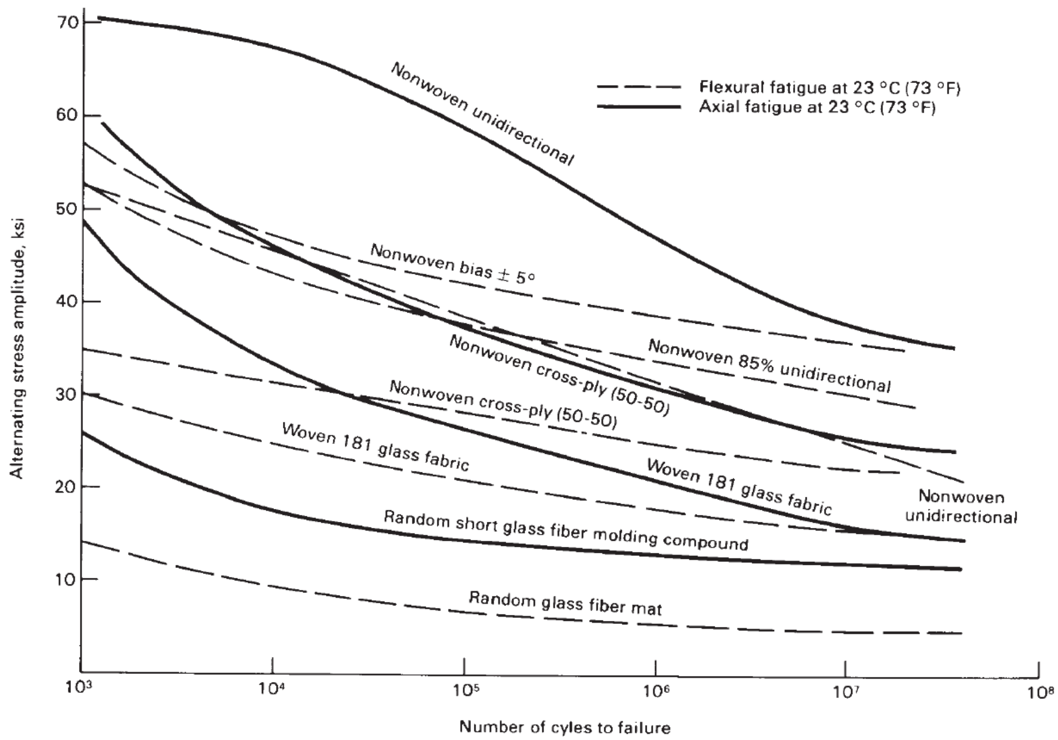

Comparative Fatigue Strengths of Nonwoven Unidirectional Glass Fiber Reinforced Plastic Laminates [ASM Engineers' Guide to Composite Materials]

Resin Comparison S-N Curves

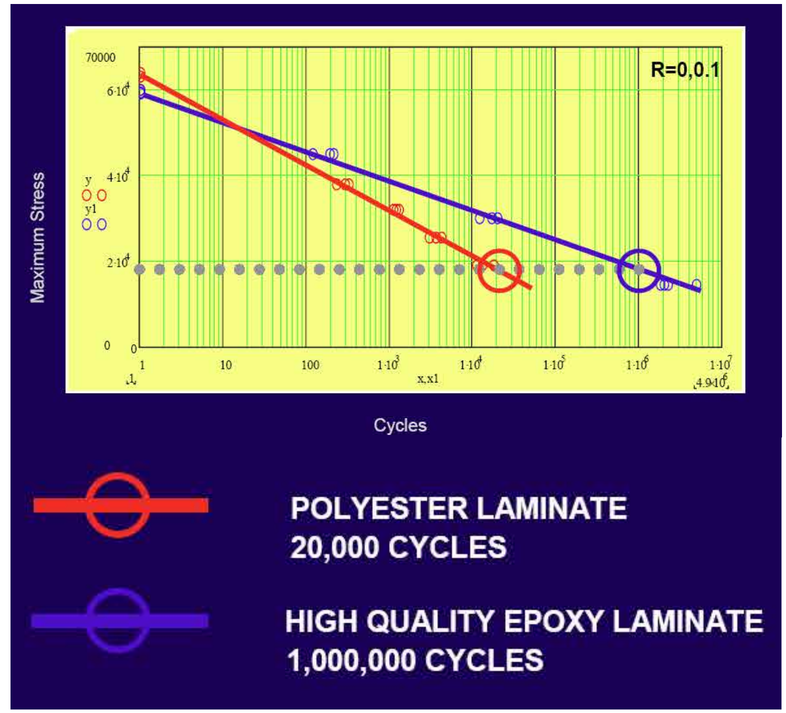

Comparison of Fatigue Behavior of Epoxy and Polyester Resin

Design for Fatigue

- Composite materials generally are less subject to fatigue damage because fiber architecture inhibits crack growth
- Fatigue loading sources include main hull girder bending for larger ships; slamming loads for high-speed craft; rotating machinery; and road transport for smaller boats
- Avoid structural natural frequencies coincident with loading
- Joints are more susceptible to fatigue damage than panels

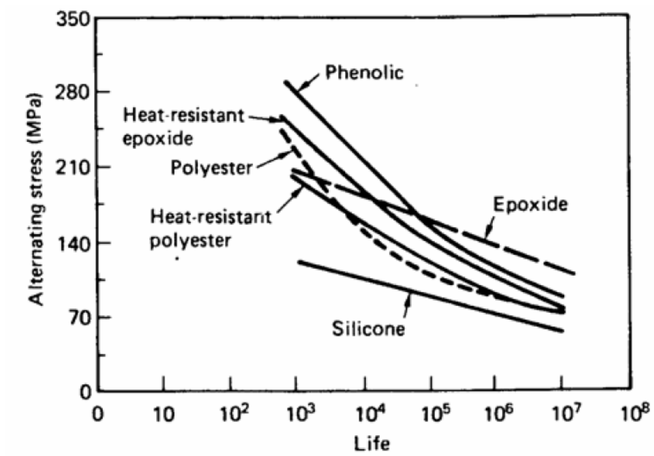

S-N Curves for various Resin Systems [Konur & Matthews "Effect of the properties of the constituents on the fatigue performance of composites: a review," Composites, vol 20, no 4, July, 1989]

- Inadequate laminate stiffness can contribute to composite laminate fatigue damage

Types of Point Impact Load Damage

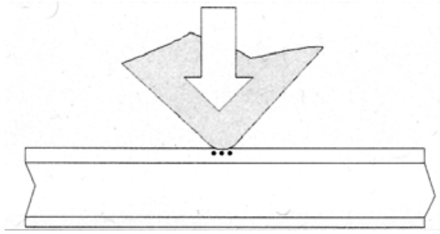

Face Crushing

The face fails in through-thickness compression under the impactor tip

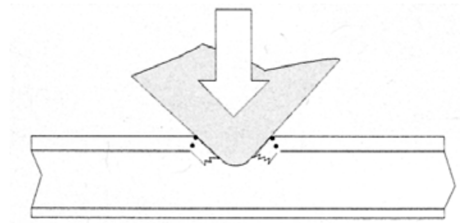

Face Shear Failure

The face fails locally in interlaminar shear near the sides of the impactor

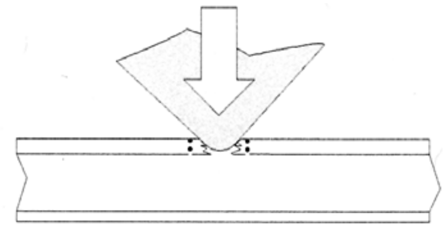

In-Plane Failure of Faces

The face fails in local in-plane tension or compression near the sides of the impactor

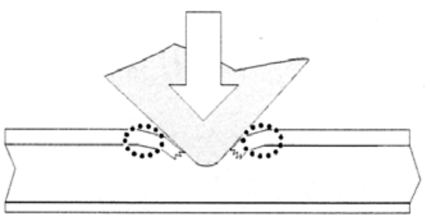

Flexural Failure of Faces

The face fails locally in bending near the sides of the impactor

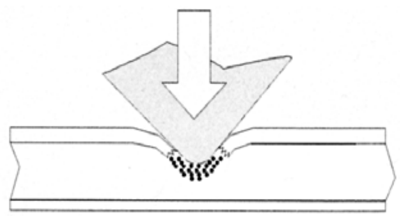

Core Crushing

The core is locally crushed, which manifests as buckling with honeycomb cores

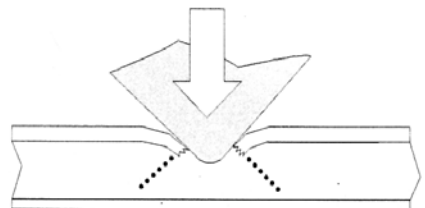

Core Shear Failure

The core fails in shear near the impactor. With brittle cores, the shear failure can spread over a wide area

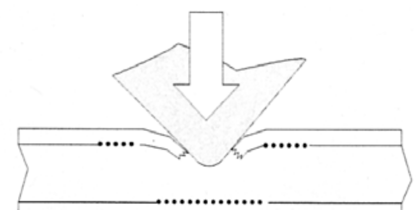

Delamination between Outer Face & Core

Typical failure mode with stiffer cores, such as balsa.

reported by Martin Hildebrand in VTT pub 281, “A comparison of FRP-sandwich penetrating impact test methods”

eric greene associates

Impact Damage

Front-Face (left) and Back-Face (right) Damage

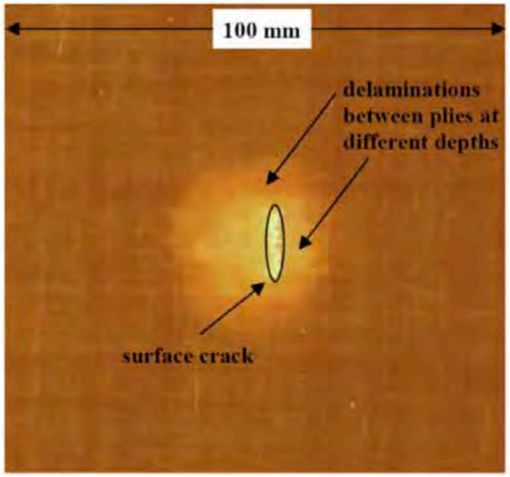

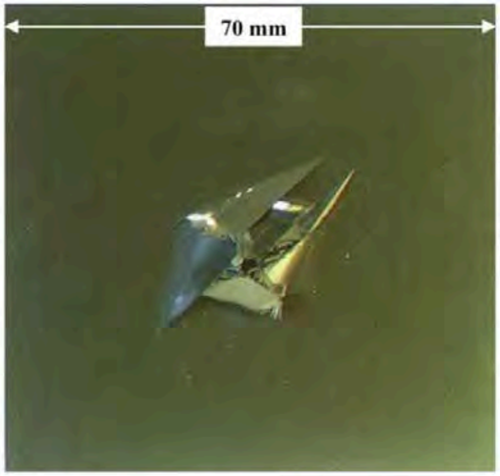

M. Gower

Blunt Object Impact

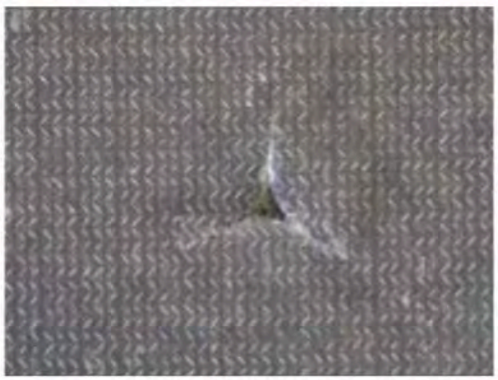

D. Zenkert

Damage to Viking 60 from Collision with Whale

Team Bad Company

Hull Skin Delamination

Tony Guild

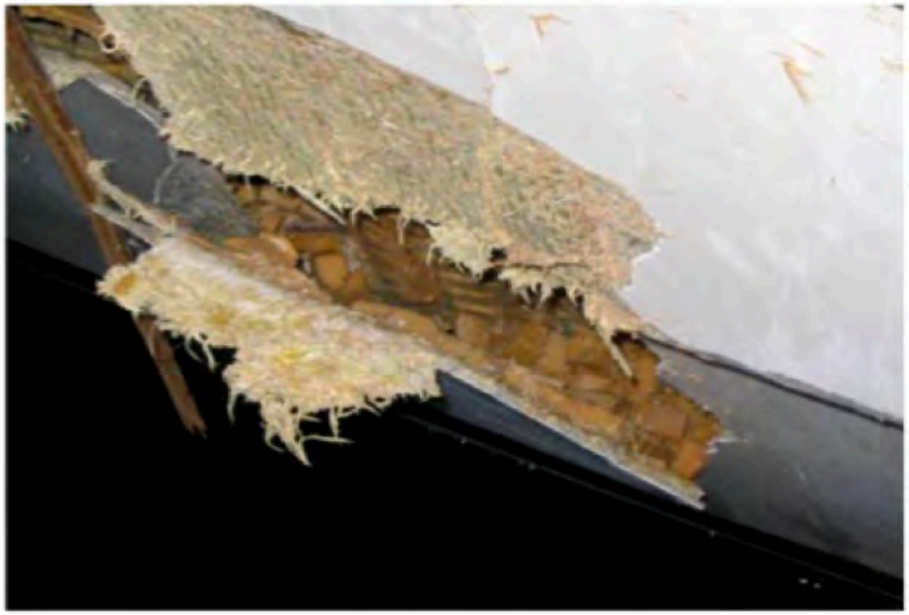

YachtForums.com

Sandwich Laminate Failure Modes

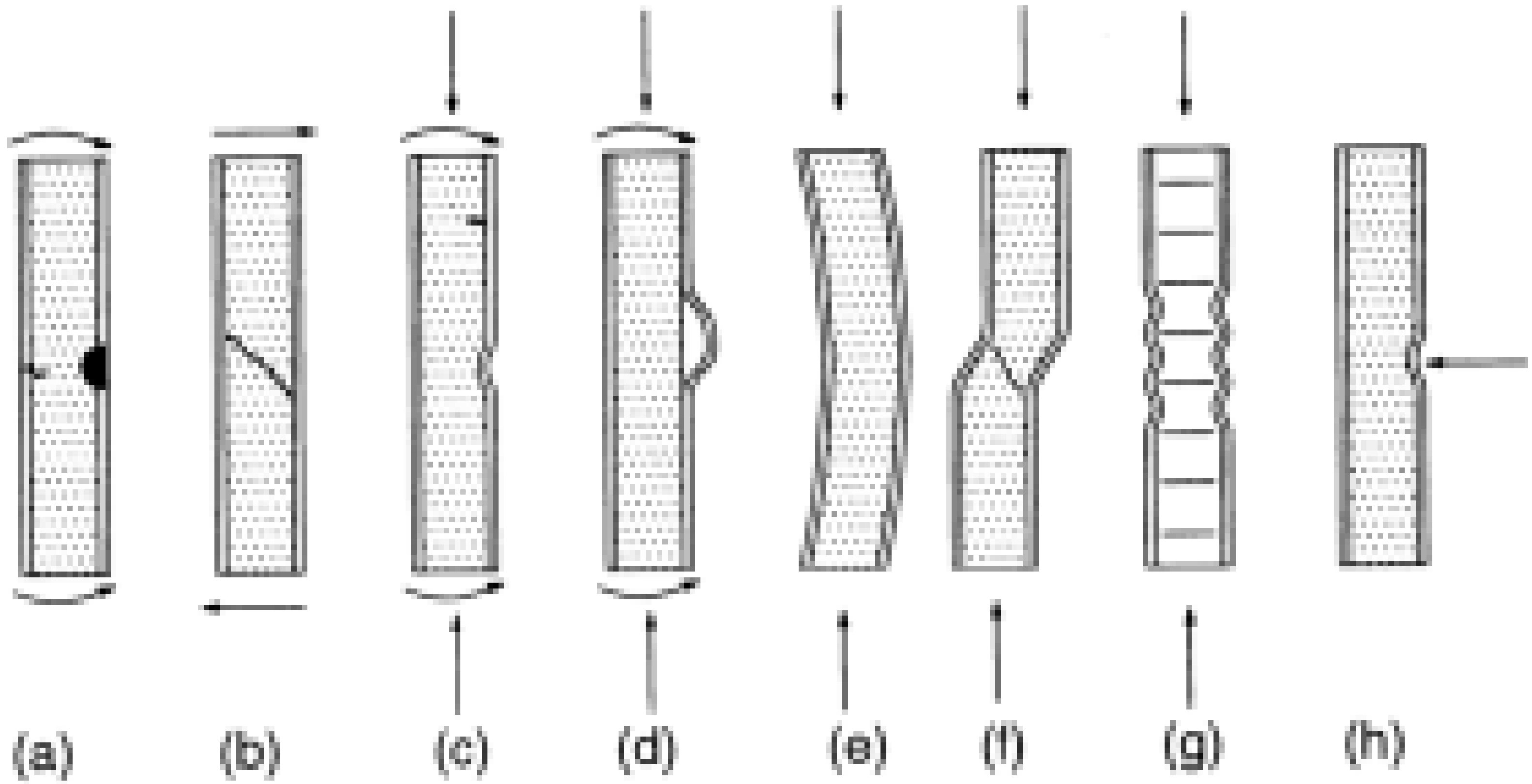

(a) face/core yielding/fracture
(b) core shear
(c) buckling - face wrinkling
(d) delamination
(e) general buckling
(f) buckling - shear crimping
(g) buckling - face dimpling
(h) core indentation - core yield

Det Norske Veritas Offshore Standard DNV-OS-C501, Composite Components, January 2003.

Summary of Sandwich Failure Loads

Failure Mode		Failure Load
Face Yielding	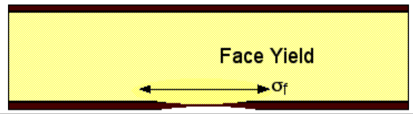	$P \geq \sigma_{yf} \cdot \frac{B_3 btc}{l}$
Face Wrinkling	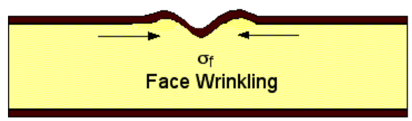	$P \geq \frac{B_3 btc}{l} \cdot 0.57 \left(E_f E_s^2 \left(\frac{\rho_c^*}{\rho_s} \right)^4 \right)^{1/3}$
Core Shear	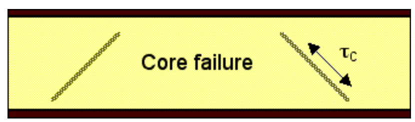	$P \geq C B_4 bc \cdot \left(\frac{\rho_c^*}{\rho_s} \right)^{3/2} \sigma_{ys}$
Core Fracture	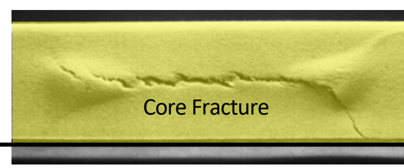	$P \geq C B_4 bc \cdot \left(\frac{\rho_c^*}{\rho_s} \right)^{3/2} \sigma_{cf}^* \sqrt{\frac{l^*}{a}}$
Bond Failure	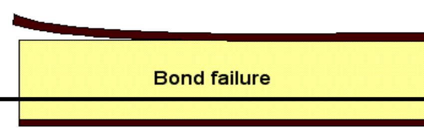	$P \geq \frac{B_3 btc}{l} \sqrt{\frac{G E_f}{t}}$

Sandwich failure presentation developed by Dr. John Pilling, Technical Director of Electric Park Research [http://home.comcast.net/~brandihampson/ep.html]

Core Failure

Shear Failure

D. Roosen

Skin-to-Core Debond

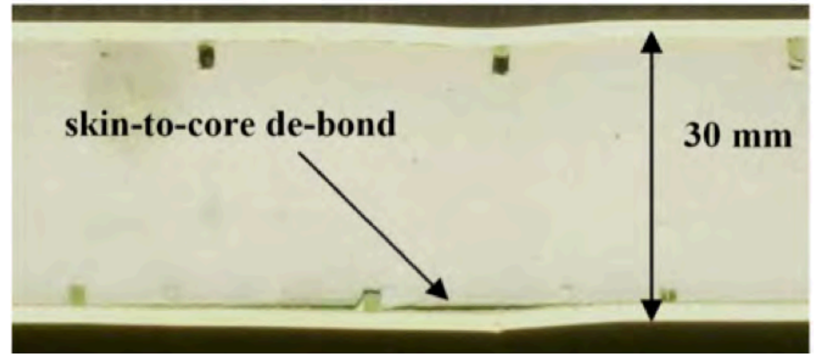

M. Gower

Crushing

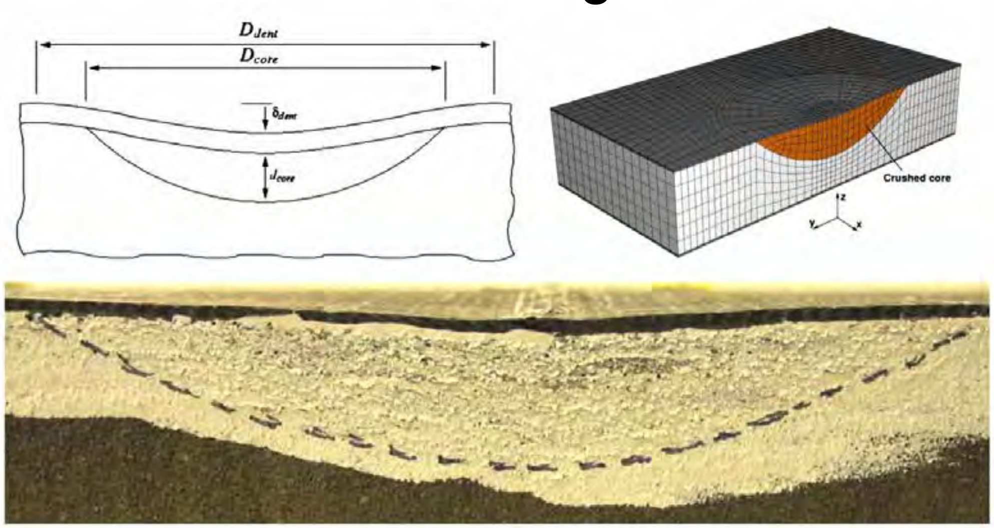

D. Zenkert

Fatigue Skin-to-Core Debond

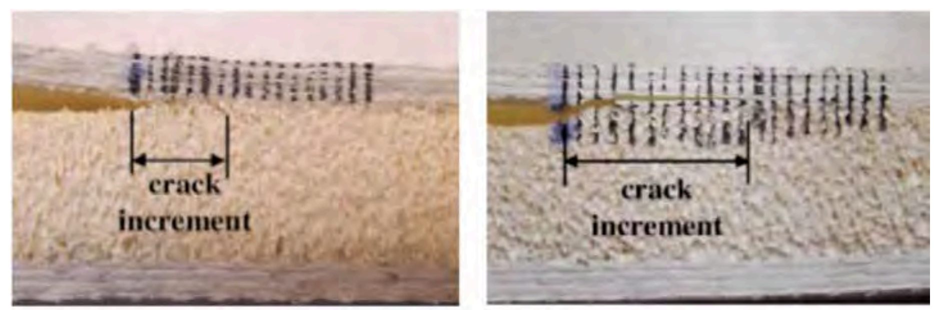

C. Berggreen

Core Shear Failure

"EGB-150" Balsa Core Material, Vacuum-Infusion (top), Hand Lay-up (bottom)

"SAN-95" Foam Core Material, Vacuum-Infusion (top), Hand Lay-up (bottom)

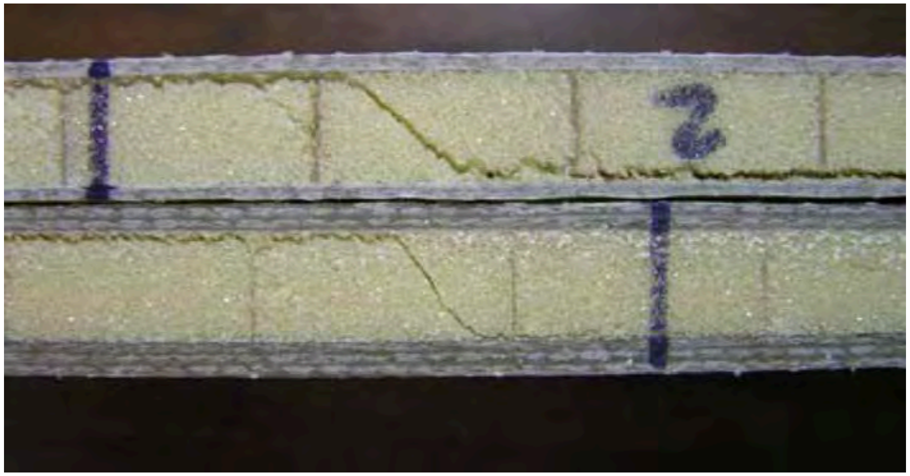

"PUR-130" Foam Core Material, Vacuum-Infusion (top), Hand Lay-up (bottom)

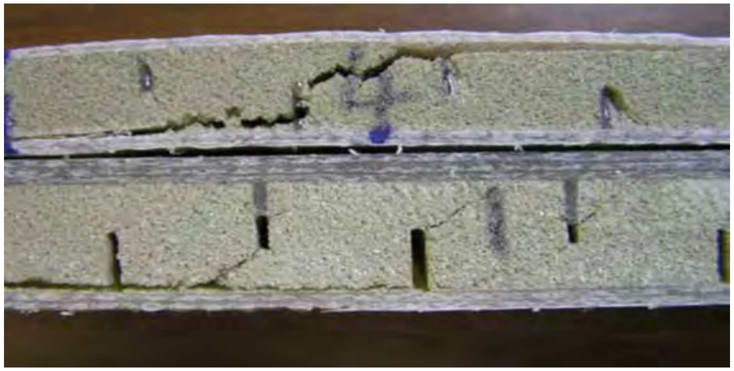

"PPHC-100" Polypropylene Honeycomb Core Material, Hand Lay-up

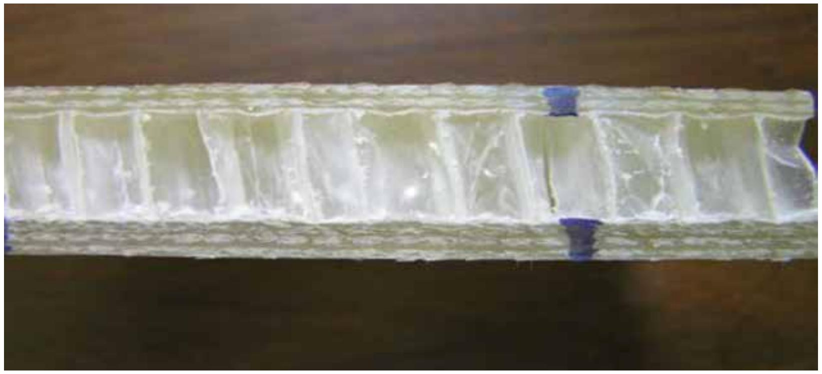

Kurt Feichtinger, Wenguang Ma and Russell Elkin, "Properties of Structural Sandwich Core Materials: Hand Lay-up vs. Vacuum-Infusion Processing," COMPOSITES 2006

Honeycomb & Foam Core Failures

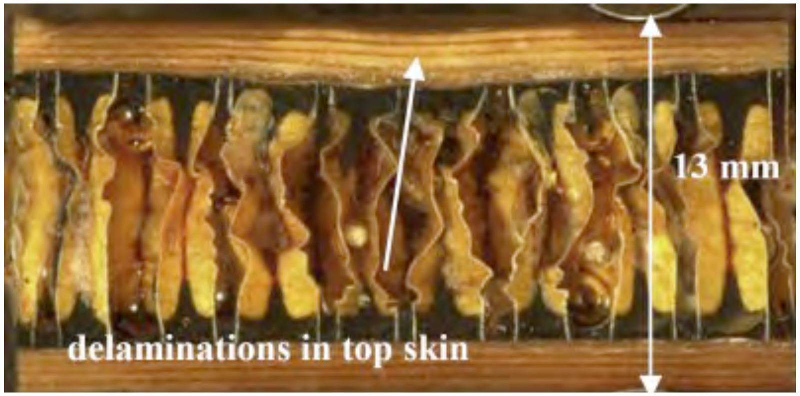

Digital photograph of impact delaminations in top skin of a sandwich construction

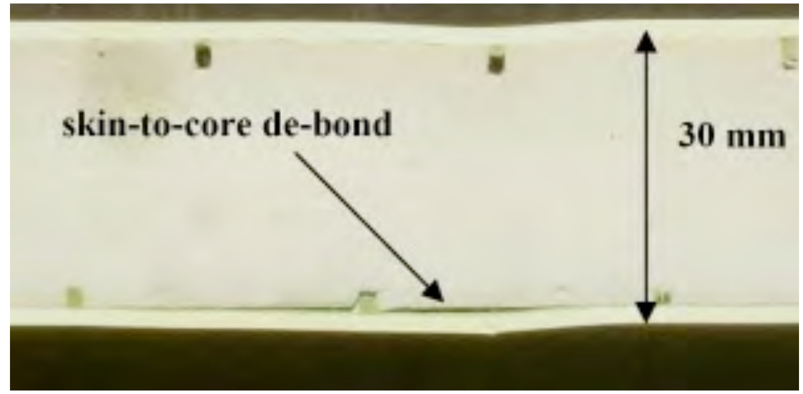

Digital photograph of skin to-core de-bond in a GRP skin, PU foam sandwich

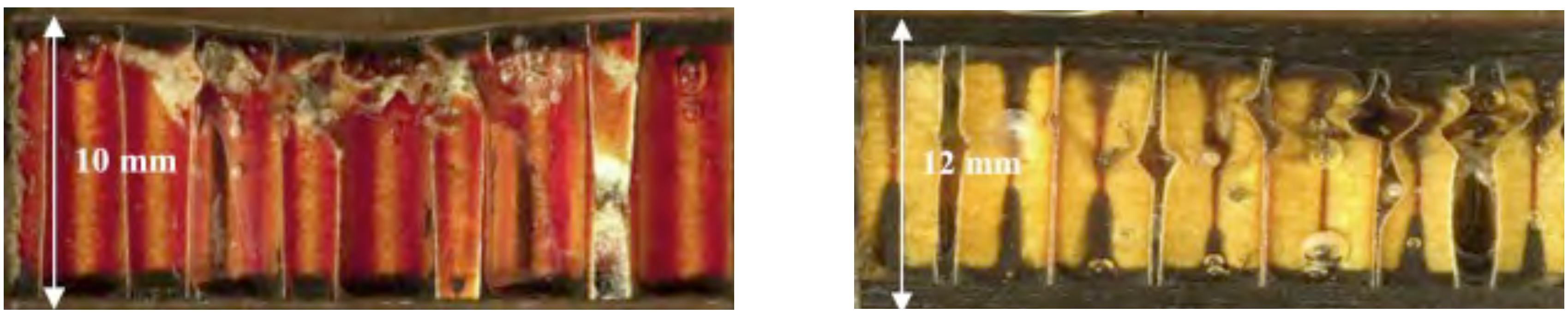

Digital photographs showing core crushing in (left) GRP-high density Nomex and (right) CFRP-medium density Nomex sandwich constructions

Gower, M., Sims, G., Lee, R., Frost, S. and Wall, M., “Assessment and Criticality of Defects and Damage In Material Systems," National Physical Laboratory, Teddington, Middlesex, United Kingdom, June 2005

Honeycomb Core Failures

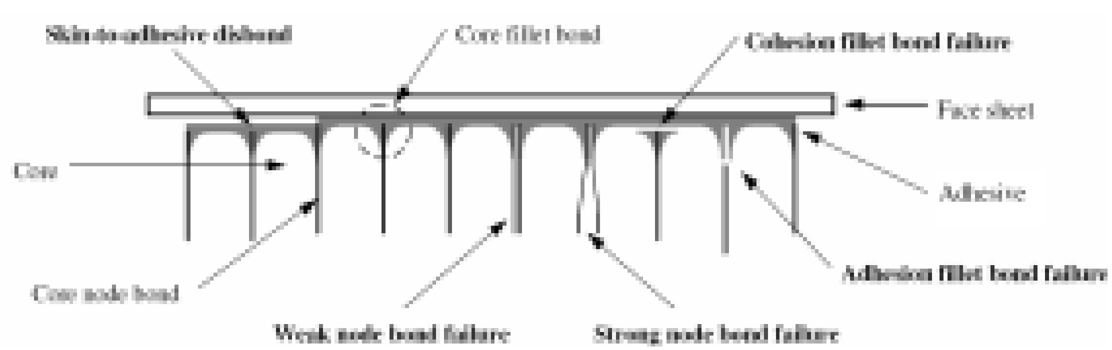

Adhesive bond failure modes for honeycomb sandwich panels

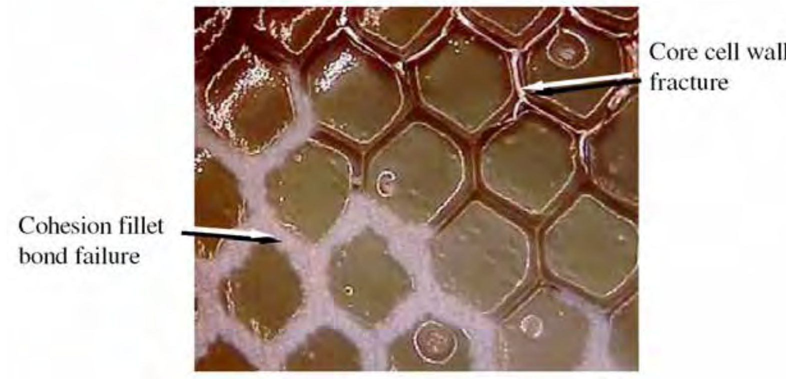

Flatwise tension failure of a sandwich panel

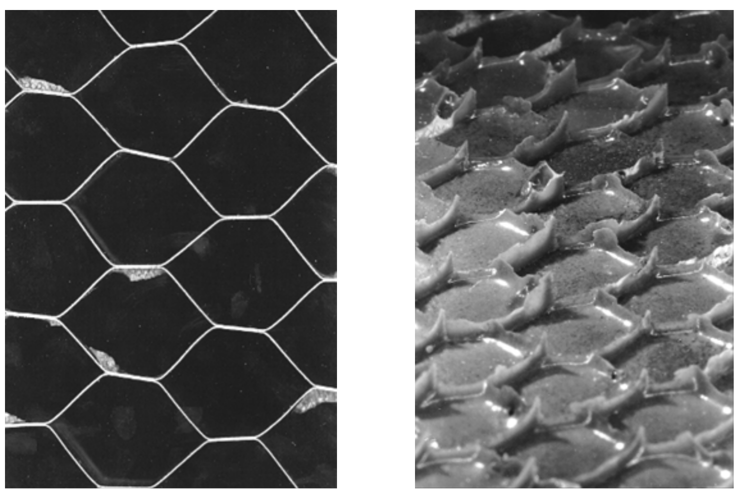

Core (left) and adhesive (right) surfaces after adhesion fillet bond failure. Note the minimal amount of cohesion fillet bond damage to the adhesive (right).

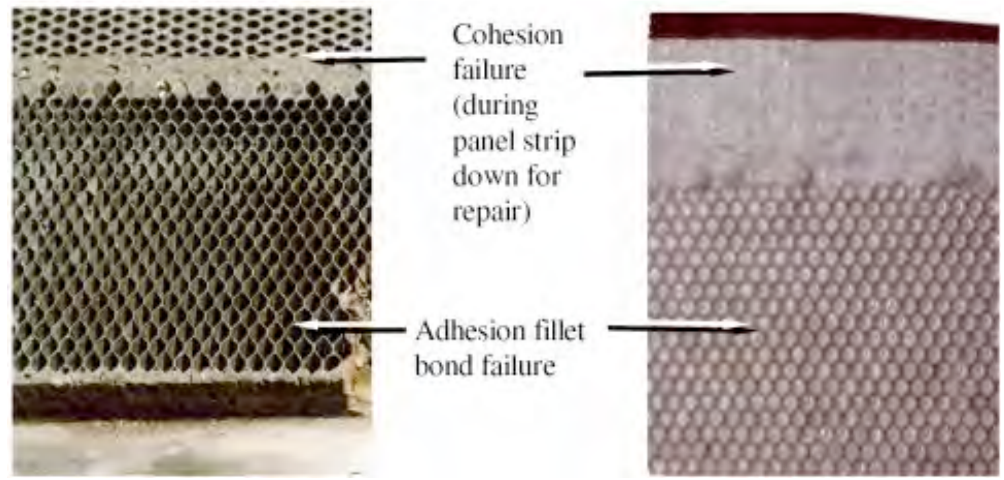

Disbonded sandwich panel: core (left) and skin (right)

Davis, M.J. and Bond, D.A., “The Importance of Failure Mode Identification on Adhesive Bonded Aircraft Structures and Repairs,,” Royal Australian Air Force, Melbourne, Australia, Sep 2008.

eric greene associates

Adhesive Failure Modes

Adhesive bond failure modes for honeycomb sandwich panels

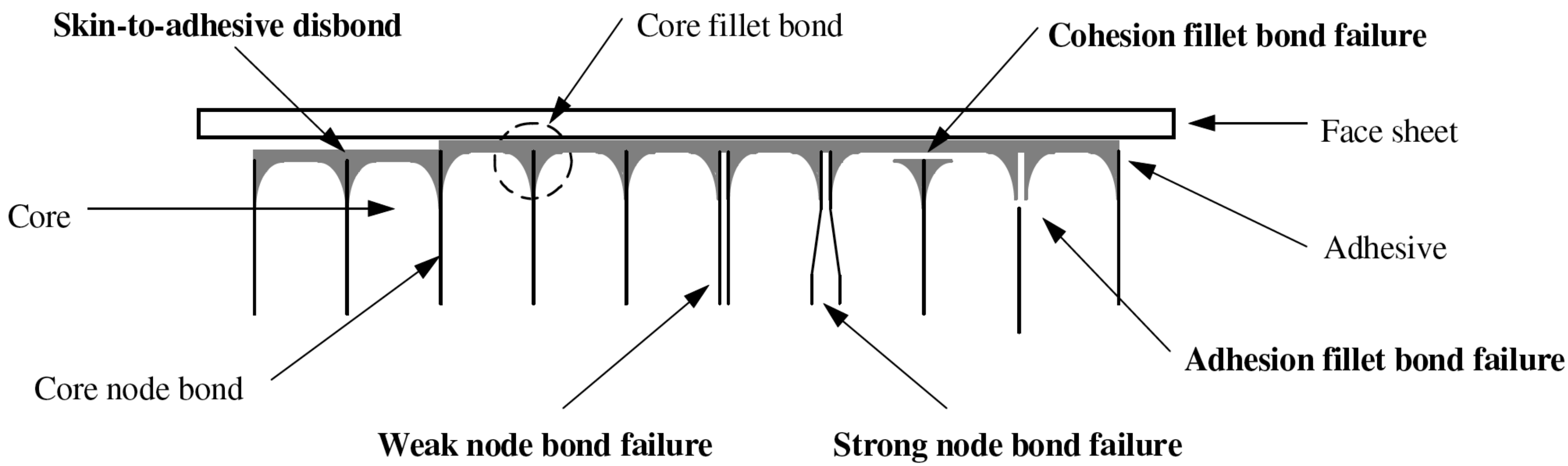

M.J. Davis and D.A. Bond, "The Importance of Failure Mode Identification in Adhesive Bonded Aircraft Structures and Repairs," Royal Australian Air Force

Bonded Joint Failures

Adhesive Failure: Failure of a bonded joint between the adhesive and the substrate

- Primarily due to a lack of chemical bonding between the adhesive and the bonding substrate
  - Can be indicative of poor surface preparation or contamination
  - Or, incorrect adhesive selection for the substrate materials

Cohesive failure: Failure of an adhesive joint occurring primarily in the adhesive layer

- Optimum type of failure in an adhesive bonded joint when failure occurs at predicted loads
- Lower failure loads are indicative of poorly cured adhesive or moisture or other contaminants present in the adhesive

Bolted Connection Failure Modes

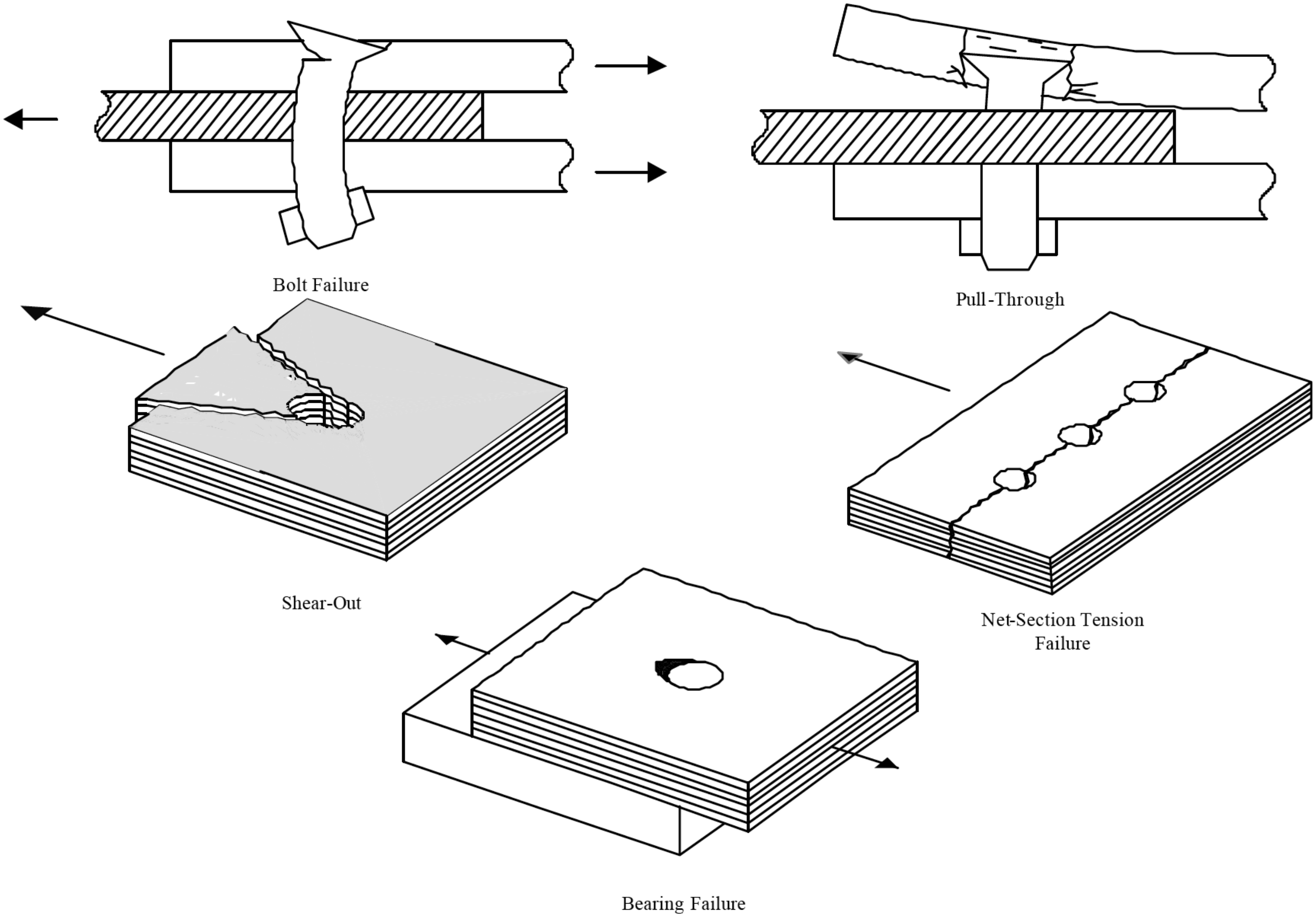

Visible Surface Damage

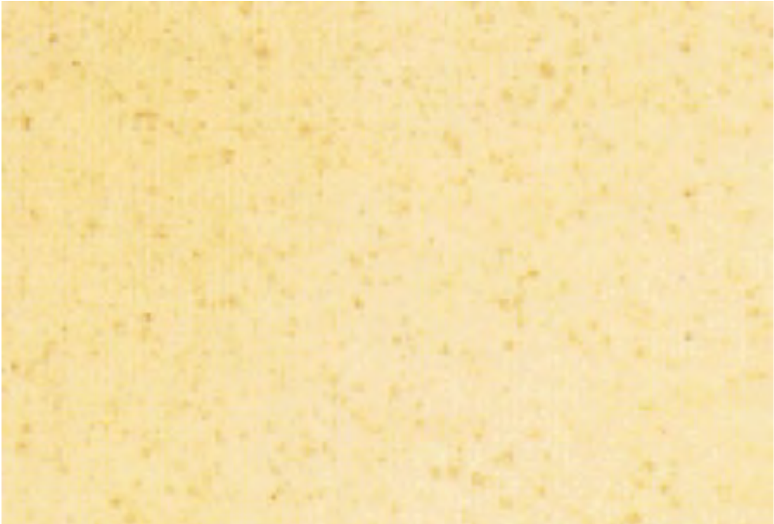

Air bubbles, voids Air entrapment in and between plies; noninterconnected spherical voids

Blisters Rounded, sometimes sharply defined elevations of laminate surface resembling blisters.

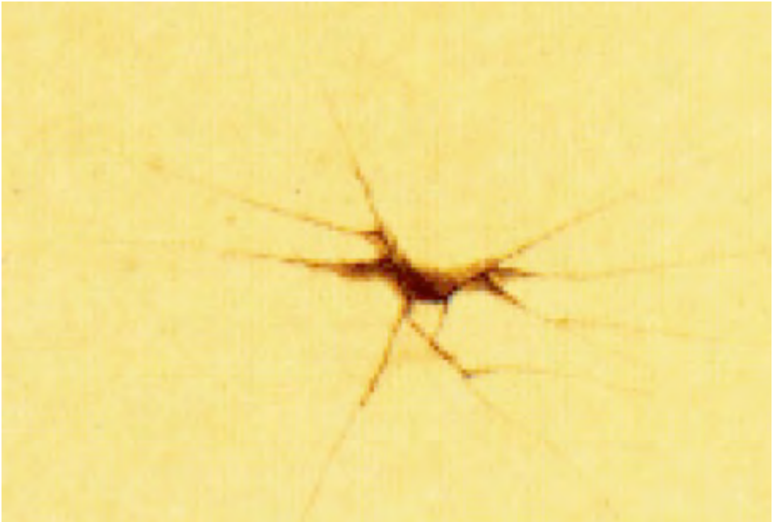

Impact cracks Separation of material through entire thickness and visible on surfaces.

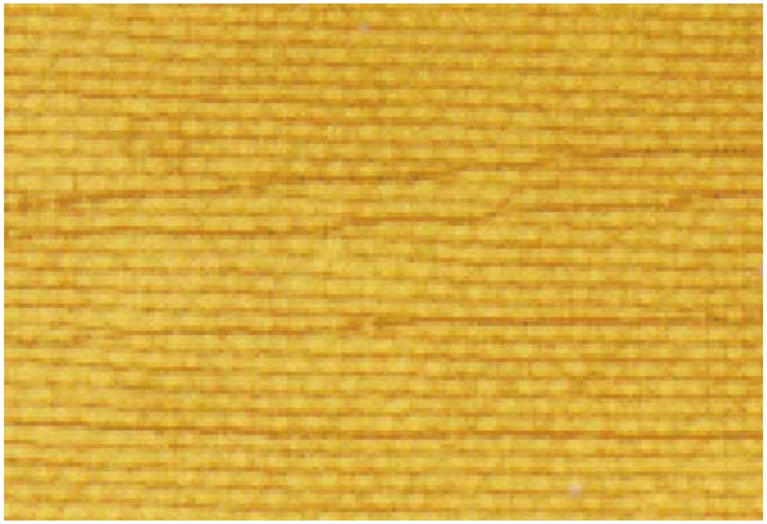

Crazing Pattern of fine cracks on or beneath surface.

Dow Chemical Company

Visible Surface Damage

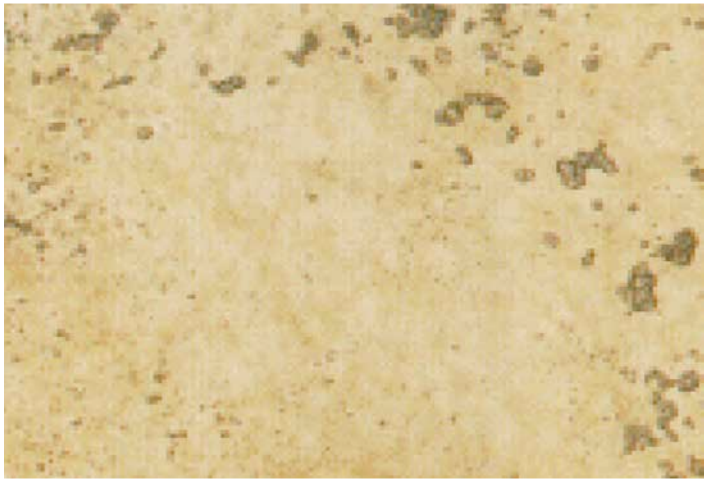

Pit or pinhole Small regular or irregular crater on surface, usually with nearly equal width and depth

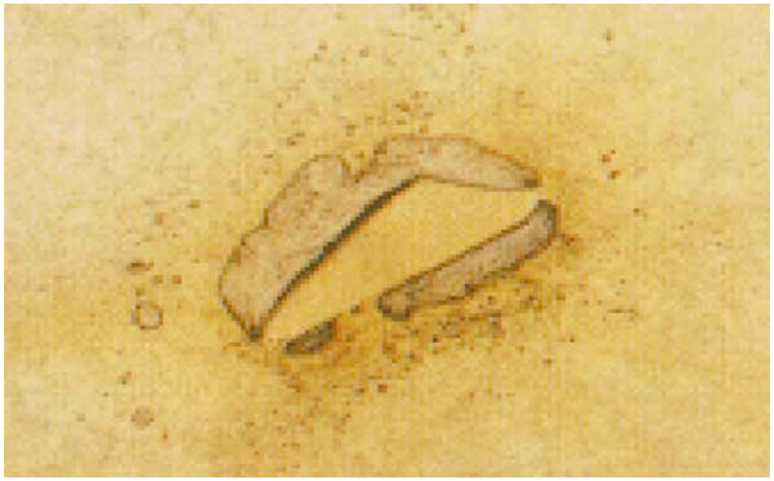

Resin pocket Apparent accumulation of excess resin in a small localized area

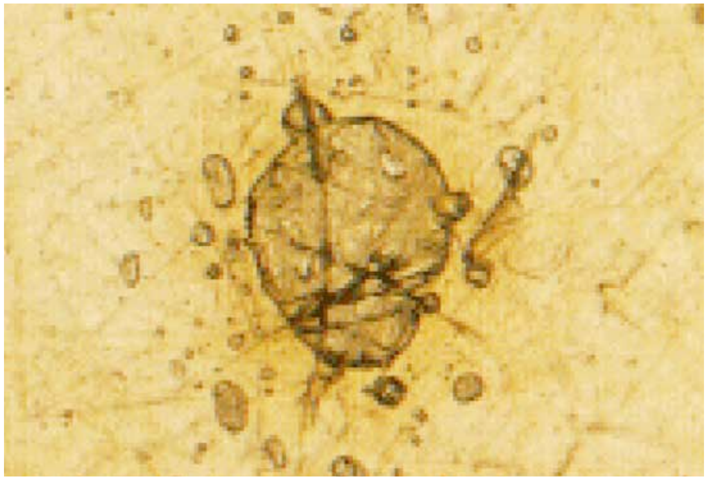

Worm hole Elongated void in surface or covered by thin film of cured resin.

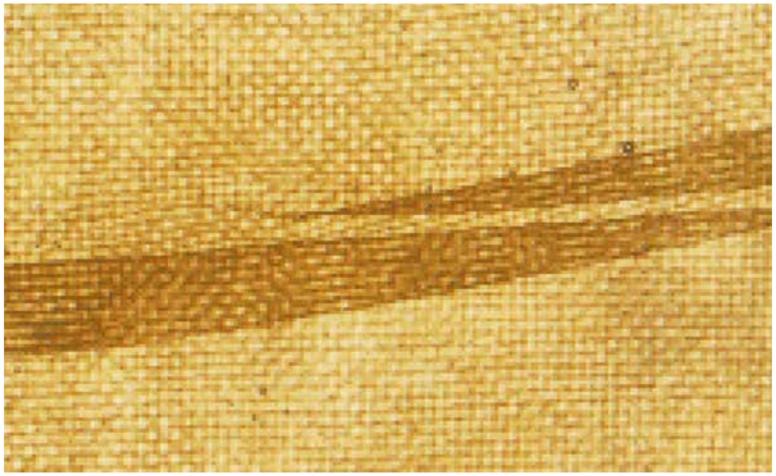

Wrinkle Crease or wrinkle-like surface imperfection in one or more plies of molded-in reinforcement.

Dow Chemical Company

Visible Surface Damage

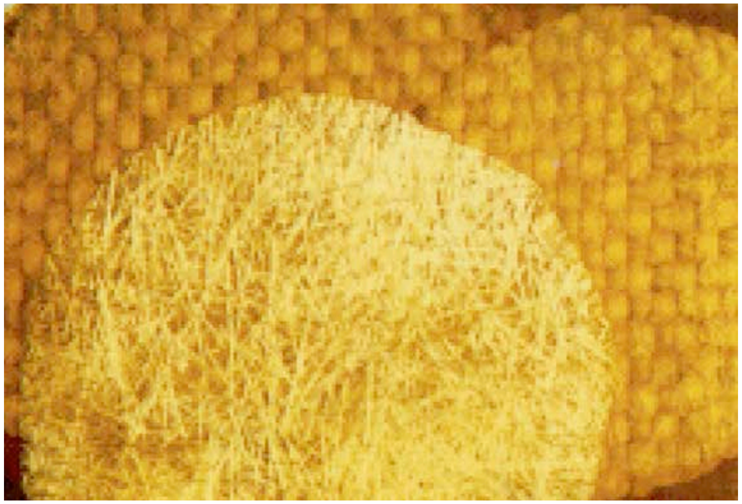

Delamination Separation of layers

Fisheye Small globular mass that has not blended into surrounding material. Particularly evident in transparent or translucent materials

Dry Spots Area of reinforcement that was not wetted with resin. Usually at laminate edge.

Pimple Small sharp or conical pimple-like elevation on surface. Usually resin-rich.

Dow Chemical Company

Gel Coat Cracking

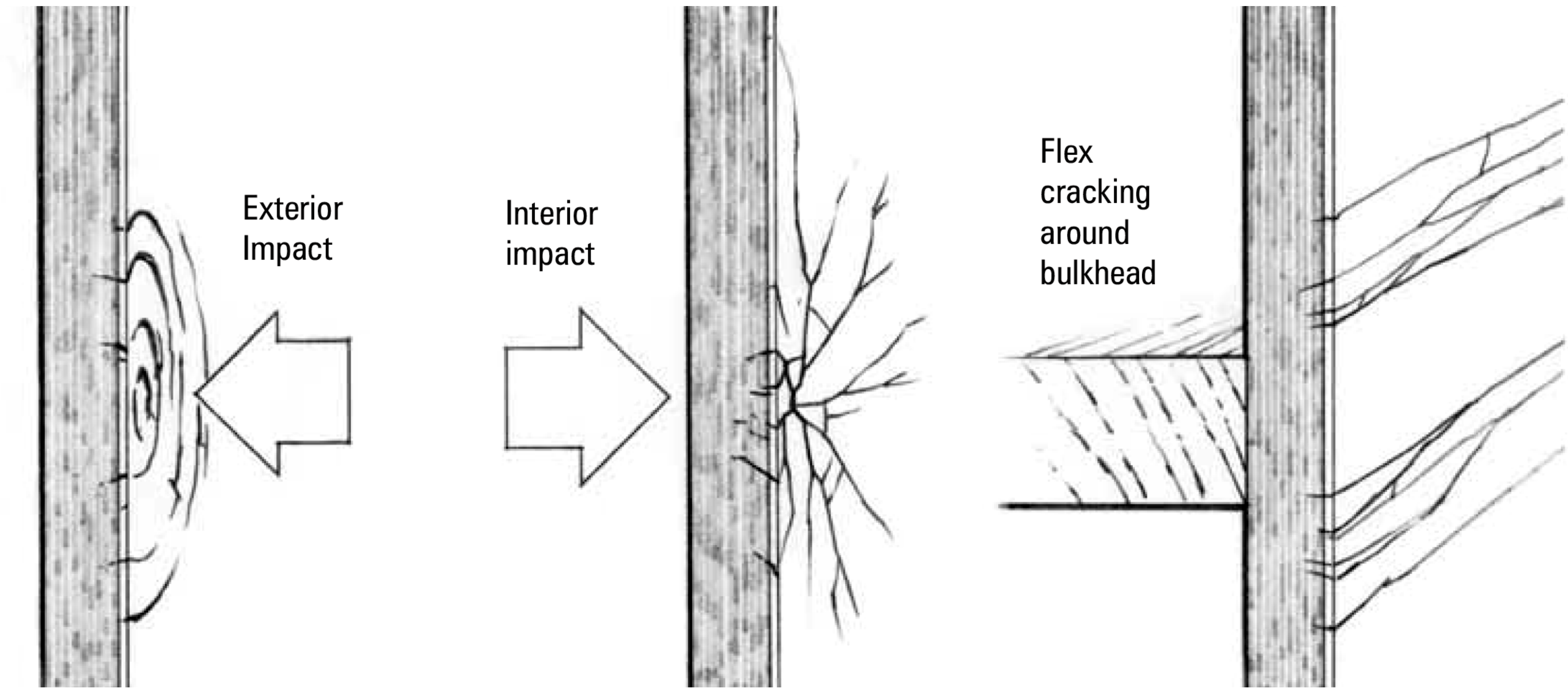

Gougeon Brothers Inc., "WEST System Fiberglass Boat Repair & Maintenance," 15th Edition, April 2011

Gelcoat Cracking

photo credit: Tony Guild

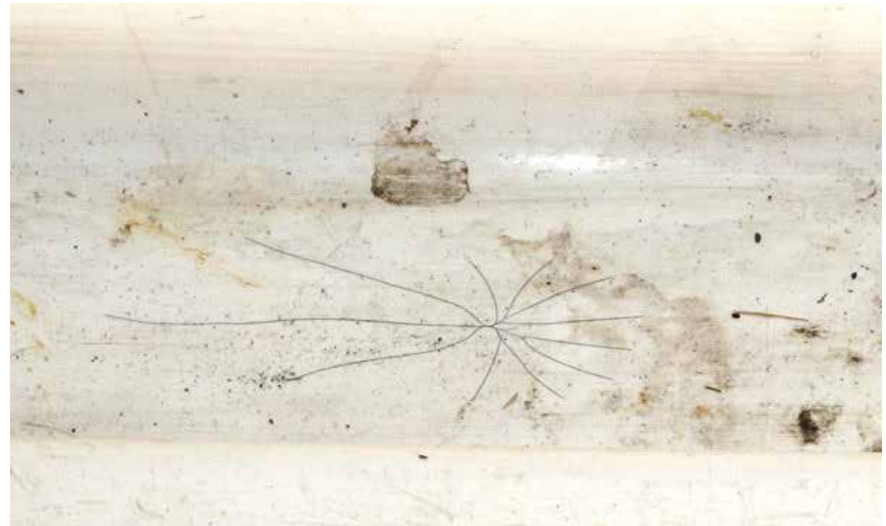

www.walshsurveyor.com

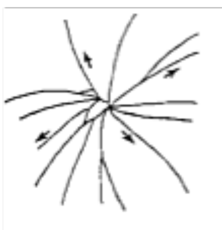

Secondary cracks diverge to less density

Adjacent stress fields influence pattern

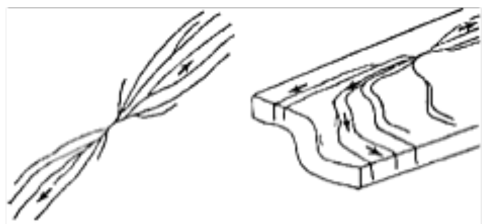

Type I Radial or Divergent Configuration

Type II Randomly Spaced Parallel and Vertical Fractures

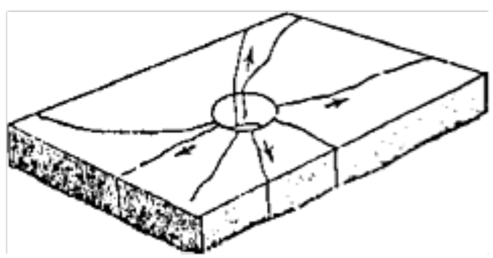

Type III Cracks at Hole of Other Stress Concentration

illustration credit: J.W. Smith

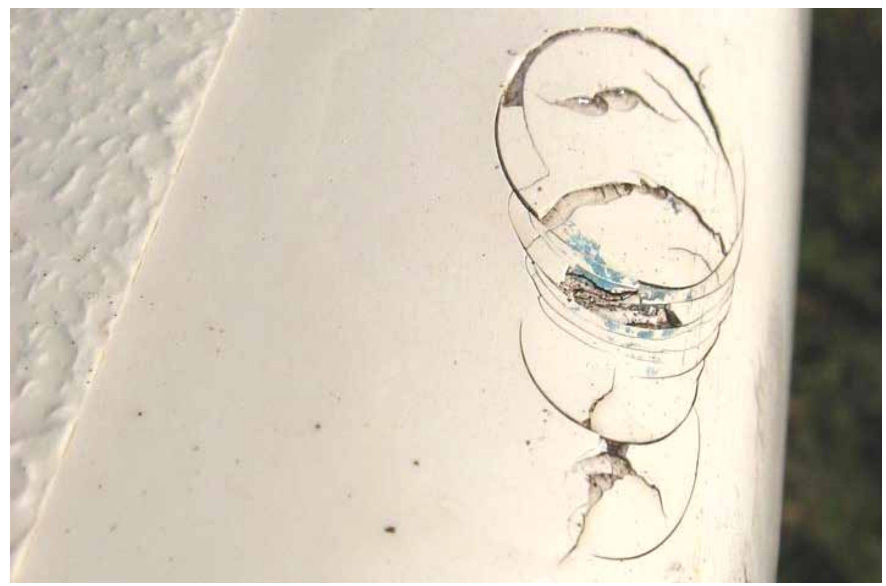

www.cautionwater.com

Voids

Micrographs of voids in (left) unidirectional pre-preg and (right) filament wound CFRP materials

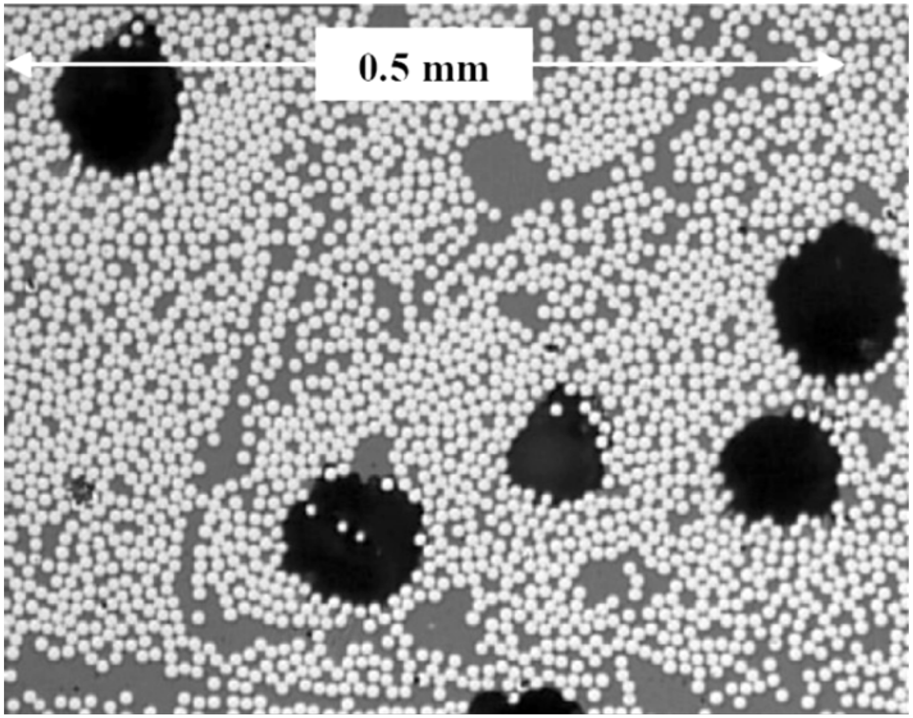

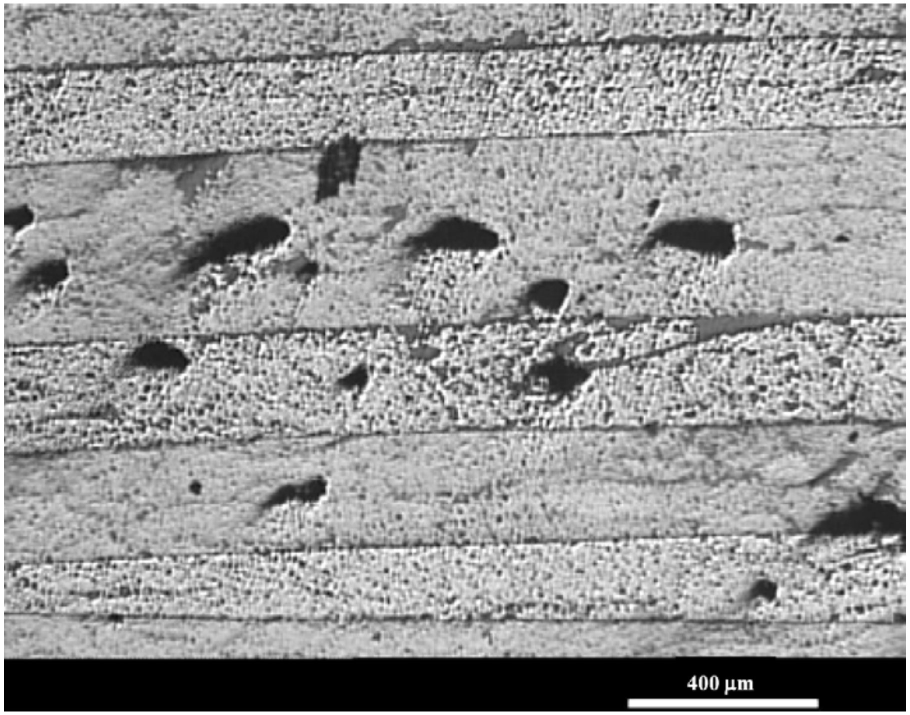

Gower, M., Sims, G., Lee, R., Frost, S. and Wall, M., Measurement Good Practice Guide No. 78 "Assessment and Criticality of Defects and Damage In Material Systems," National Physical Laboratory, Teddington, Middlesex, United Kingdom, June 2005

Lightning Damage

Lightning damage to wind turbine blades

Kithil, R., Knight & Carver, "Case Study of Lightning Damage to Wind Turbine Blade," National Lightning Safety Institute (NLSI), June 2008.

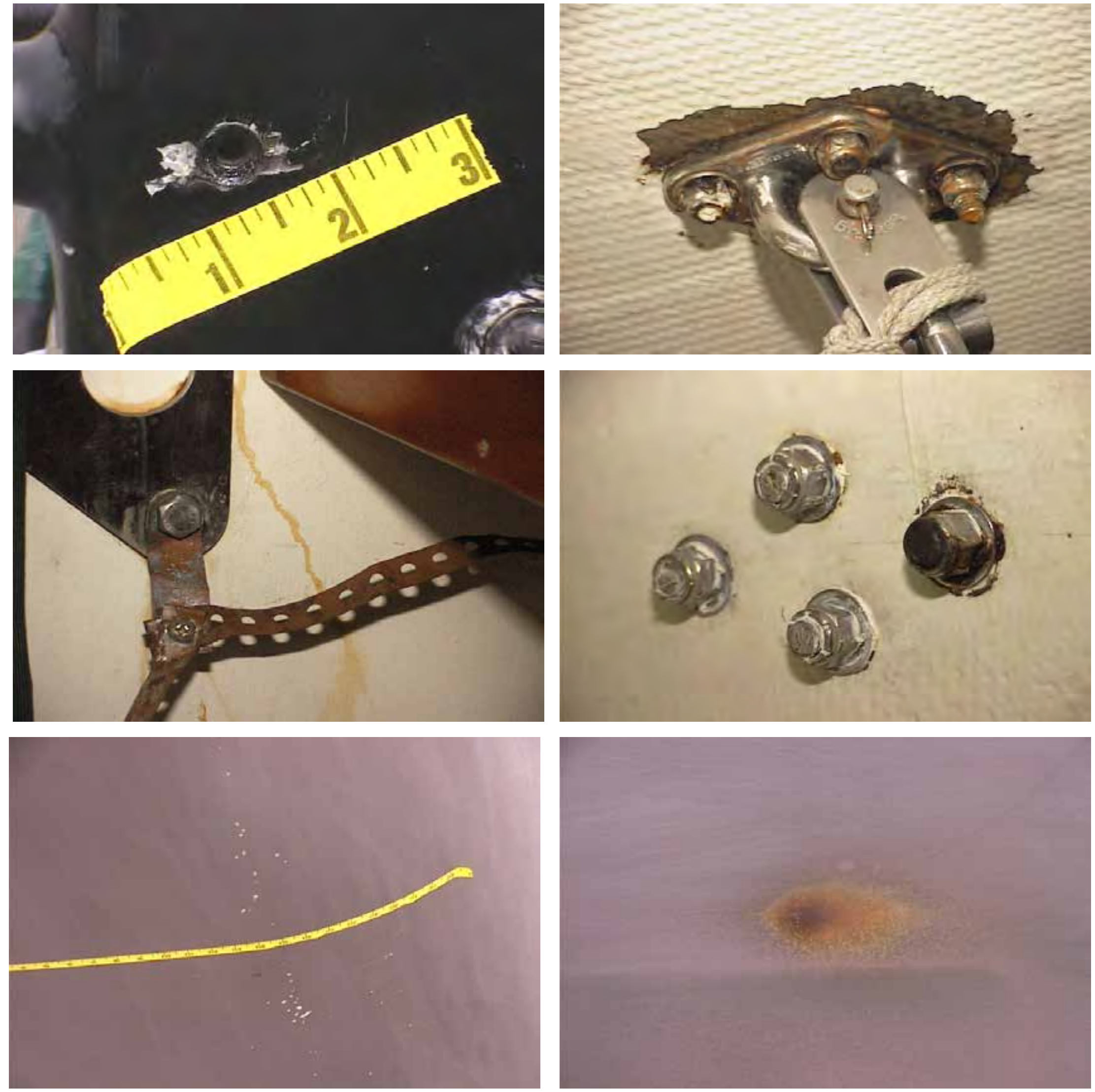

Lightning damage to carbon fiber yacht mast showing discharge path

Eric Greene Associates, Inc. survey of Santa Cruz 72, July 2002.

Lightning Damage

Micrographs of (left) resin burn-off and matrix micro-cracking in CFRP panel containing lightning strike protection and (right) large scale delaminations in unprotected panel

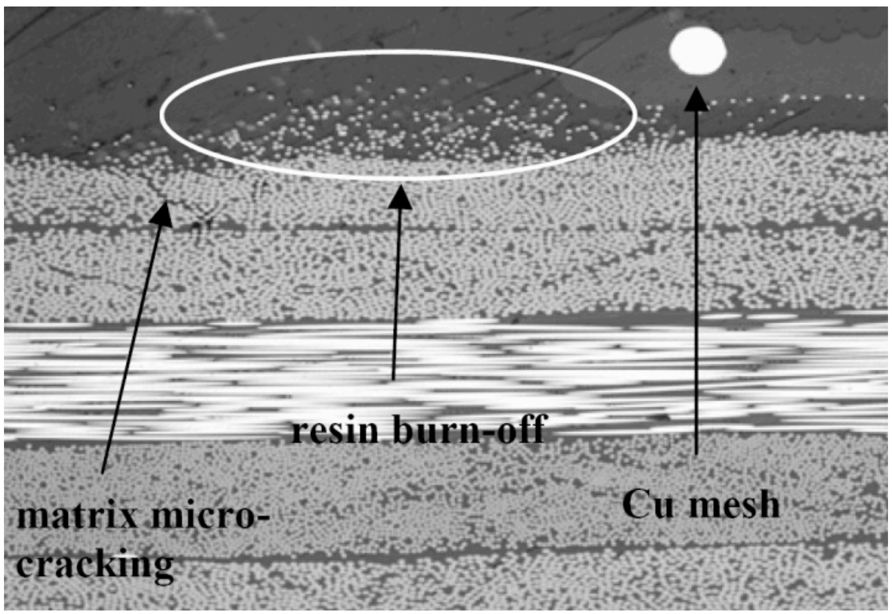

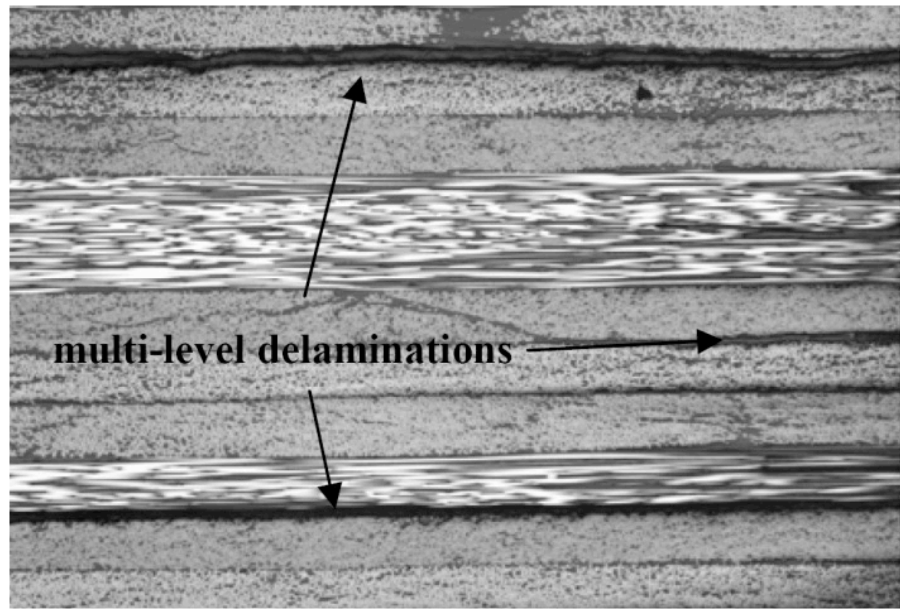

Gower, M., Sims, G., Lee, R., Frost, S. and Wall, M., Measurement Good Practice Guide No. 78 “Assessment and Criticality of Defects and Damage In Material Systems," National Physical Laboratory, Teddington, Middlesex, United Kingdom, June 2005

Damage in Foil Spar Structures

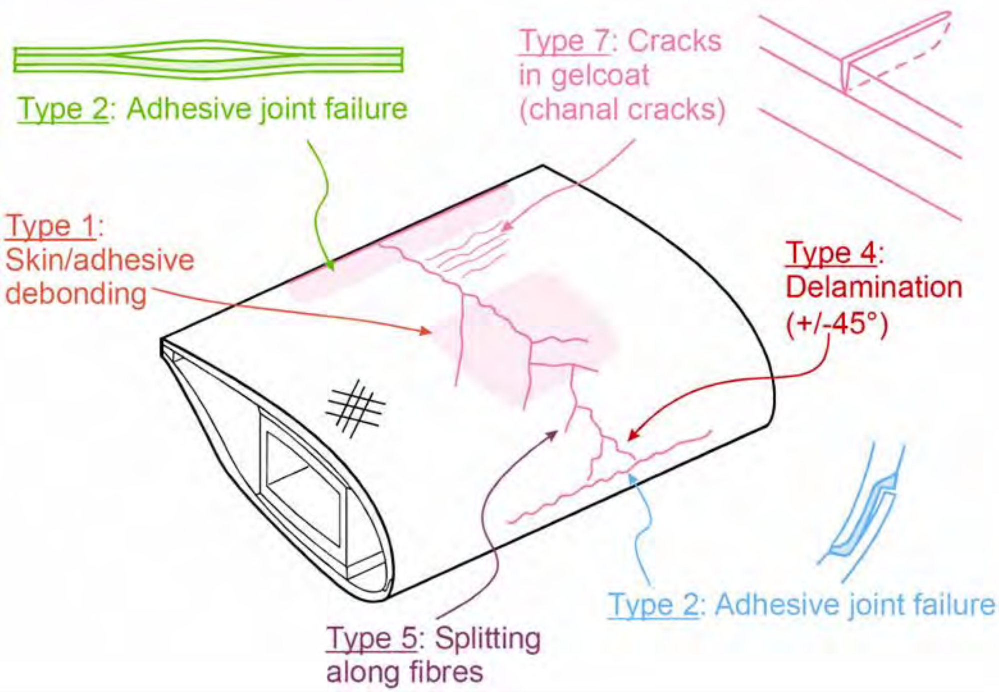

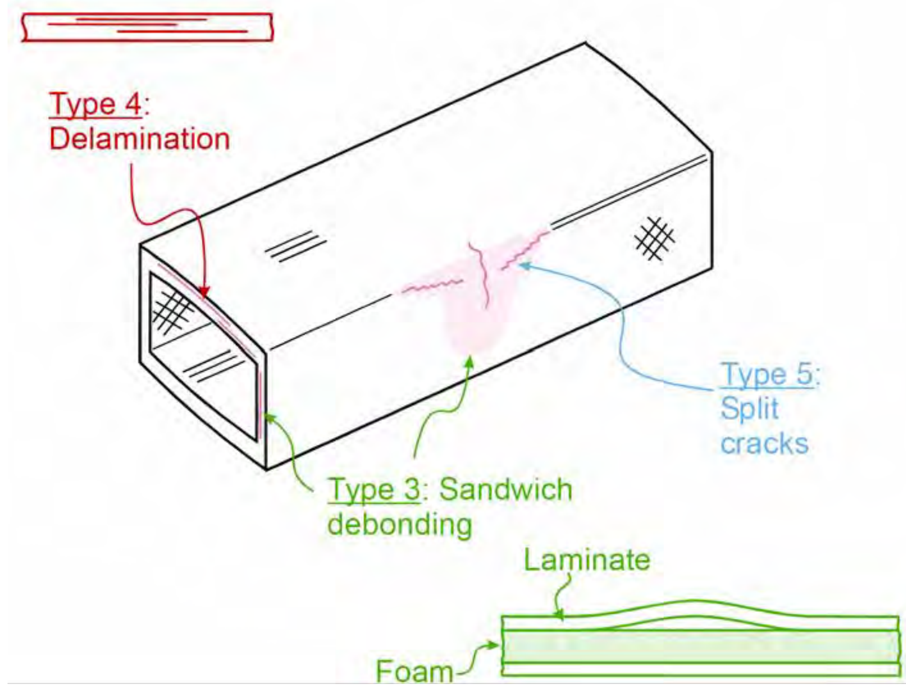

Types 1 (skin/adhesive debonding) and 2 (adhesive joint failure between skins) at the leading as well as the trailing edge. Types 4 (delamination driven by a buckling load), 5 (laminate failure in compression) and 7 (gel-coat cracking and gel-coat/skin debonding)

Damage types 4 (delamination driven by buckling load) in upper flange and 5 (fiber failure in tension; laminate failure in compression) in the web

Sørensen, B.F., Jørgensen, E, Debe, C.P., Jensen, F.M., Jensen, H.M., Jacobsen, T.K.and Halling, K.J., "Improved design of large wind turbine blade of fibre composites based on studies of scale effects (Phase 1) - Summary Report," Risø National Laboratory, Roskilde, Denmark, September 2004.

Ship Structural Failures

Indonesian Trimaran Fire

High-speed Catamaran Bow

Bulbous Bow

Examples of Impact Damage

Roll stabilizer damaged after grounding (top) and resulting hull damage (below)

Just before 2 a.m., a 1992, 38-ft. Fountain power boat slammed into a fixed, channel marker, ripping a 17-ft. gash in the forward hull & becoming impaled on the steel piling holding the channel marker.

Sailboat hit by powerboat on autopilot in the open ocean

Impact Damaged Boats




www.yachtpals.com

Impact Damaged Boats

Submarine Impact Damage

SSN 711 *San Francisco* hit an uncharted seamount in Jan 2005

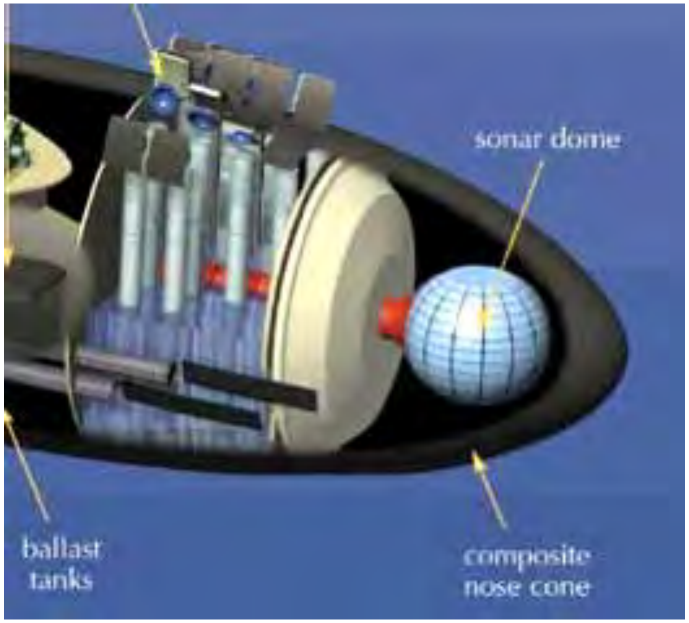

Internal Damage

Crew repairs damage to ring frame sustained in 50 knot winds on Irish entry in the 2011-12 edition of the Volvo Ocean Race

Guo Chuan/Green Dragon Racing

Stringer damaged from grounding event

Examples of Slamming

Sail

Power

Illustrations of Sail, left [High Modulus] and Power, right [Structural Composites] High-Speed Vessel Slamming Events

Catamaran Slamming

Crowther design 318 slamming locations

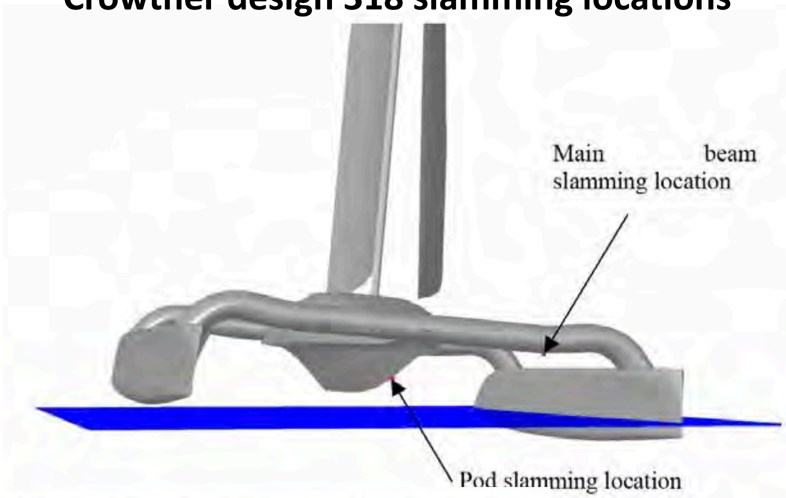

Typical Slam Impact Pressure

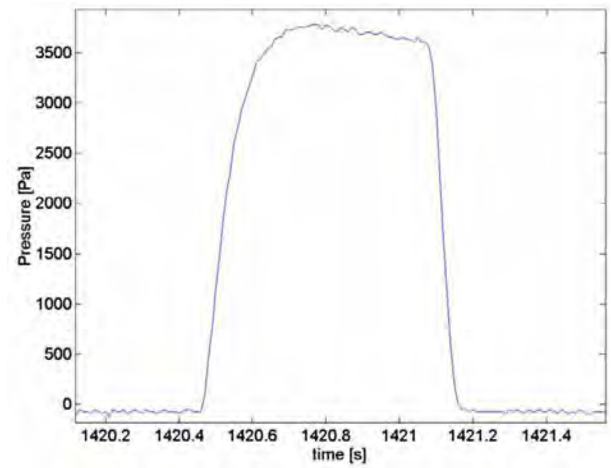

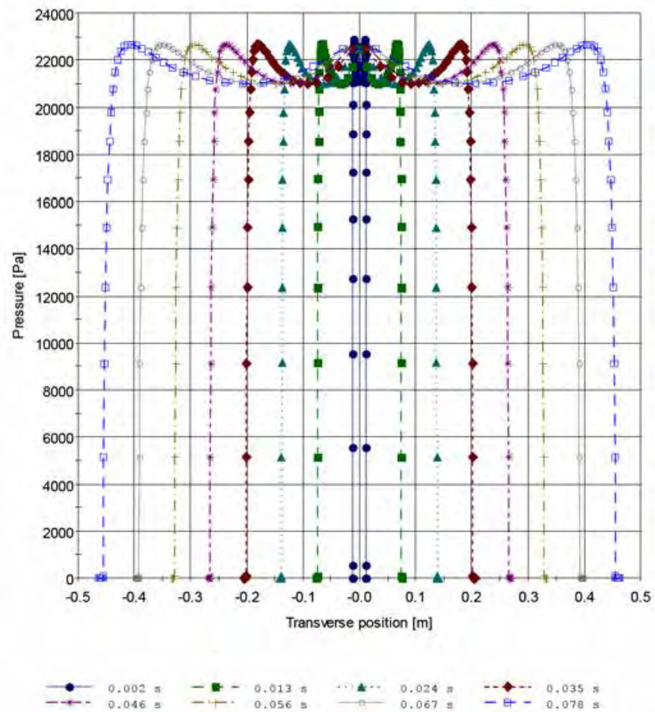

Transverse distribution of Crowther 318 pod slamming pressure for 4 m/s impact

Longitudinal distribution of Austal H 63 slamming pressure for 4 m/s impact

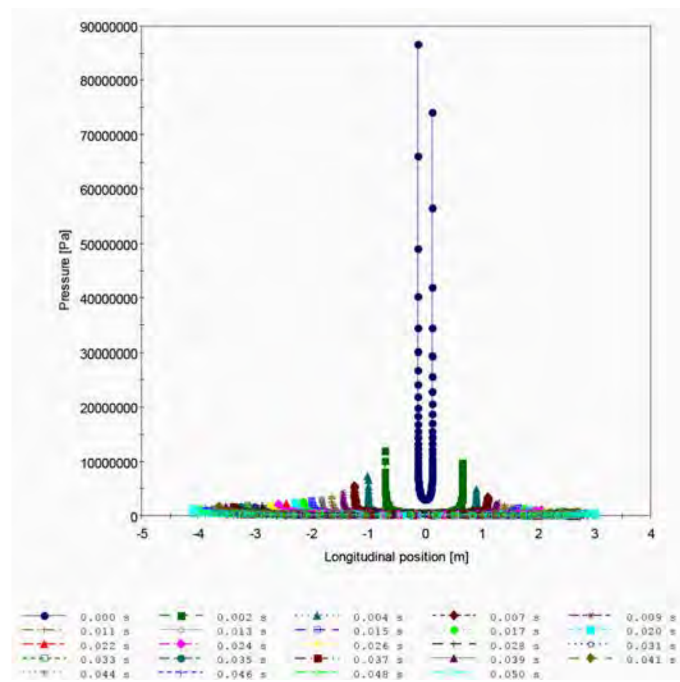

Kristoffer Grande, “Prediction of Slamming Occurrence of Catamarans,” Aug 2002.

Slamming Phenomenon

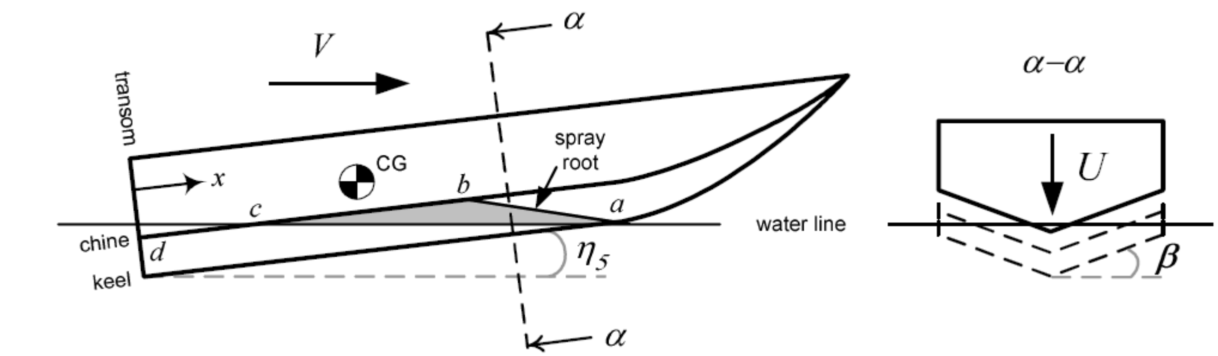

Planing Craft
Wave Impact

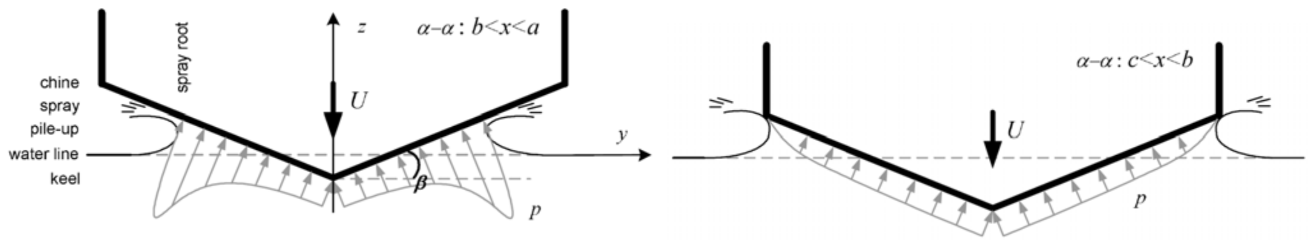

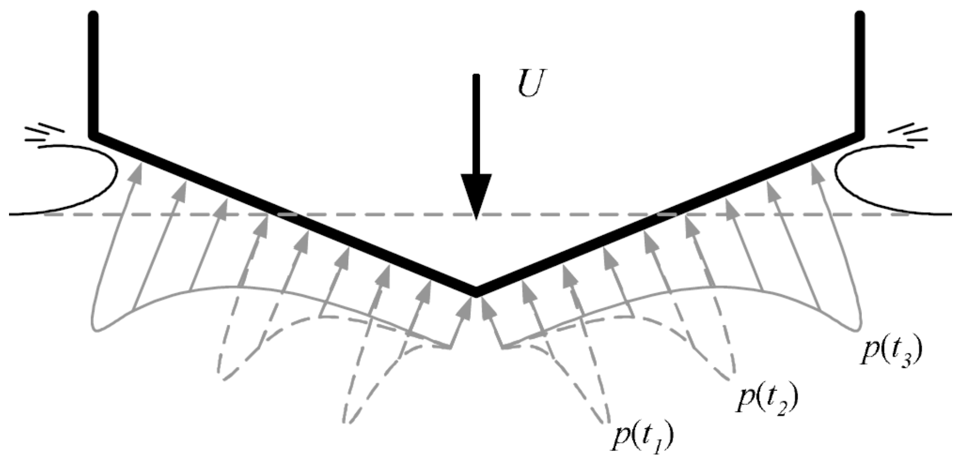

Pressure Distribution During Hull-Wave Impact

Slamming Pressure Distribution

$$p_{bxx} = \frac{N_1 \Delta}{L_w B_w}[1 + n_{cg}]F_D F_v$$

Δ = *Displacement*
L_w = *Length*
B_w = *Beam*

Vertical Acceleration Distribution Factor F_V

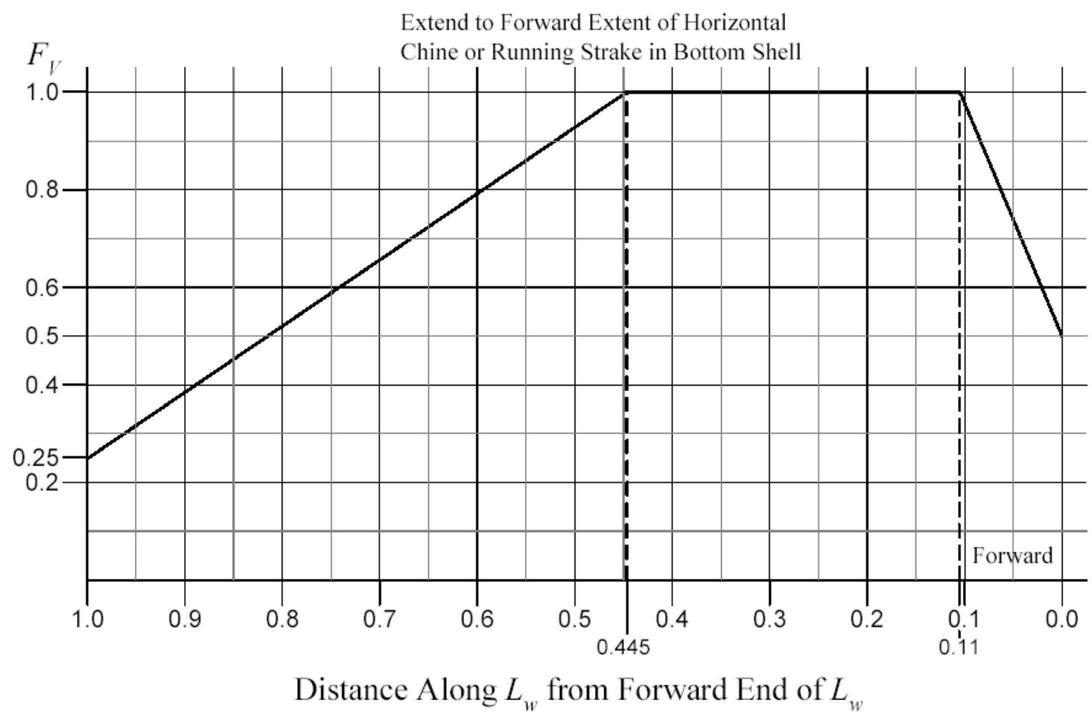

n_{cg} = the vertical acceleration of the craft as determined by a model test, theoretical computation, or service experience

Deadrise Angle

Peak pressures plotted against deadrise angle for 3 different velocities.

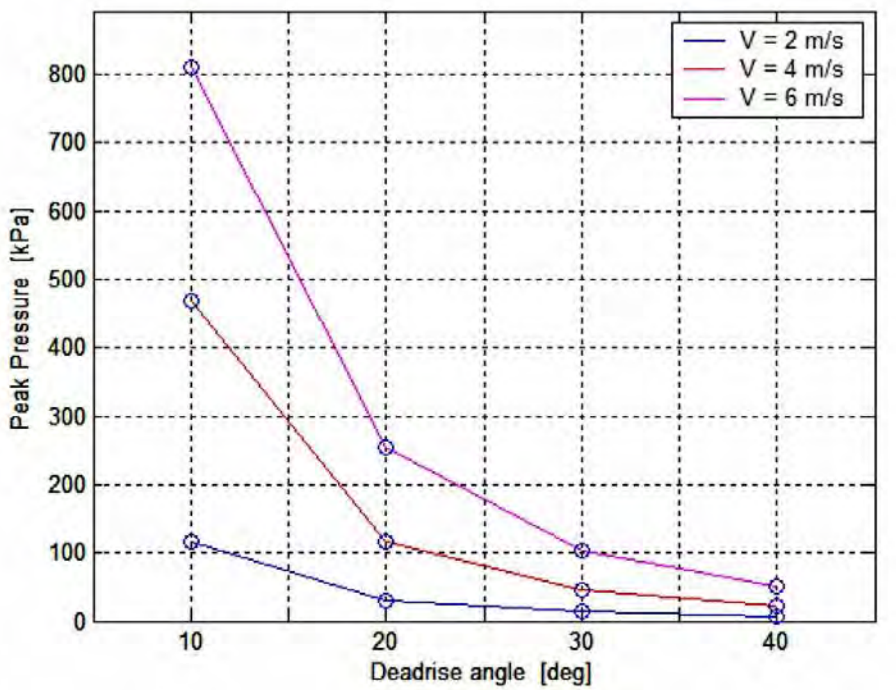

Johan Breder, “Experimental Testing of Slamming Pressure on a Rigid Marine Panel,” Stockholm, Sweden 2005

Predicted water jet flows and pressure contours in water by LS-DYNA for the wedge with 30° and 60° deadrise angle (scale is 5x for 30° deadrise)

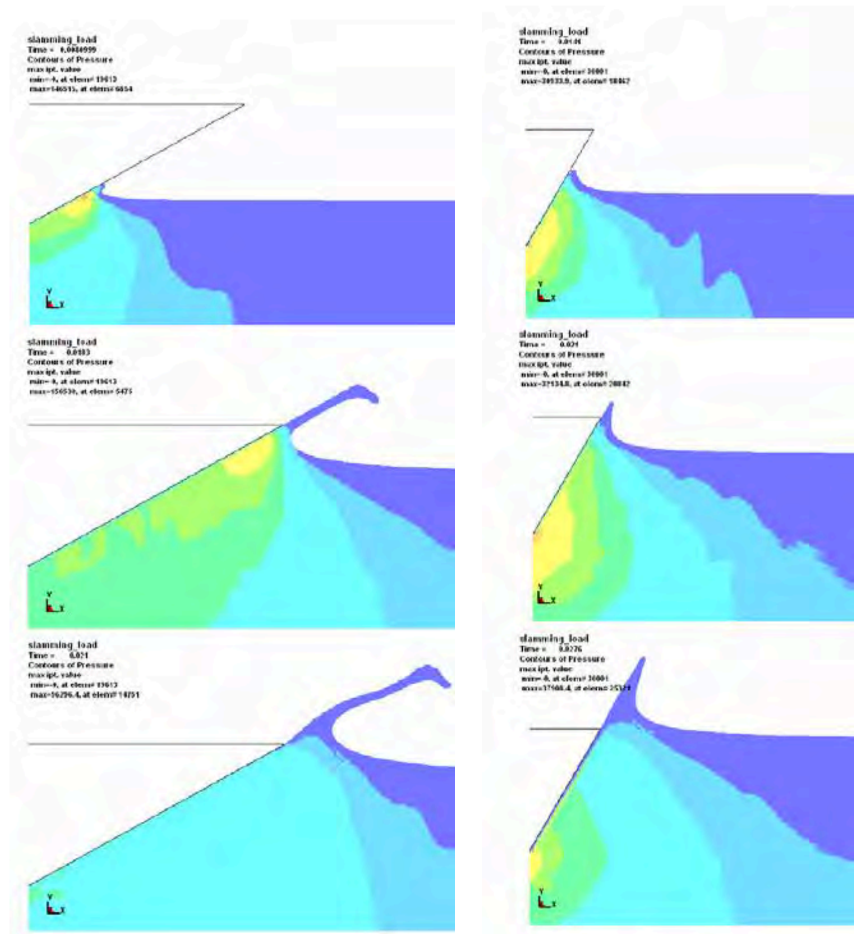

Shan Wang, “Assessment of slam induced loads on two dimensional wedges and ship sections,” Dec 2011.

Slam Pressure Distribution

Example of momentary pressure distribution on a planing craft in head seas

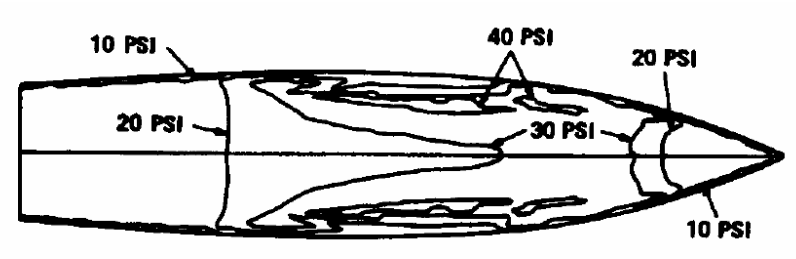

Allen & Jones 1978

Bottom slamming design pressure

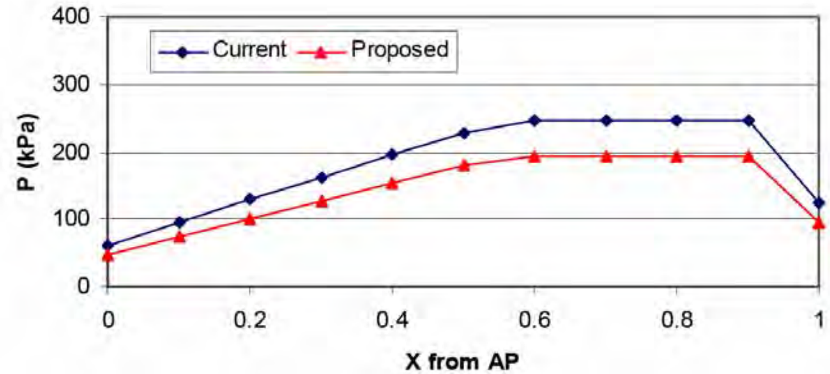

Peter Kim, Derek Novak, Kenneth Weems & Hamm-Ching Chen, "Slamming Impact Design Loads on Large High Speed Naval Craft," 2008

Time History of Panel Deflection (left) and Deflection at time of maximum deflection for "3D" Pressure Distribution [mm] (right)

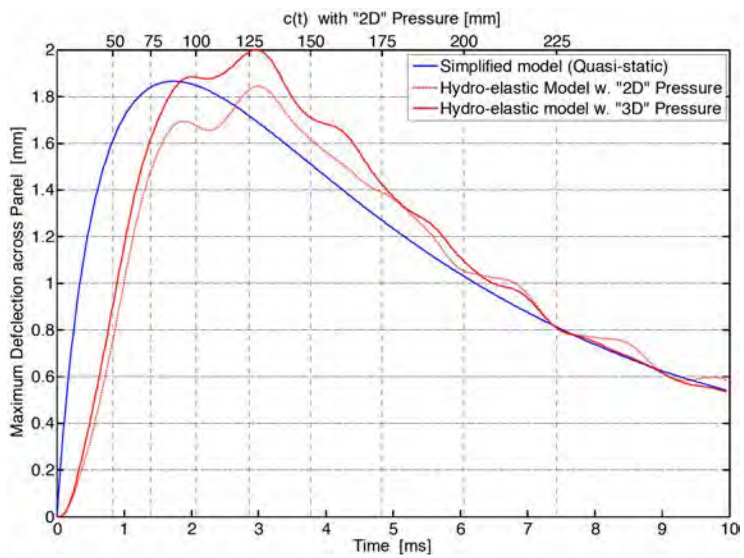

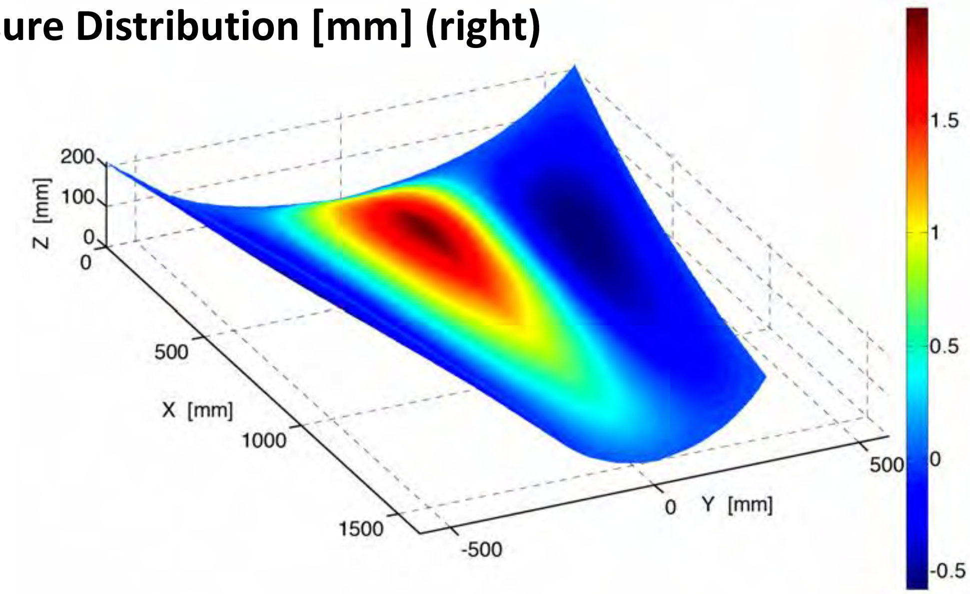

Frederic Louarn and Paolo Manganelli, "A simplified slamming analysis model for curved composite panels," 21st International HISWA Symposium, Dec 2010.

eric greene associates

Impact Damage Types

Low-Energy Impact

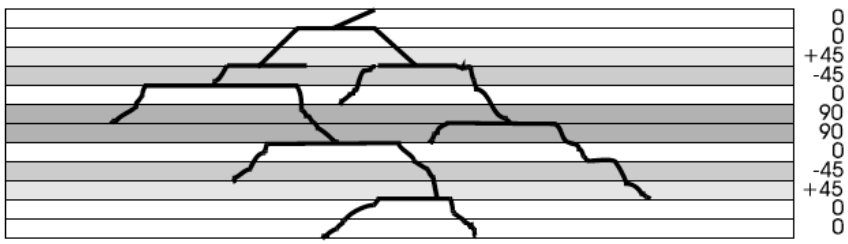

Pyramid Pattern Matrix Crack from impact.

Medium-Energy Impact

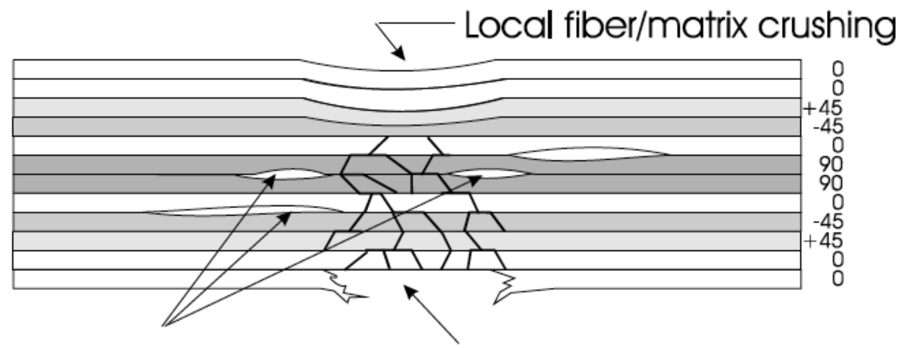

High-Energy Impact

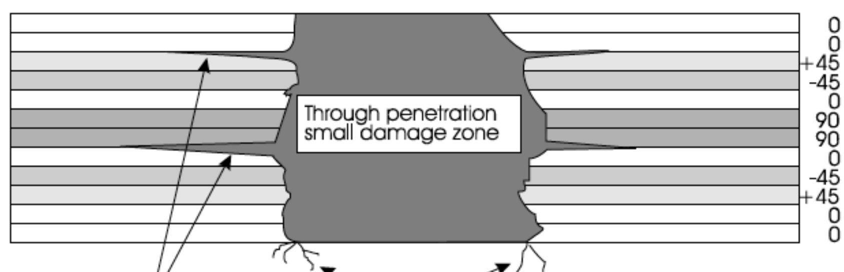

Abaris Training Resources Incorporated

Modeling Impact Damage

Impact rig for the large-scale plate tests

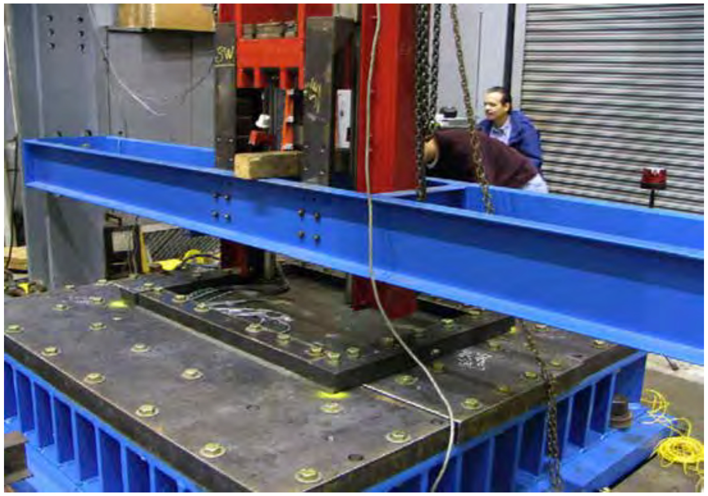

Damage predictions for test

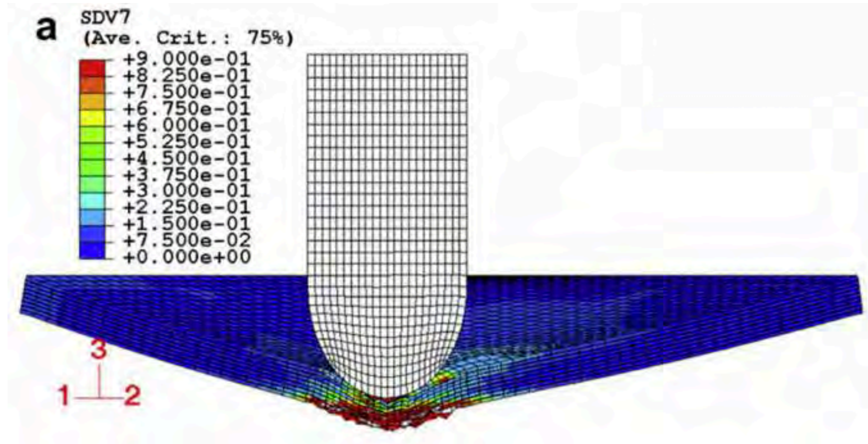

Damage viewed from top (left) and bottom (right)

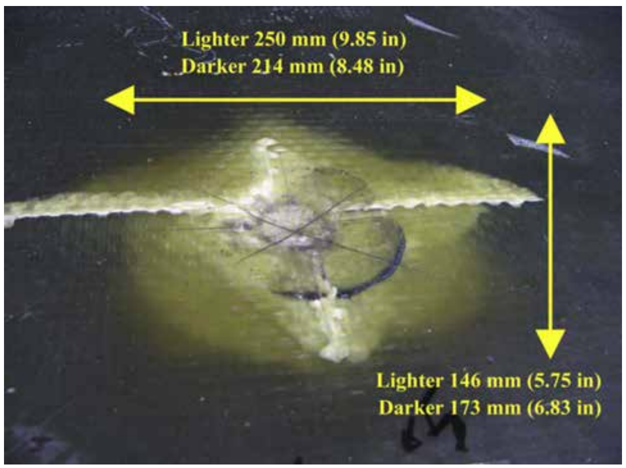

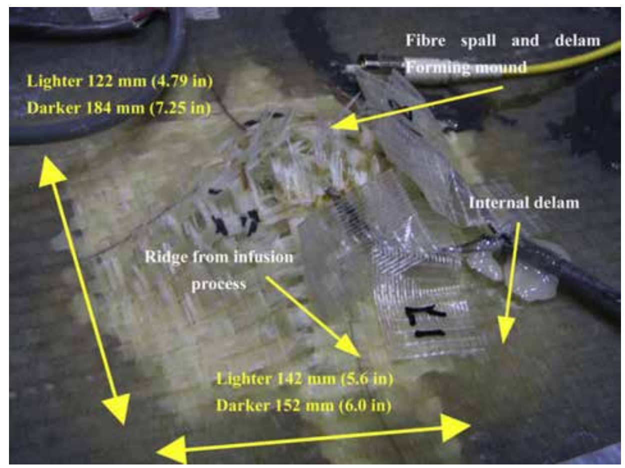

H.E. Johnson, L.A. Louca, S. Mouring, A.S. Fallah, “Modelling impact damage in marine composite panels,” International Journal of Impact Engineering 36 (2009) 25–39

Free-Fall Lifeboats

Schat-Harding freefall lifeboat

55 meter freefall test

Norsafe lifeboat structural grid

Skin-to-Core Bond Influence on Core Impact Damage

Schematic diagram of the instrumented impact test (left) and "high-density" sample following impact 39.3 J (right)

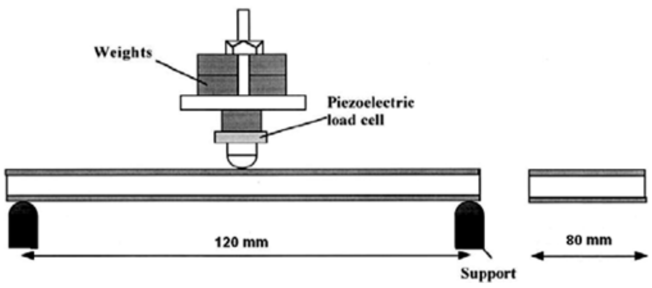

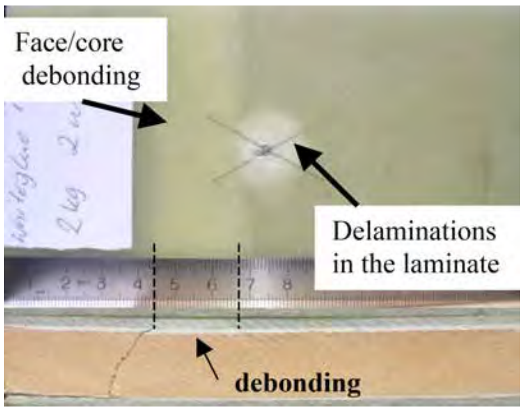

Impact damage area as a function of impact energy for sandwich structures: visual inspection and C-scan results

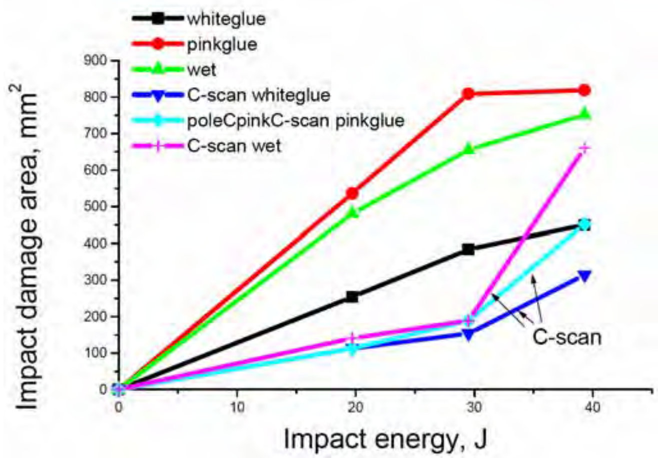

Illustration of damage observed visually on the surface of the samples subjected to impact 19,7J: (a) whiteglue", (b) "pinkglue", (c) "wet" sample.

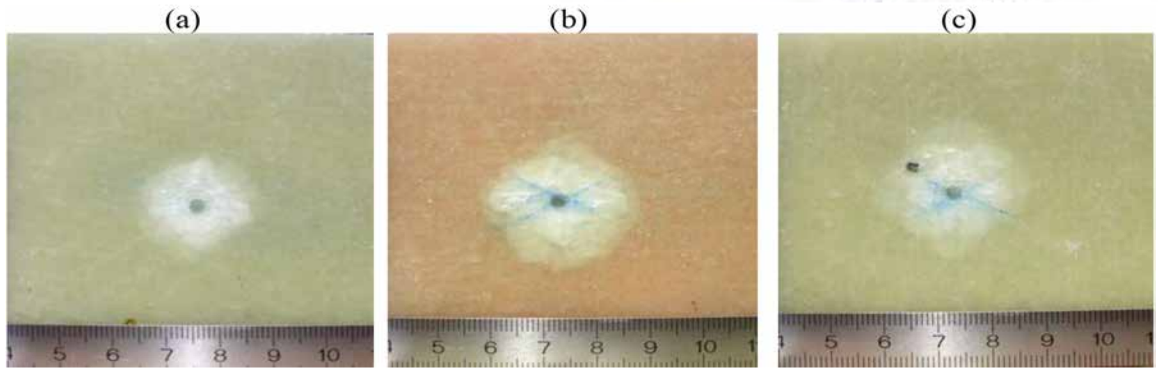

In terms of impact damage size, in each case the size of C-scan damage area was significantly smaller than in visual inspection of the sample.

K. Imielińskaa, L. Guillaumatb, R. Wojtyrac, and M. Castaingsd, "Effects of manufacturing and face/core bonding on impact damage in glass/polyester–PVC foam core sandwich panels," *Composites Part B: Engineering*, September 2008

Servo-hydraulic Slam Testing System (SSTS)

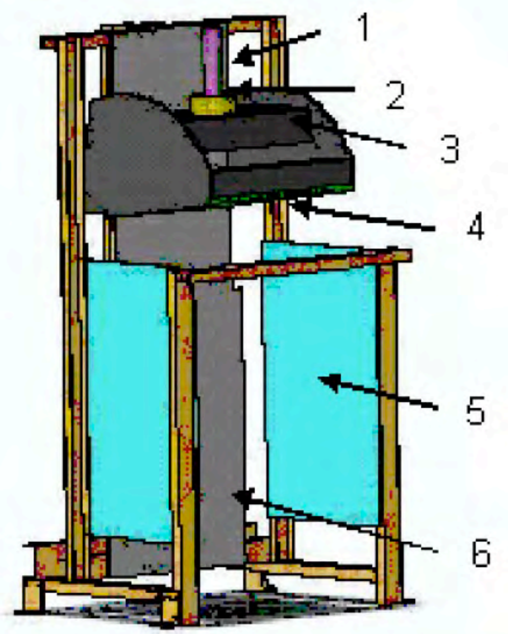

Elements of the Servo-hydraulic Slam Testing System (SSTS) including Ram (1), Load Cell (2), Specimen Fixture (3), Test Panel (4), Side Plates (5), and Back Plate (6). Top left is Overall Equipment Setup with Computer Control and bottom Sequence is of Slam Test Event [Mark Battley, University of Auckland & Susan Lake, High Modulus]

Slam Testing Results

time [m/s]	load1 [KN]	acc1 [m/s2]	Panel Disp [mm]	velocity [m/s]	velocity [mm/s]	strain0 [microstrain]	strain1 [microstrain]	strain2 [microstrain]	acc dec	320 -22.9
min/max	min/max	min/max	min/max	min/max	min/max	min/max	min/max	min/max	scan rate	10000
0	-10.6	-534	-17.45	-0.6	-569	-80	-30	-29	panel depth	410
1000	41.5	516	9.14	4.2	4167	610	2572	821	end phase 2	826.1

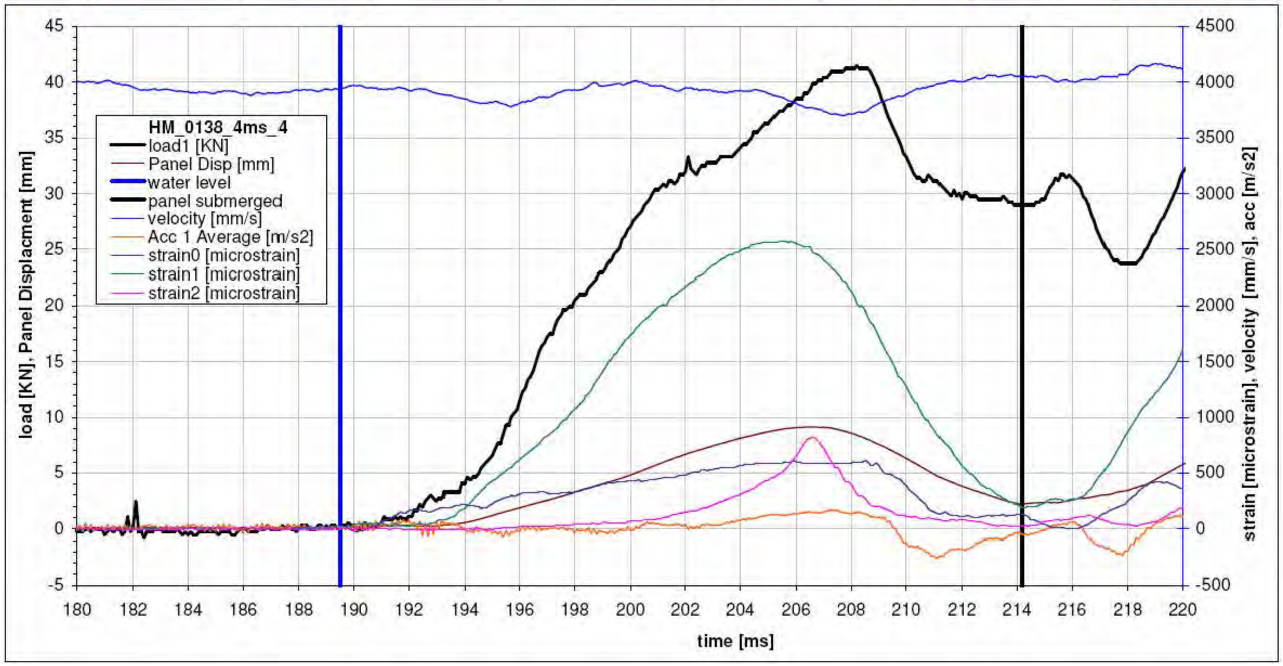

Typical Results from Slam Testing in the SSTS [High Modulus]

Servo-hydraulic Slam Testing System (SSTS)

Shear fracture of C70.130 core beam specimen

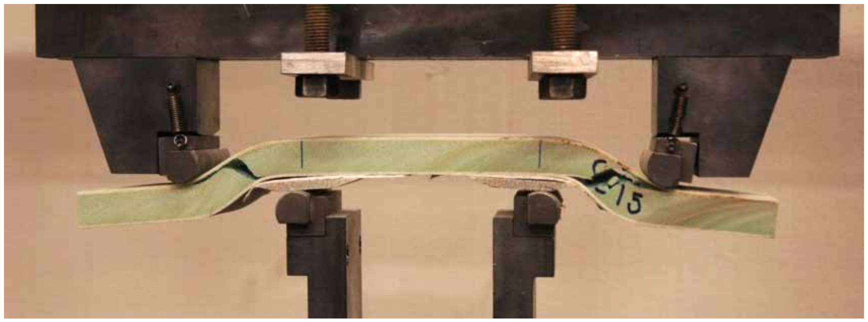

Shear deformation of R63.140 core beam specimen

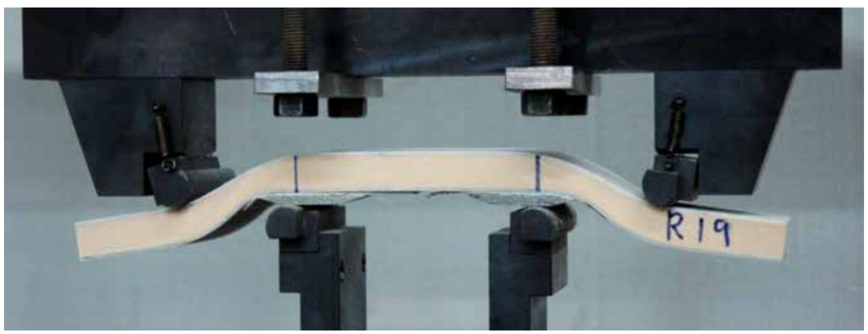

Mark Battley, Ivan Stenius, Johan Breder and Susan Edinger, “Dynamic Characterisation of Marine Sandwich Structures,” 7th International Conference on Sandwich Structures, Aalborg, Denmark, August 2005

Deflection vs. panel center strain

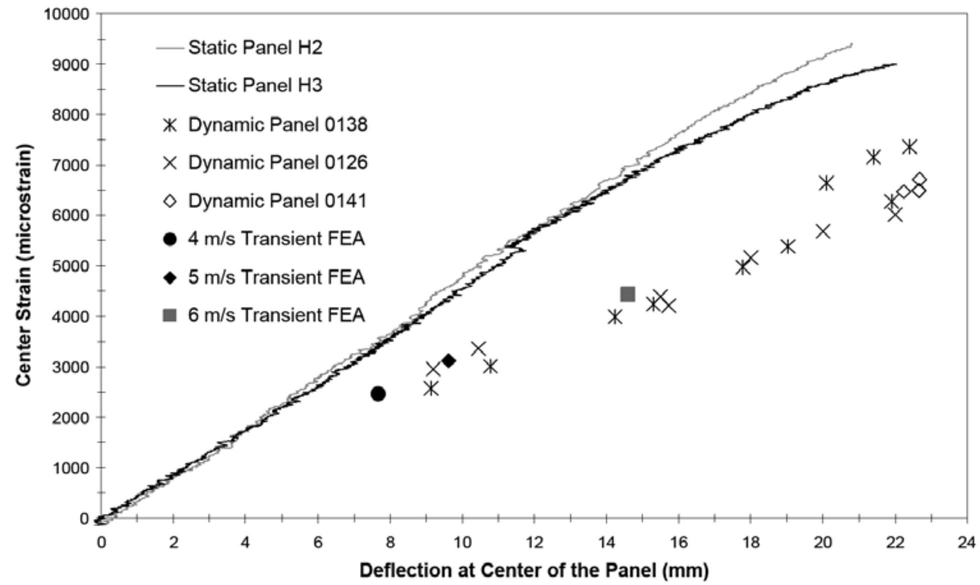

Deflection vs. panel edge strain

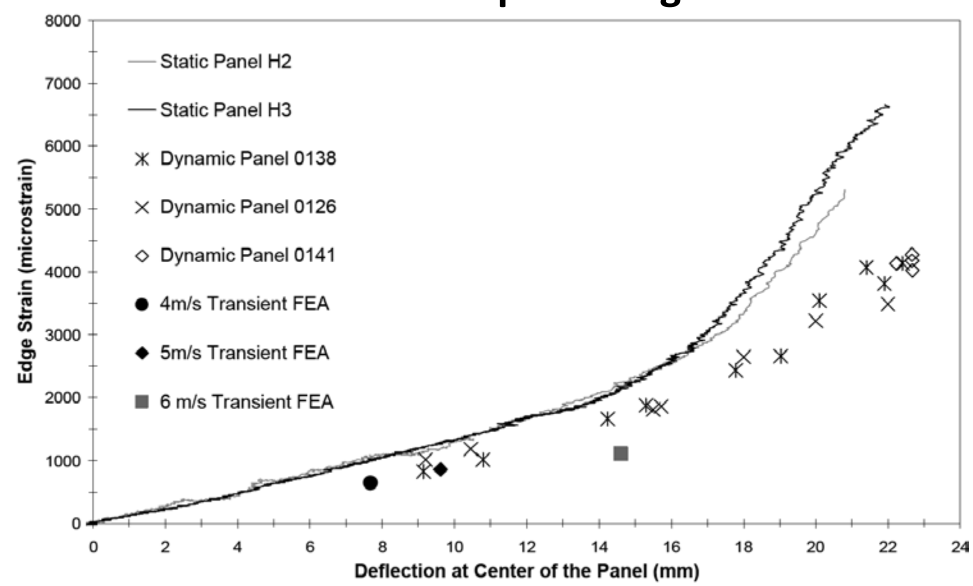

Servo-hydraulic Slam Testing System (SSTS)

Slam event of 10° panel at 4m/s with transient FEA predictions. The blue vertical line represents the water surface, and the black line full immersion of the panel

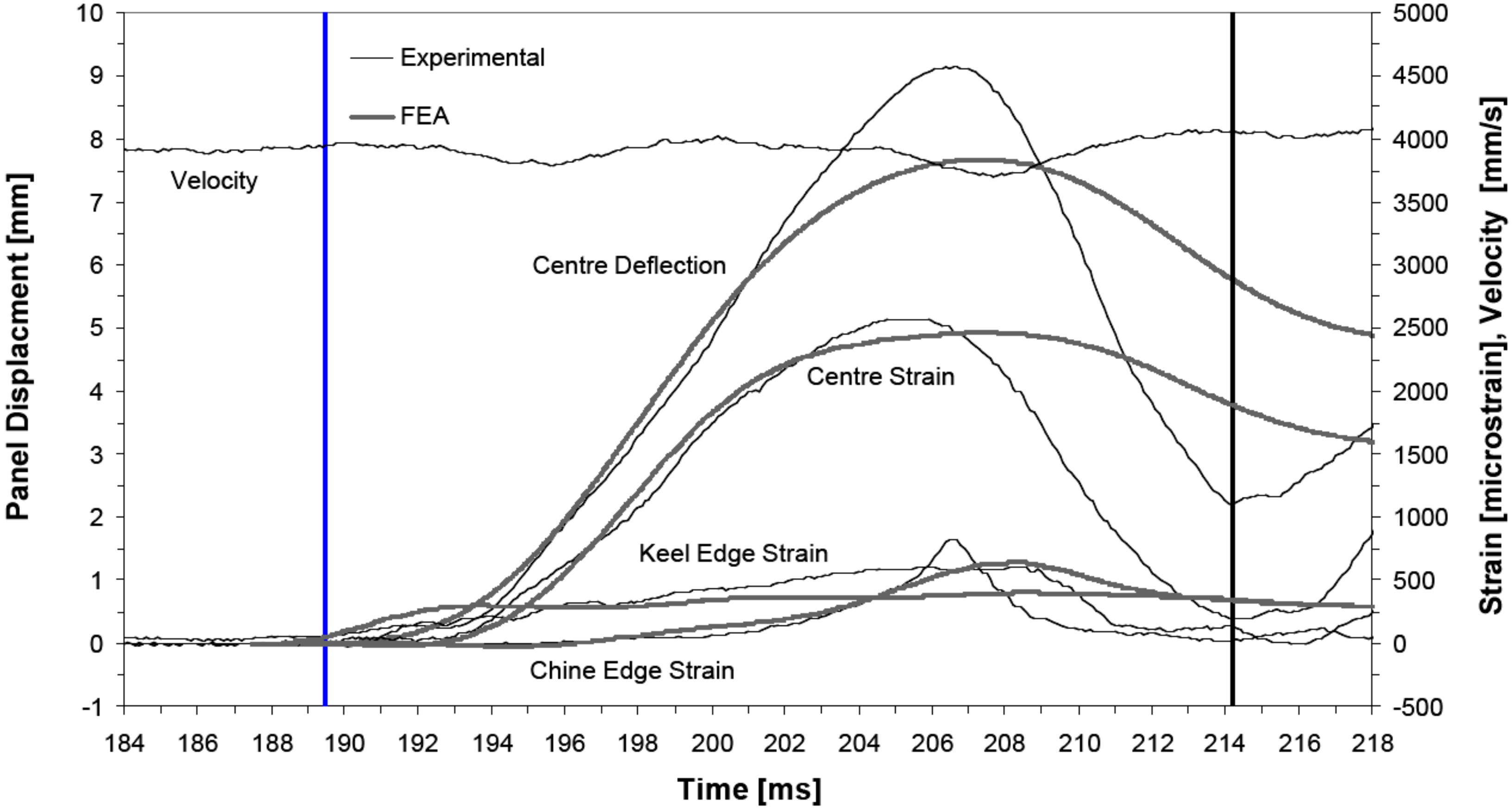

The dynamic panels have higher deflections relative to bending strains, confirming that the load distribution is not well represented by a uniformly distributed pressure. Under dynamic loading the transverse shear is more significant than bending compared to a uniformly loaded panel.

Mark Battley, Ivan Stenius, Johan Breder and Susan Edinger, "Dynamic Characterisation of Marine Sandwich Structures," 7th International Conference on Sandwich Structures, Aalborg, Denmark, August 2005

Slam Testing Takeaway Concepts

- The testing method used for characterization of core materials can have a significant effect on the shear strength obtained.
- The peak ratio of edge strain to center strain increases with velocity of impact
- Slam-loaded panels are subjected to higher shear loads relative to bending than is the case for uniform pressure-loaded panels.
- There are significant performance advantages for high-elongation foam cores in slam loaded hull panels (few scantling codes distinguish between rigid, low elongation cores; medium elongation foams; and high elongation linear cores).
- A Slam Tester larger than the SSTS is required to break panels of interest to the marine industry.

Design for Slamming
Safe Haven Marine's Interceptor 42




Photographs showing Pilot Boat operating conditions, including storm with 100-knot wind gust and 10 m waves [www.safehavenmarine.com]

The hulls scantlings are very closely spaced @ 500mm centers giving a 4300mm panel width, the frames themselves are a huge 150 x 150mm resulting in a massively strong structure

Hull Bottom Laminate

Isophthalic gel coat to minimum 10mm (300 & 2 x 900gm/m^2 layers) (white pigment used below water line to prevent osmosis)

300gm/m^2 using isophthalic resin. Composite as follows-

900gm/m^2 CSM. isophthalic resin

900gm/m^2 CSM. isophthalic resin

300gm/m^2 CSM stitched in combination to

600gm/m^2 Woven Roving

900gm/m^2 CSM

300gm/m^2 CSM stitched in combination to

600gm/m^2 Woven Roving

900gm/m^2 CSM

300gm/m^2 CSM stitched in combination to

600gm/m^2 Woven Roving

900gm/m^2 CSM

Operator Tolerance

Acceleration limits for operator fatigue and injury

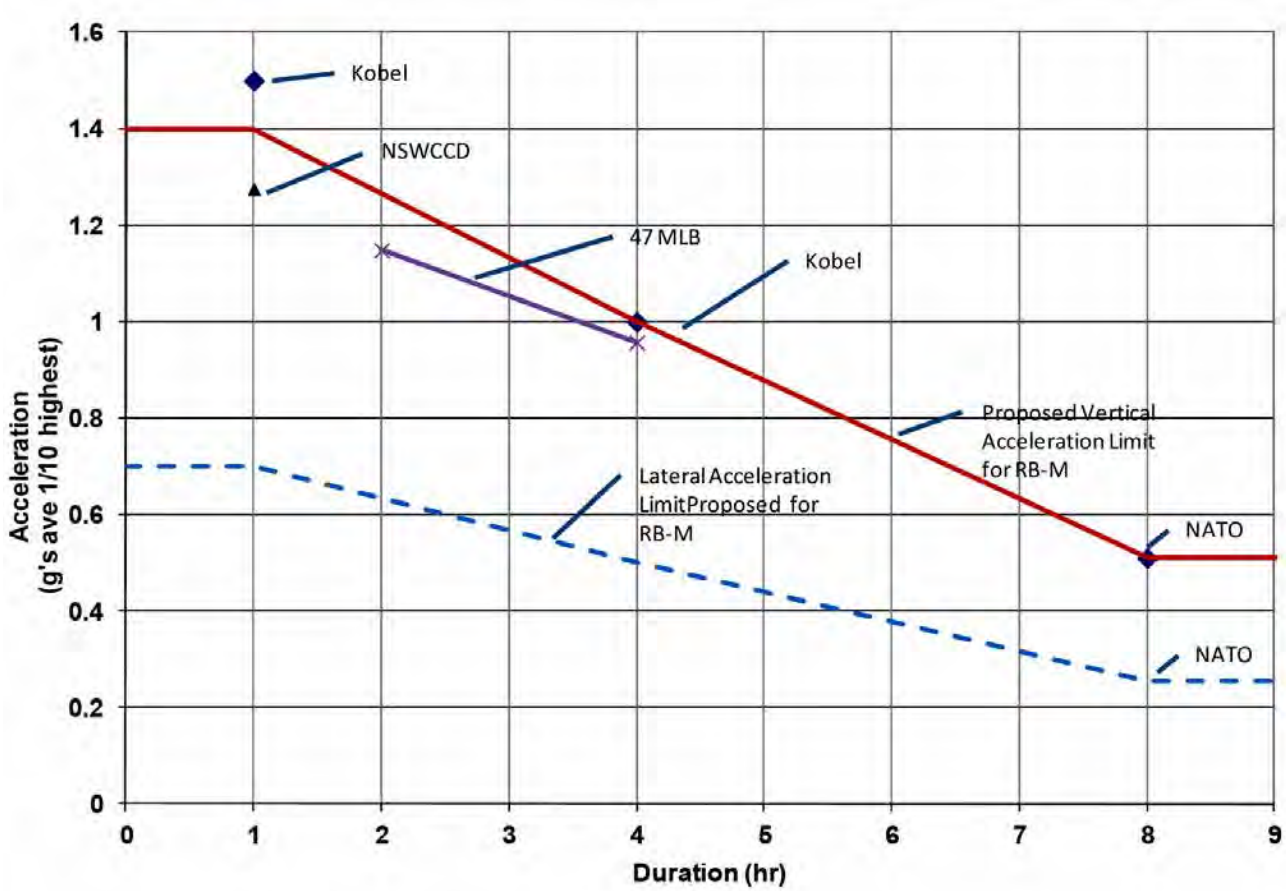

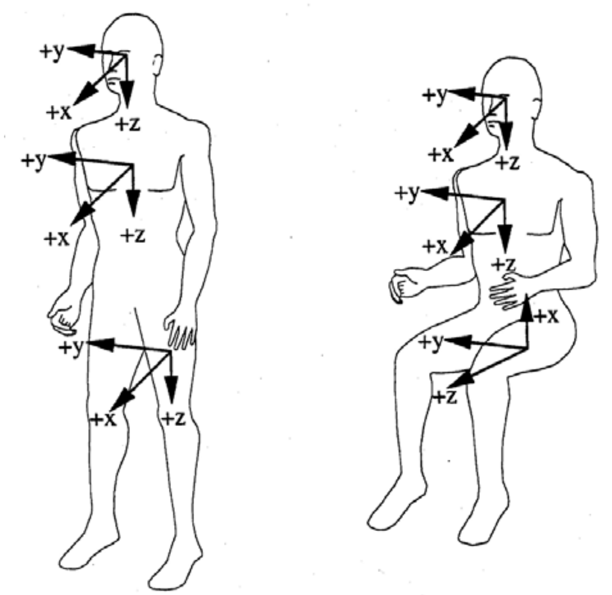

Frank DeBord, Karl Stambaugh, Chris Barry and Eric Schmid, "Evaluation of High-Speed Craft Designs for Operations in Survival Conditions," 3rd Chesapeake Bay Powerboat Symposium, June, 2012.

Hydro-Structural Shock Mitigation

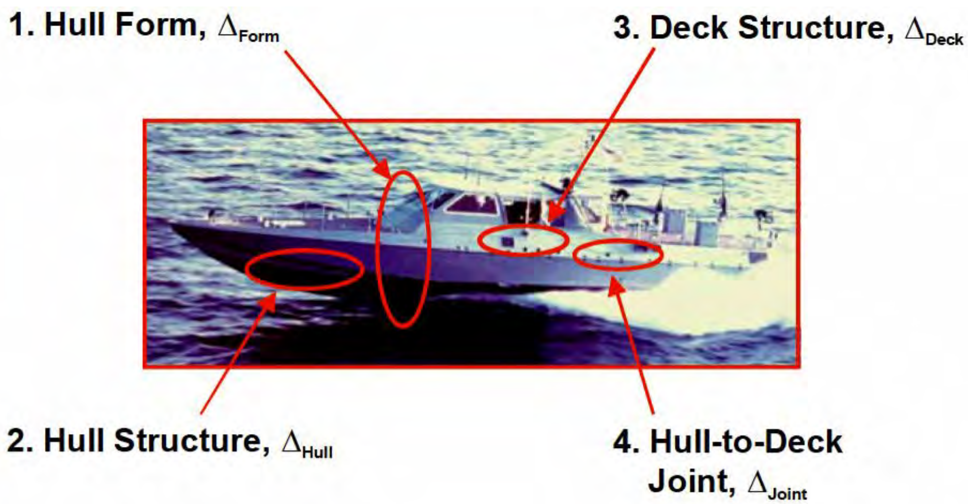

Total Ride Improvement = $\Delta_{Form} + \Delta_{Hull} + \Delta_{Deck} + \Delta_{Joint}$

Hull Structure Improvement Methodology

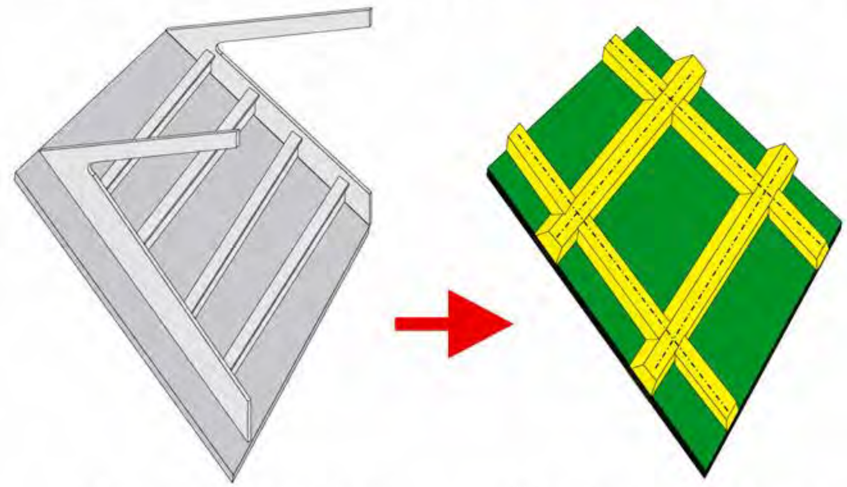

Transverse-Framed Aluminum Grillage

Solid Composite Laminate with Low Profile Stiffeners

Deck Structure Improvement Methodology

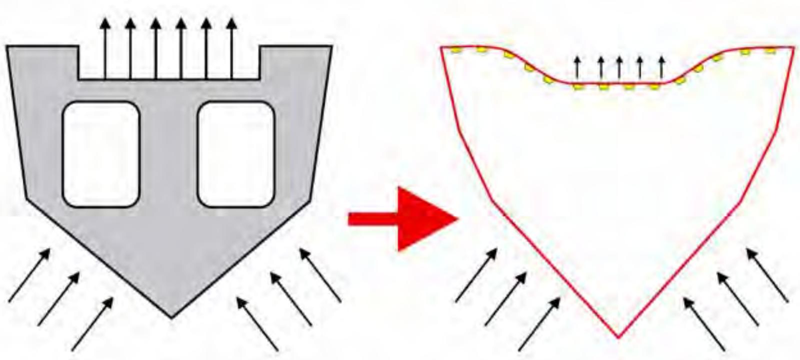

Transverse Framing that Creates Hull & Deck Coupling

Longitudinally Stiffened Deck will Minimize Shock Transmission

Hull-to-Deck Joint Improvement Methodology

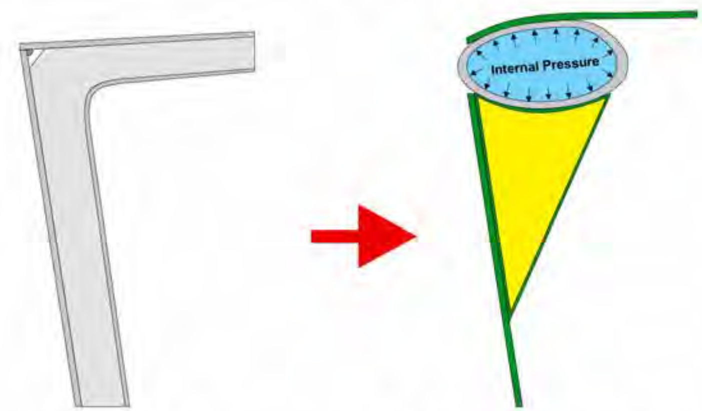

Transverse Knees at Deck Joint

Compliant Deck Joint Utilizing Tube with Variable Internal Pressure

RHIB Shock Mitigation

SBIR Program Objectives

- Low Section Framing
- Membrane Structure
- Suspended Cockpit Design
- SharkSkin^{tm} Coatings
- Air Support
- VARTM/Infusion Manufacturing

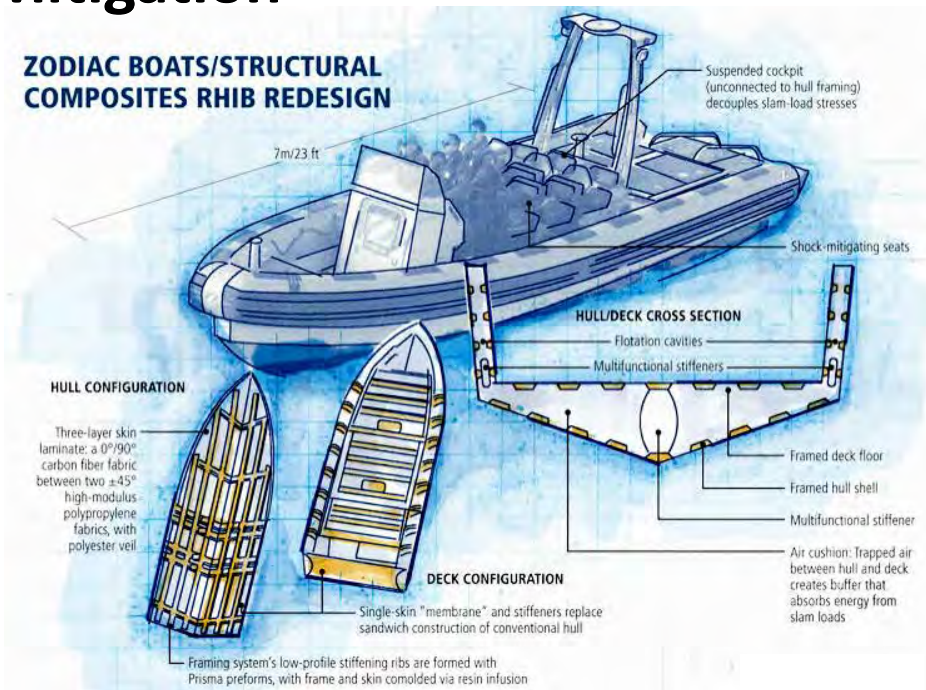

Karl Reque, *Composites World*

Helm Deck (green) and Hull (red) acceleration data seems to indicate peak g values are reduced by over 50% between the hull and the deck

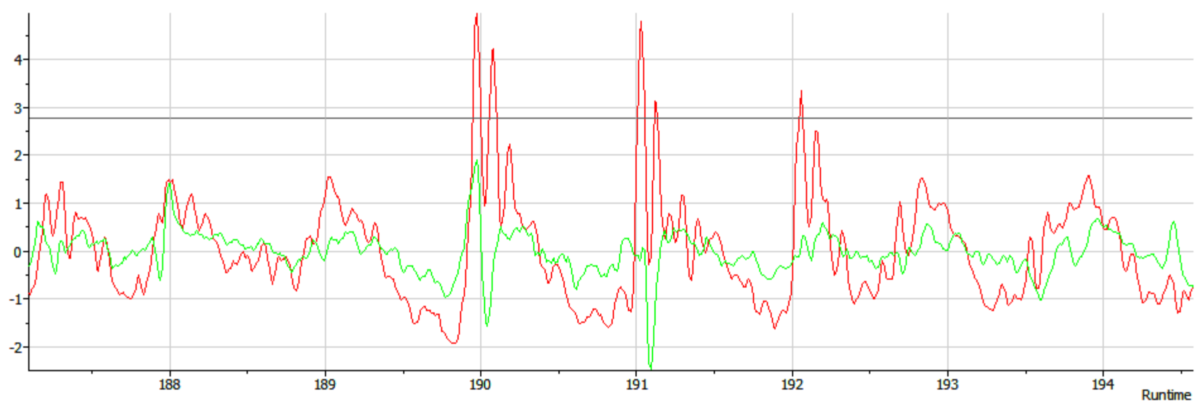

Scott Lewit, Structural Composites, Inc.

Impact Testing

ASTM D256 - Izod Impact Strength Testing of Plastics

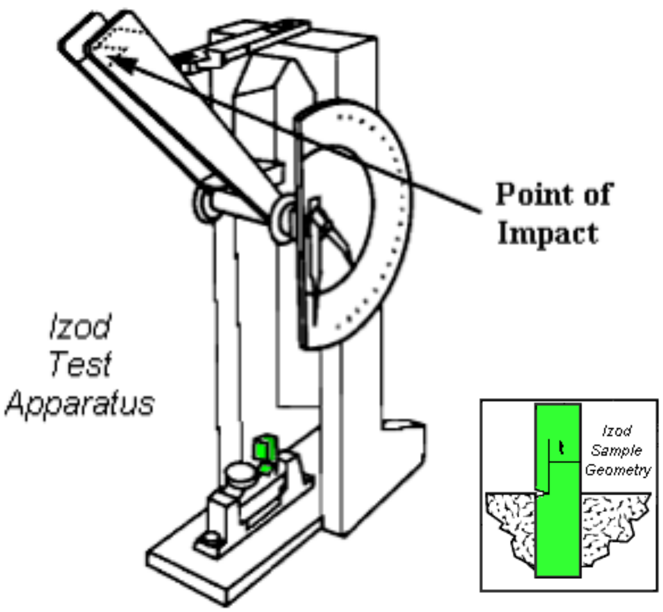

A pendulum swings on its track and strikes a notched, cantilevered plastic sample. The energy lost (required to break the sample) as the pedulum continues on its path is measured from the distance of its follow through.

ASTM D5628 - Impact Resistance of Flat, Rigid Plastic Specimens by Means of a Falling Dart

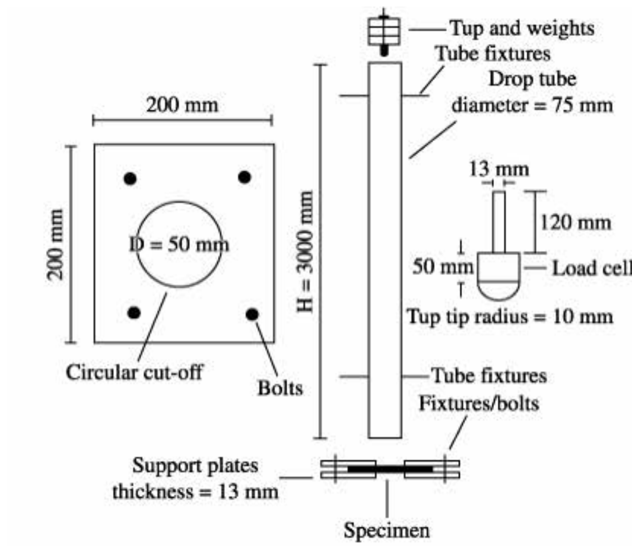

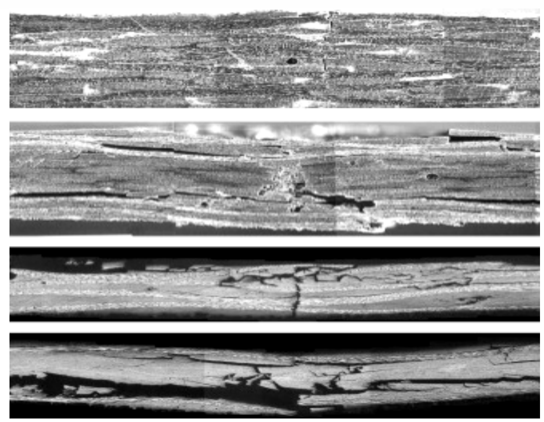

Impact Testing




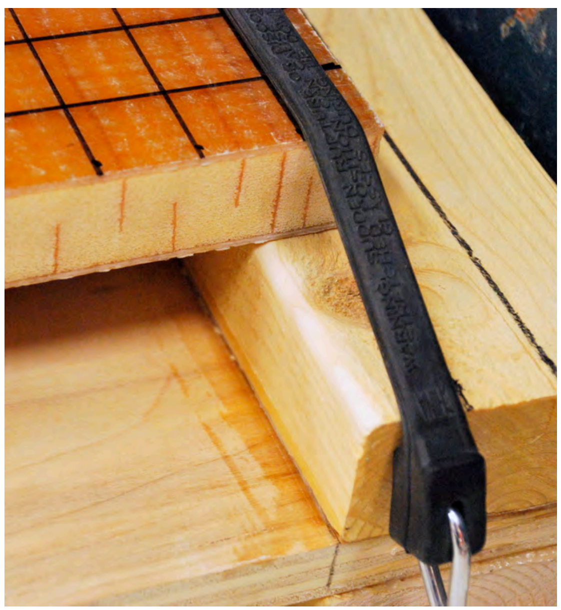
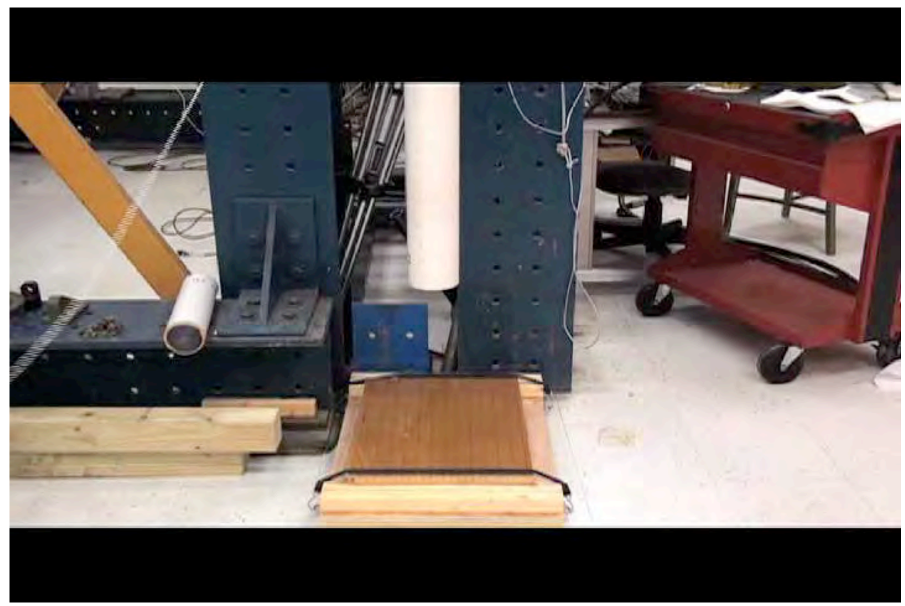

eric greene associates

Foreign Object Impact

Types of Boating Accidents

	Vessels Involved	Fatalities
TOTALS	**8,591**	**865**
Grounding	390	14
Capsizing	545	289
Swamping/Flooding	252	60
Sinking	210	11
Fire/Explosion (fuel)	274	14
Fire/Explosion (other)	97	2
Collision with another vessel	**4,422**	**81**
Collision with fixed object	**864**	**76**
Collision with floating object	262	13
Falls overboard	451	239
Falls within boat	139	1
Struck by boat or propeller	191	7
Other	470	29
Unknown	24	29

U.S. Coast Guard Boating Safety Circular 72

The number of shipping containers lost overboard has been reported to be somewhere between 2,000 and 10,000 each year.

Tool Drop Impact Damage

Aircraft Impact Damage Tolerance Criteria

Threat	Criteria	Requirement
Small Tool Drop	48 in-lbs normal to surface.	No visible damage No non-visible damage growth for 3 design service objectives (DSOs) Accounted for in Ultimate Design Allowables
Large Tool Drop (BVID)-general acreage	Up to 1200 in-lbs or a defined dent depth cut-off (considering relaxation) based on level of visibility as related to the inspection method.	Barely visible damage which may not be found during HMV No damage growth for 3 DSOs with life extension (LEF) Capable of Ultimate strength
Large Tool Drop (BVID)-repeat impact threat areas	Consider higher than 1200 in-lbs Consider multiple, superimposed impacts Consider clustered impacts	Barely visible damage which may not be found during HMV No damage growth for 3 DSOs with LEF Capable of Ultimate strength
Visible Impact Damage No energy cut-off (VID)	No energy cut-off	Visible Damage with a high probability to be found during HMV No damage growth for 2 times the planned inspection interval with LEF Capable of residual Limit strength

Barely Visible Impact Damage (BVID)

Small damages which may not be found during heavy maintenance general visual inspections using typical lighting conditions from a distance of five (5) feet

- Typical dent depth – 0.01 to 0.02 inches (OML)
- Dent depth relaxation must be accounted for

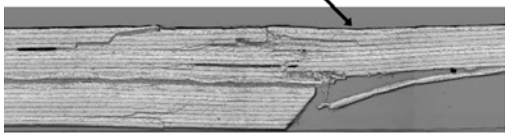

Allen J. Fawcett and Gary D. Oakes, "Boeing Composite Airframe Damage Tolerance and Service Experience," July, 2006.

Ballistic Impact

Back face view of panels impacted with .30 caliber projectiles at approximately 880 m/s

E-glass / Balsa vinyl ester

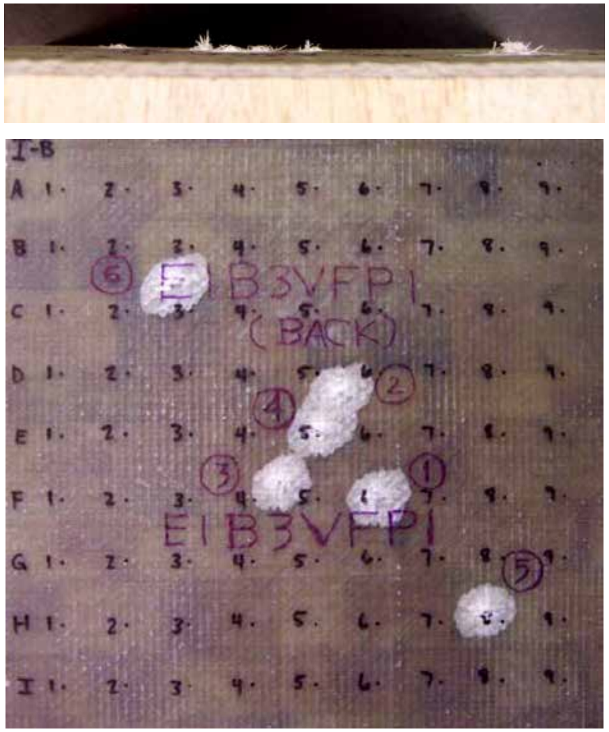

E-glass / PVC vinyl ester

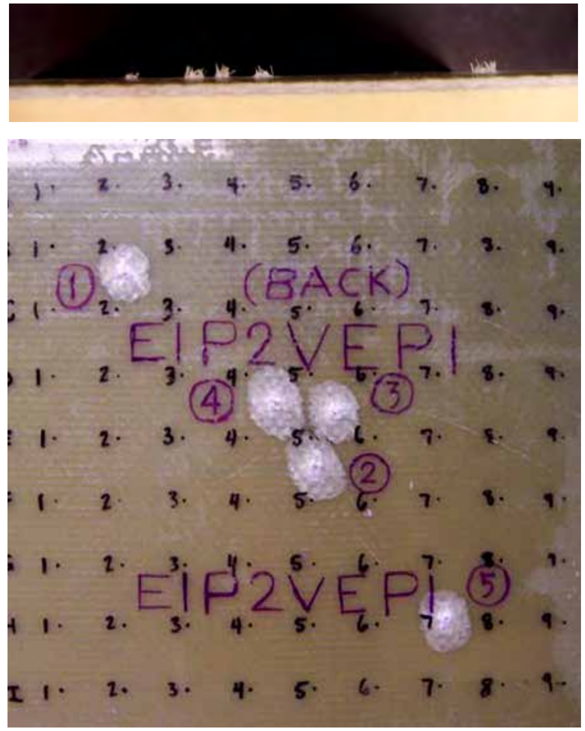

E-glass/Tycor vinyl ester

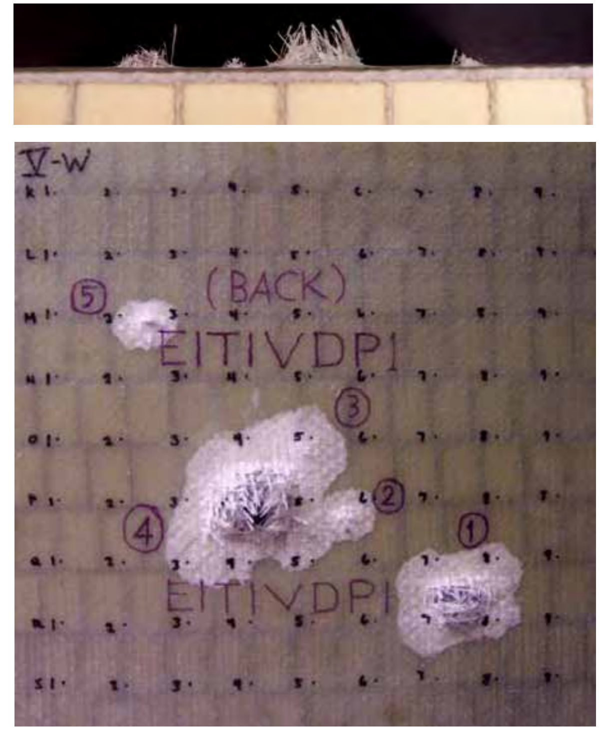

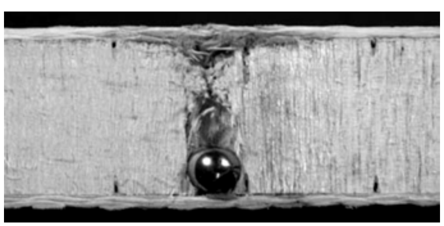

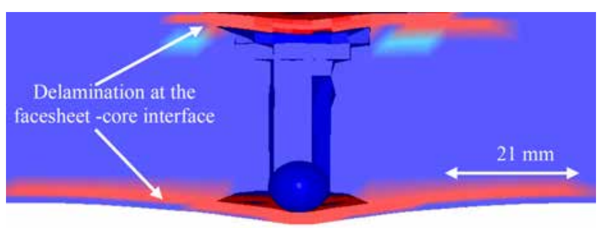

Energy absorbed by the Tycor® core when impacted at the web intersection was 575% higher than that for balsa and PVC cores. The damage in balsa and PVC core was minimal, indicating lower energy absorption capacity.

U.K.Vaidya, S.Pillay, M.Magrini and P.R.Mantena, "Ballistic Impact Testing of Balsa, PVC Foam, Glass Reinforced Polyurethane Core Sandwich Structures," July, 2009.

Theme Park Boats

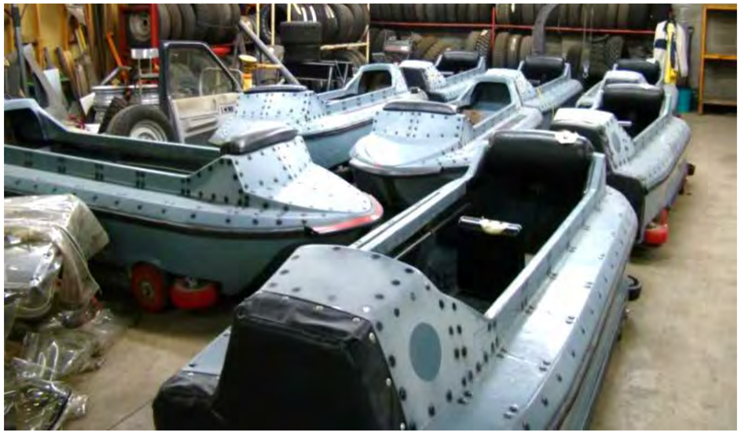






Surface Temperature

Anticipated Surface Temperature as a Function of Color and Ambient Temperature

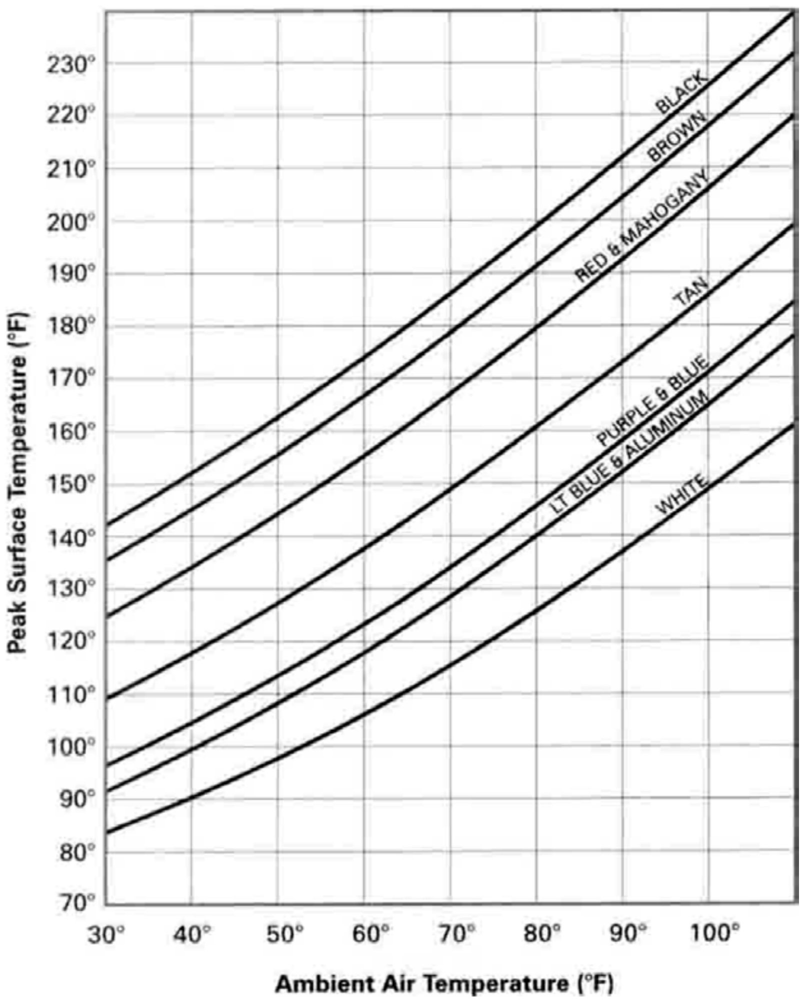

Surface temperature of curing laminate after 4 hours

Color and Surface Temperature

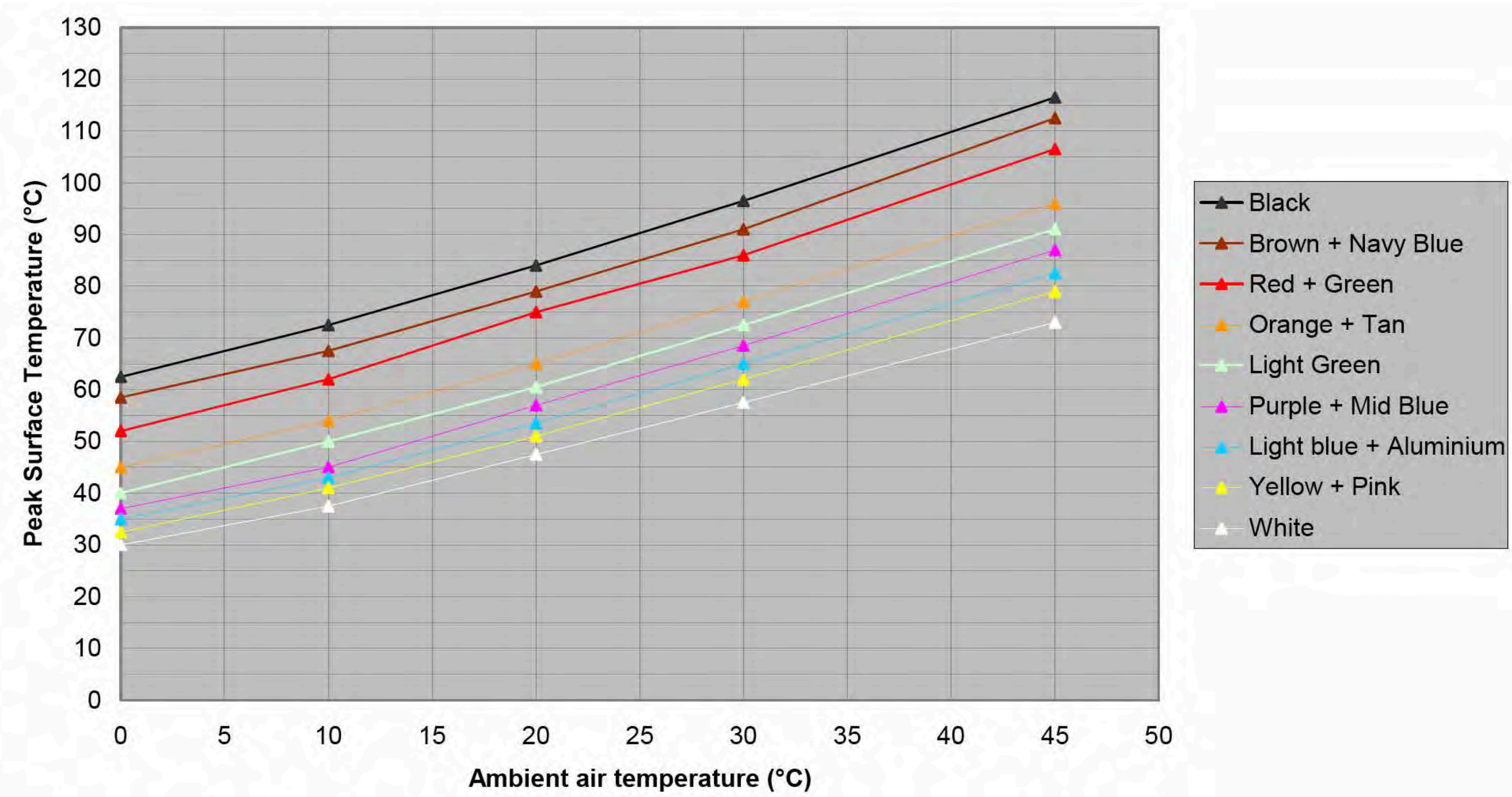

John Howard and Matt Searle, “Surface print on marine structures,” SP Systems, May 2005

Glass Transition Temperature, Tg

The glass transition temperature (Tg) of a non-crystalline material is the critical temperature at which the material changes its behavior from being 'glassy' to being 'rubbery'. 'Glassy' in this context means hard and brittle (and therefore relatively easy to break), while 'rubbery' means elastic and flexible.

Time-temperature-transformation cure diagram

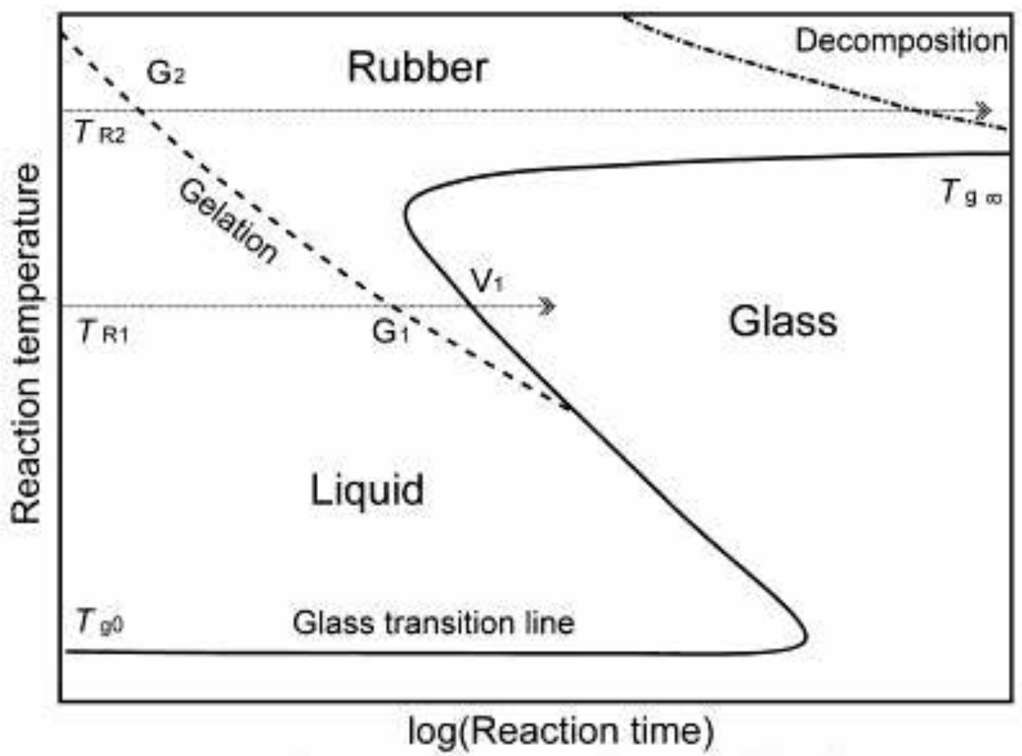

At a curing temperature T_{R2}, the gelation line (dashed line) is reached after a relatively short time, the material gels (gel point G_2) and is transformed to the rubbery state, and cross-linking continues until curing is complete. The curing temperature is thus always higher than the maximum possible glass transition temperature $T_{g\infty}$. Below T_{g0}, the resin is in the glassy state and the reaction is practically blocked.

Steve Sauerbrunn and Rudolf Riesen, "Thermosets: How to Avoid Incomplete Curing," www.americanlaboratory.com, Jan, 2010.

Resin Ultimate Tg and Shrinkage

If epoxy system 1 is exposed to temperatures just over 90°C a higher level of shrinkage will occur compared to epoxy system 2. This is because 90% of the cure as taken place, as cure has an exponential relationship less physical shrinkage will occur in the last 10% of cure.

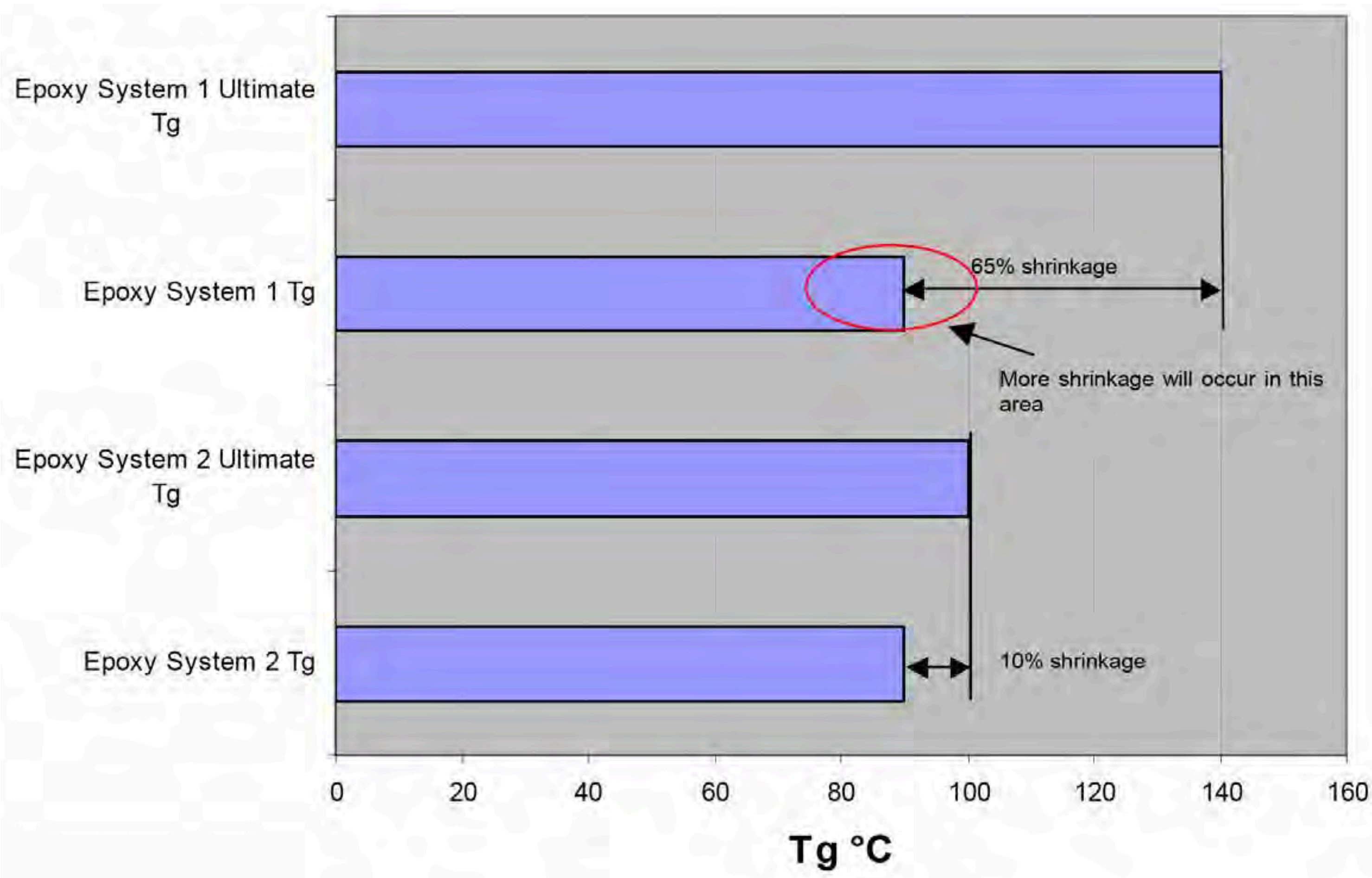

Epoxy system 1 has an ultimate Tg 140°C and epoxy system 2 has an ultimate Tg 100°C, both systems have been post cured to gain a Tg of 90°C.

John Howard and Matt Searle, "Surface print on marine structures," SP Systems, May 2005

Post Cure Print-Through

Typical reinforcement print-through problem when dark laminate "post cures"

Porous fillers can create surface defects

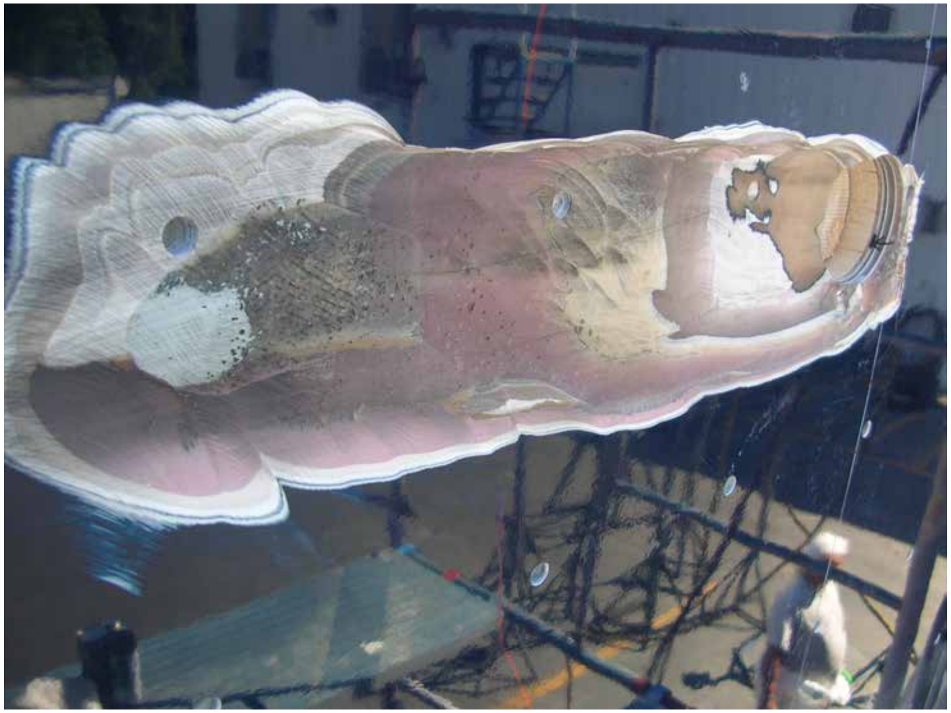

eric greene associates

Fiber Influences Print-Through

"Spread tow" is a new development in carbon fiber reinforcement whereby a sophisticated production process spreads out each tow (bundle) of carbon fibers making them significantly flatter and wider than they would be in a conventional woven fabric.

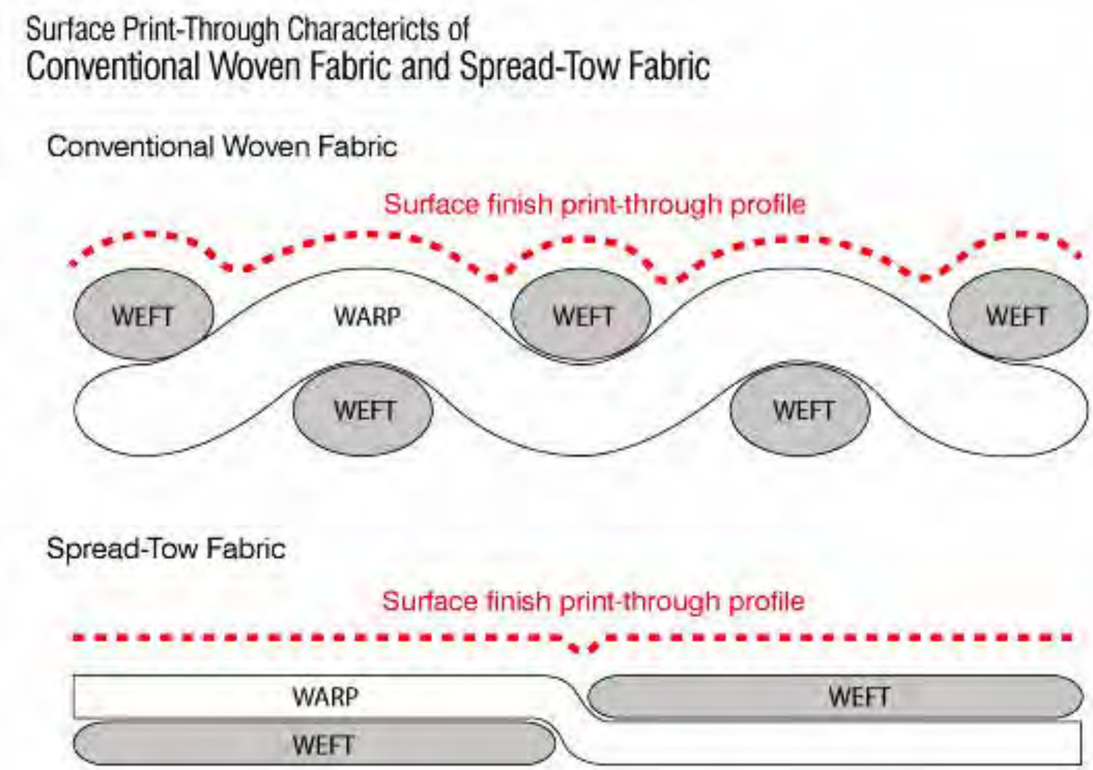

http://www.easycomposites.co.uk/products/carbon-fibre-cloth-fabric/carbon-fibre-spread-tow-20mm-very-large-pattern-plain-weave-SAMPLE.aspx

Quantifying Print-Through

Exaggerated 3D-views from the same surface area after different ageing steps. Corresponding Ra (roughness average) and Wa (waviness average) values are displayed on the right. The size of the measured area was 130 by 130 mm.

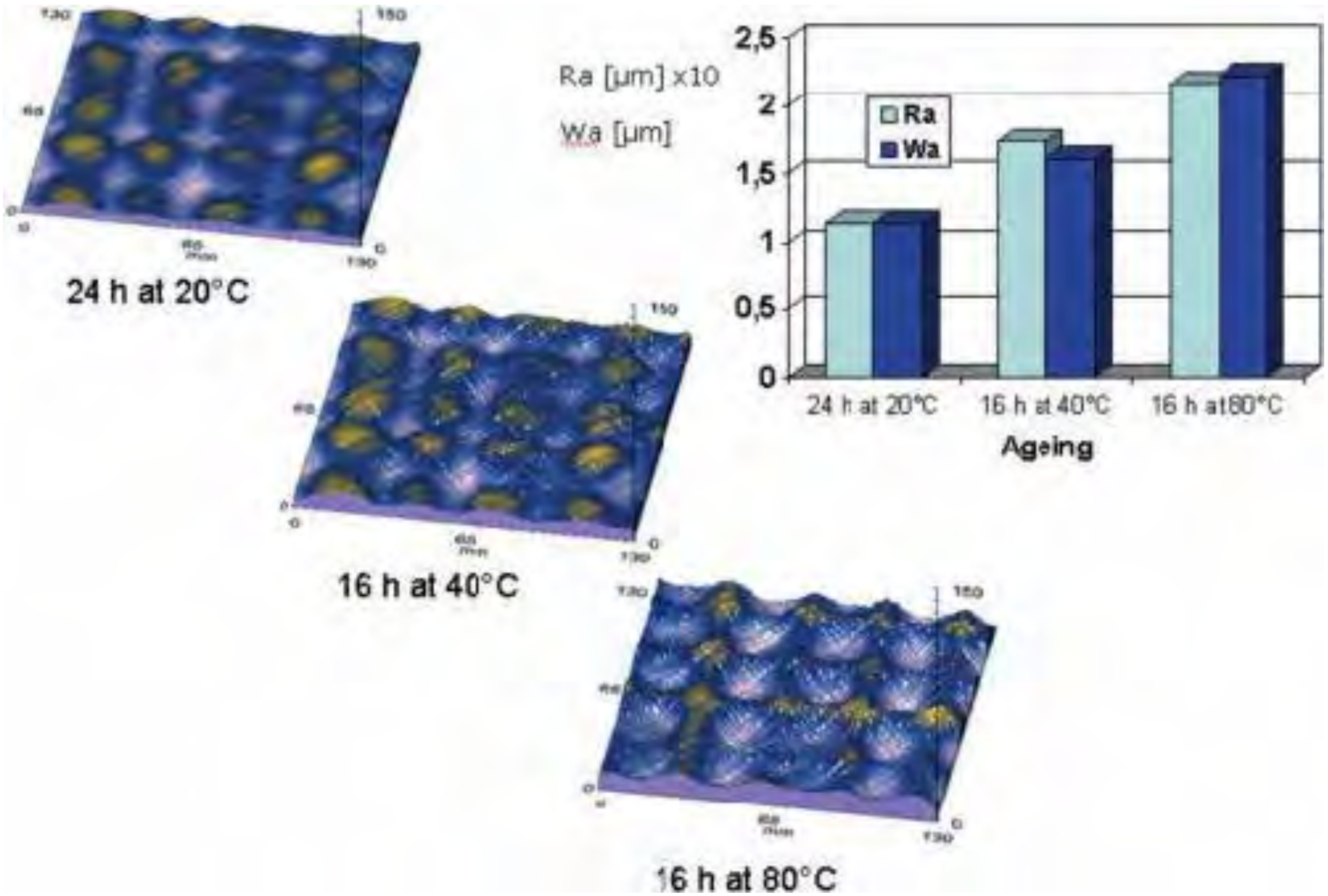

Rainer Bergström, Olli Piiroinen and Antti Ylhäinen, "Improving surface quality in vacuum infused parts," *Reinforced Plastics*, March 2008

Post Cure Print-Through Influence

Comparison between outdoor and test chamber ageing. Two different laminates showed similar change in Ra-value with both ageing methods.

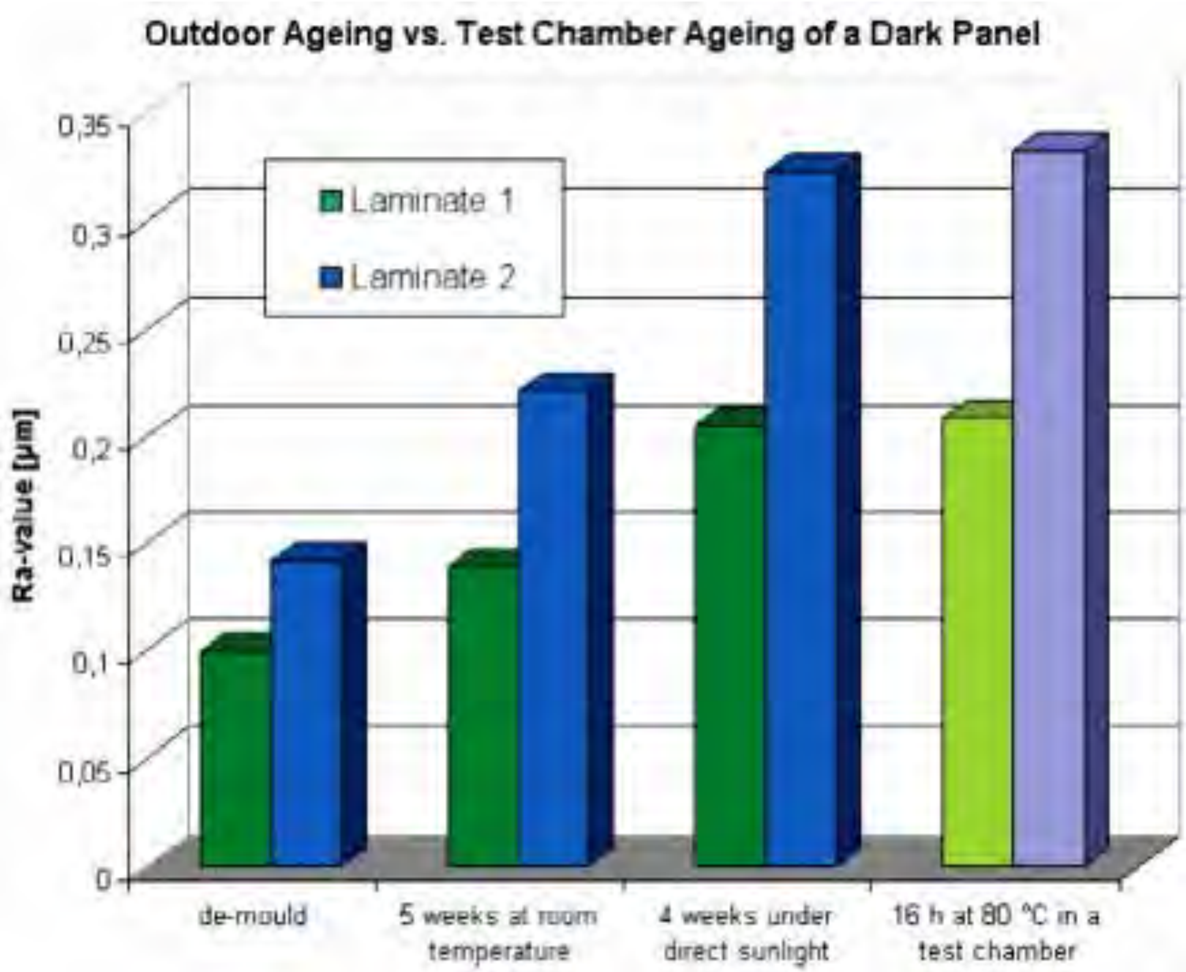

Rainer Bergström, Olli Piiroinen and Antti Ylhäinen, "Improving surface quality in vacuum infused parts," *Reinforced Plastics*, March 2008

Resin Print-Through Influence

Different resins showed different surface quality properties. Note, in resin comparison all laminates were made without using a surface improving layer (skin or barrier coat).

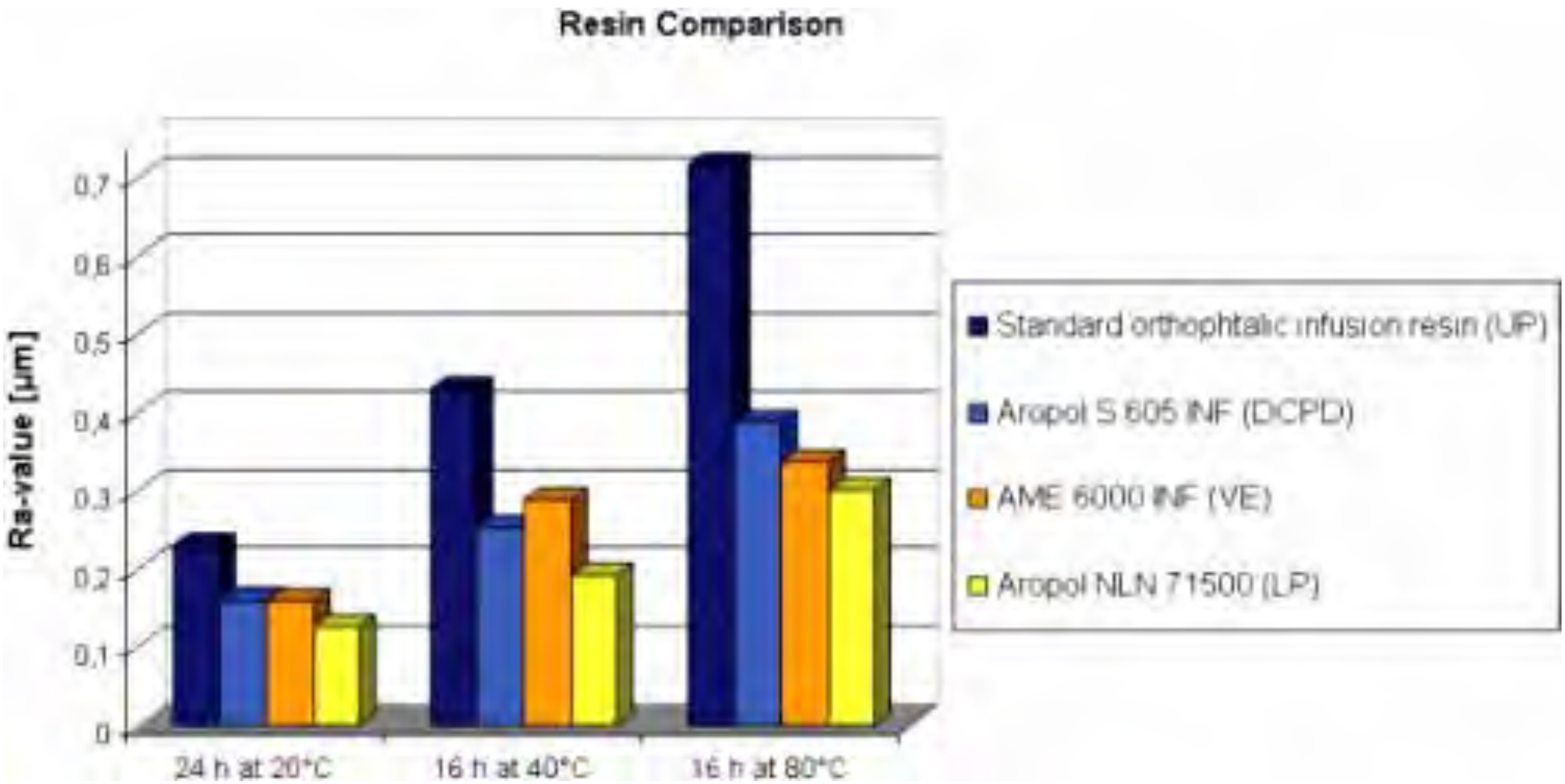

Rainer Bergström, Olli Piiroinen and Antti Ylhäinen, "Improving surface quality in vacuum infused parts," *Reinforced Plastics*, March 2008

Infusion and Print-Through

Influence of various reinforcement types and lamination methods on surface quality. Note that 2nd and 5th column consist of similar reinforcements.

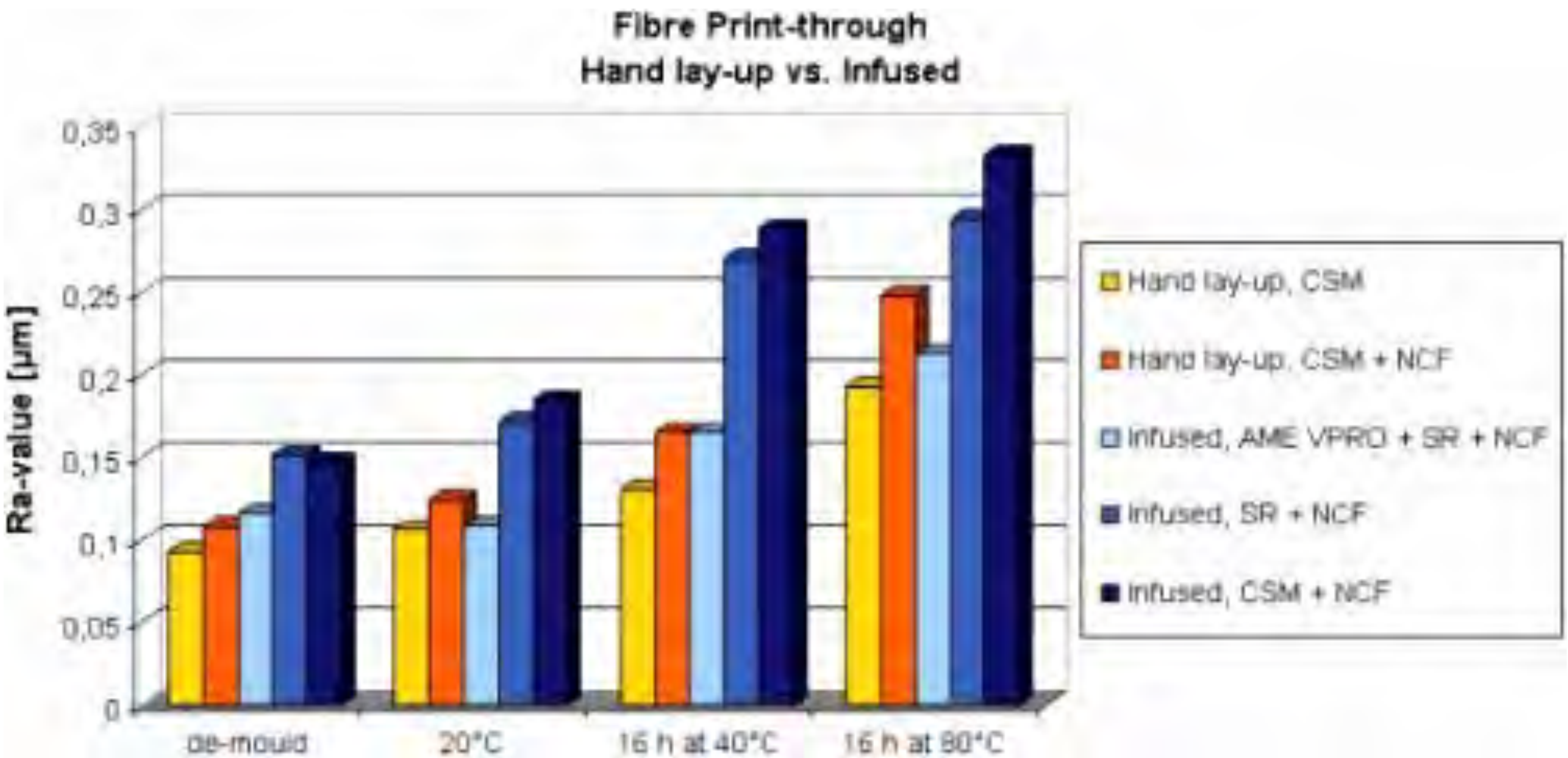

Rainer Bergström, Olli Piiroinen and Antti Ylhäinen, "Improving surface quality in vacuum infused parts," *Reinforced Plastics*, March 2008

Print-Through Barrier Layers

Both skin and barrier coats lowered the fiber print-through. The surface quality of AME VPRO barrier laminate was eventually close to a typical CSM hand laminate level.

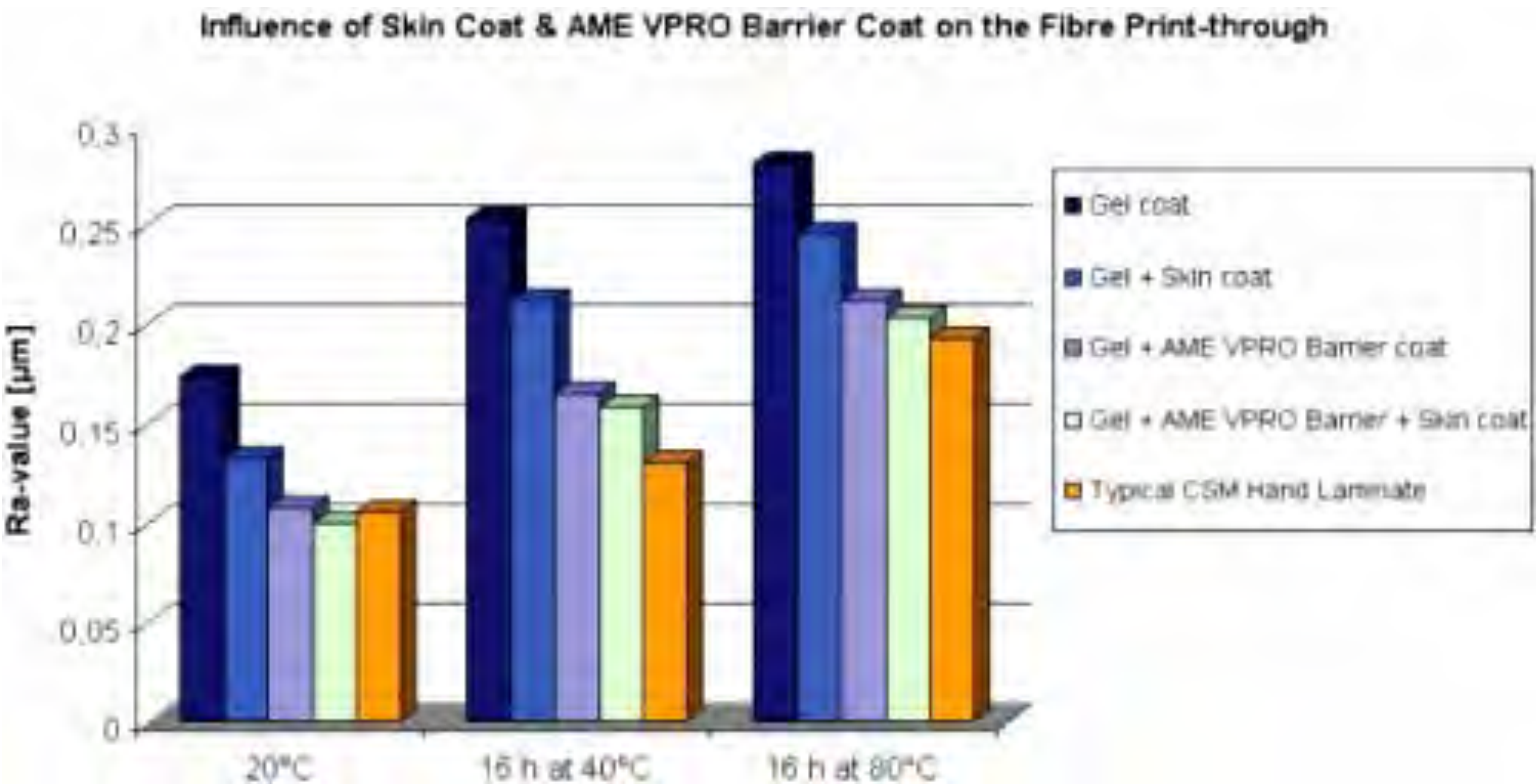

Rainer Bergström, Olli Piiroinen and Antti Ylhäinen, “Improving surface quality in vacuum infused parts,” *Reinforced Plastics*, March 2008

Typical Material Property Temperature Reduction Factors

Temperature	Infused E-Glass/ Vinylester	End Grain Balsa	Foam Cores	'H' Type Foam Cores	'HT' Type Foam Cores
23°C (74°F)	1.0	1.0	1.0	1.0	1.0
52°C (125°F)	0.85	1.0	0.9	0.70	0.90
63°C (145°F)	0.84	1.0	0.7	0.60	0.80
79°C (175°F)	0.72	1.0	0.5	0.40	0.70
88°C (190°F)	0.60	1.0	0.3	0.30	0.60

Moisture Effects

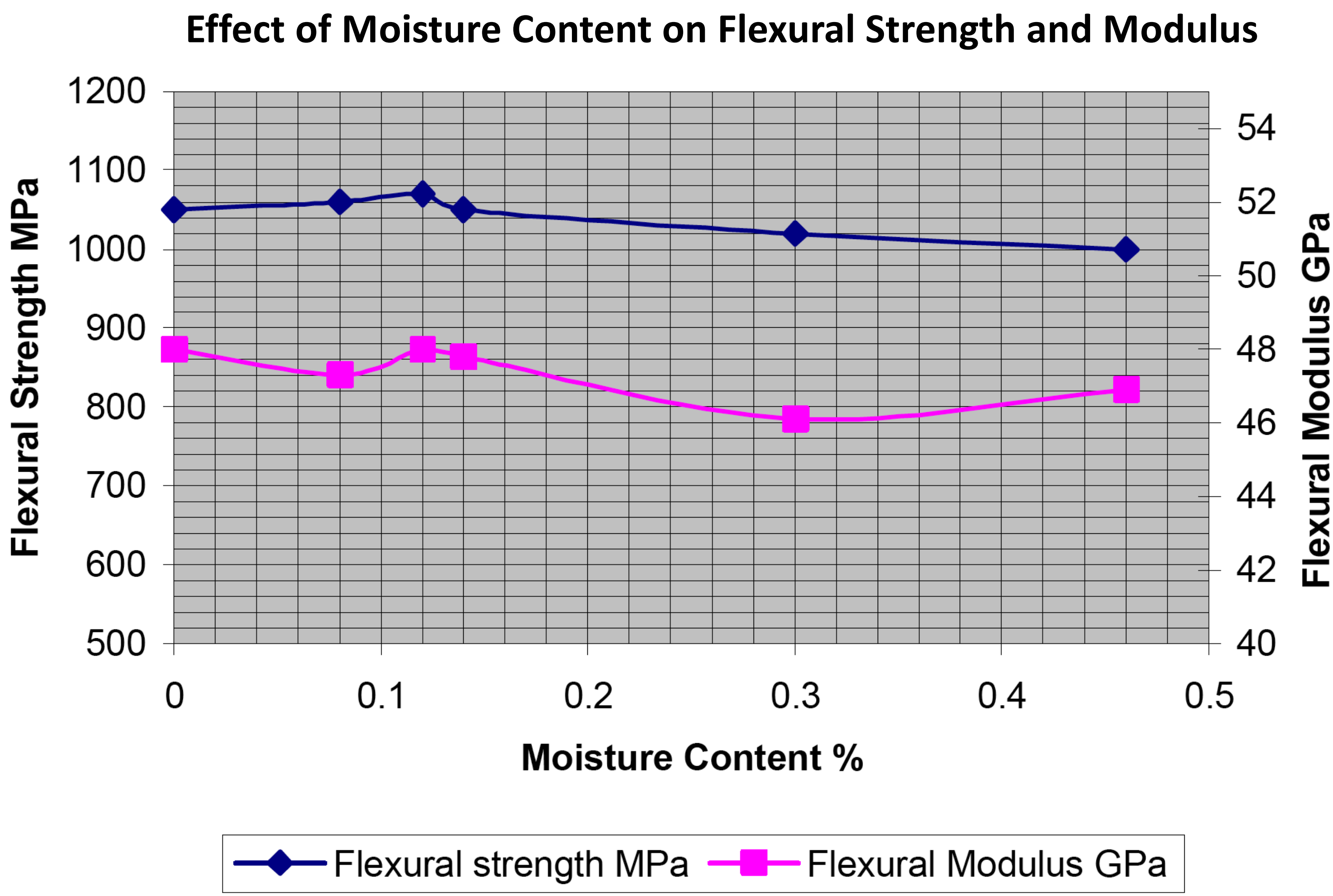

J. A. Quinn, "Composites – Design Manual," 3rd Edition, Liverpool, England, 2002.

Moisture Exclusion

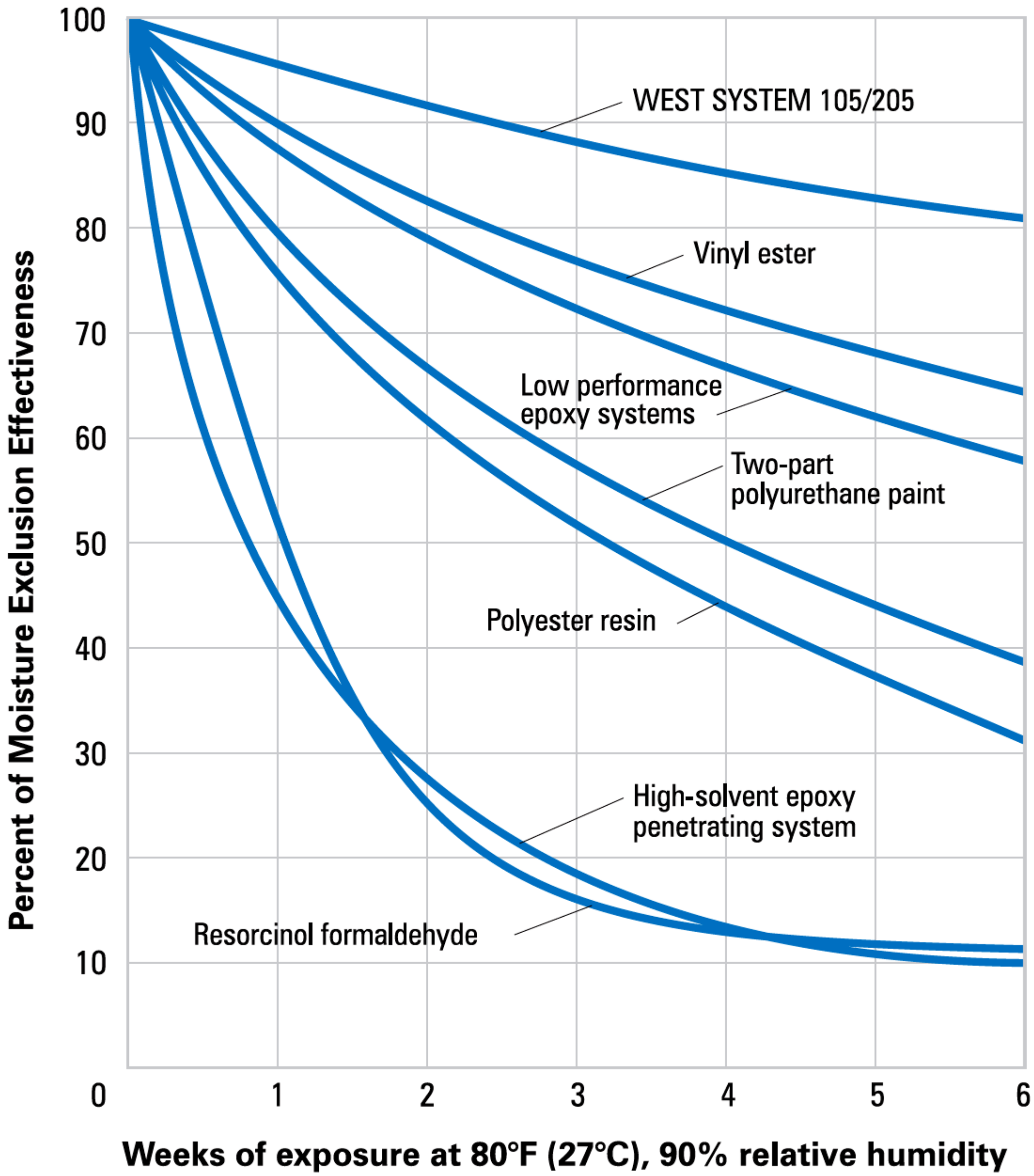

Moisture exclusion effectiveness (MEE) of various marine materials. Comparison of three coats of each material.

Gougeon Brothers, Inc., "The Problem of Gelcoat Blisters in Fiberglass Boats," 9th Edition, June 2007

Fickian Diffusion

$$\frac{\partial c}{\partial t} = D\frac{\partial^2 c}{\partial x^2} \text{ in one dimension.}$$

$$\frac{\partial c}{\partial t} = D\left(\frac{\partial^2 c}{\partial x^2} + \frac{\partial^2 c}{\partial y^2} + \frac{\partial^2 c}{\partial z^2}\right) \text{ in three dimensions.}$$

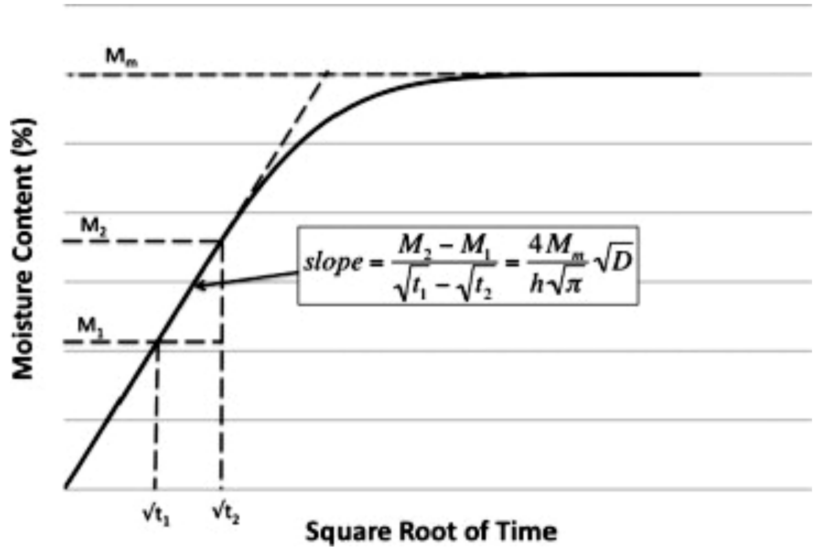

Five year sorption data for AS4/3501-6 and IM7/8551-7 coupons immersed in simulated seawater at 34 °C.

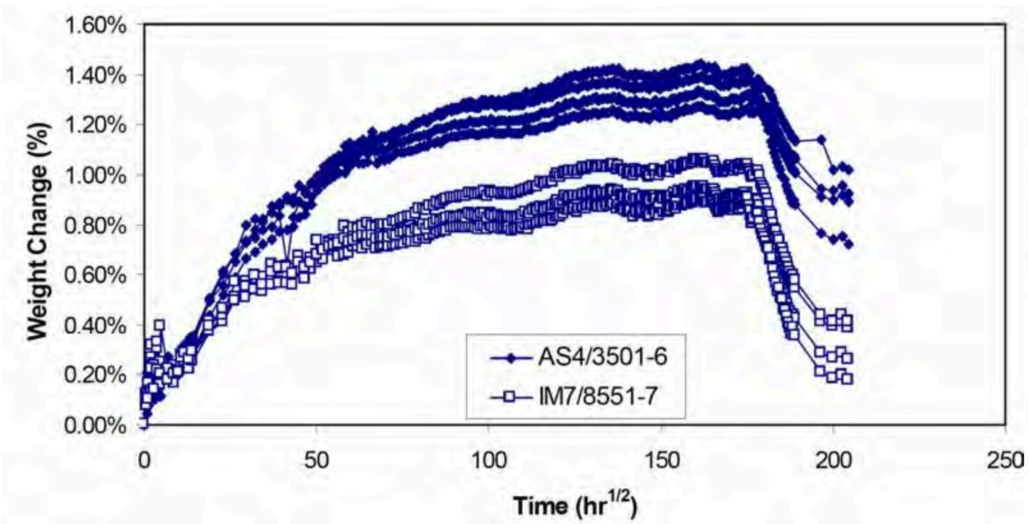

Four years weight-gain data for E-glass/NCT301 coupons immersed in simulated seawater

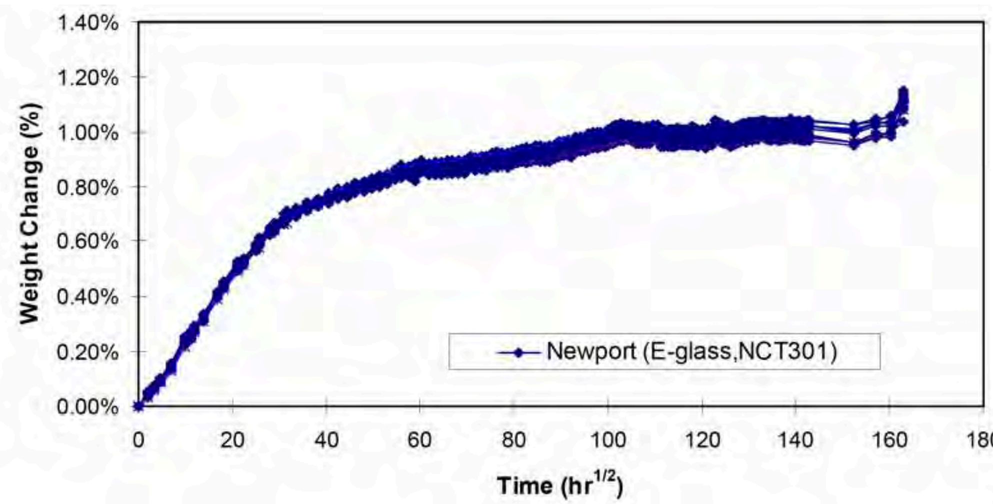

Y. J. Weitsman, “Composites in the Sea: Sorption, Strength and Fatigue,” University of Tennessee for Office of Naval Research, Oct. 1999.

Osmotic Blistering

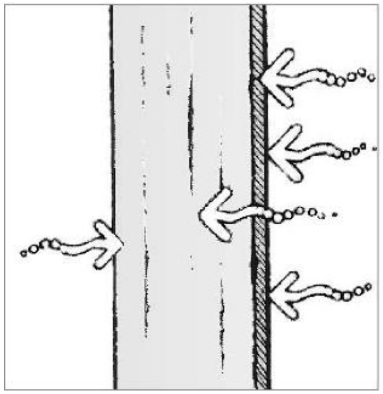

Polyester resins and gelcoats allow water molecules to migrate into the laminate and dissolve soluble materials within the laminate.

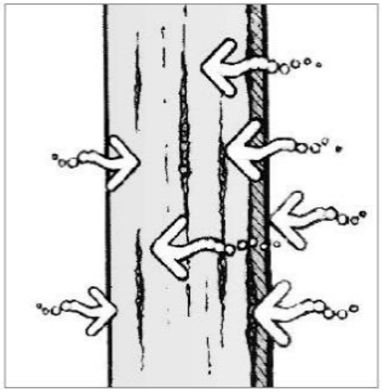

More water molecules are attracted to the voids to dilute the concentration of solutes in the blister fluid solution.

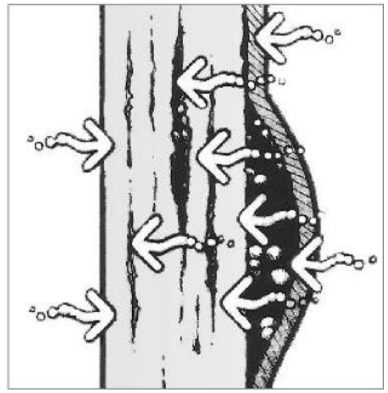

Accumulating fluid creates enough hydraulic pressure in the voids between the gelcoat and laminate to result in a gelcoat blister.

Gougeon Brothers, Inc., Bay City, MI

Tony Guild

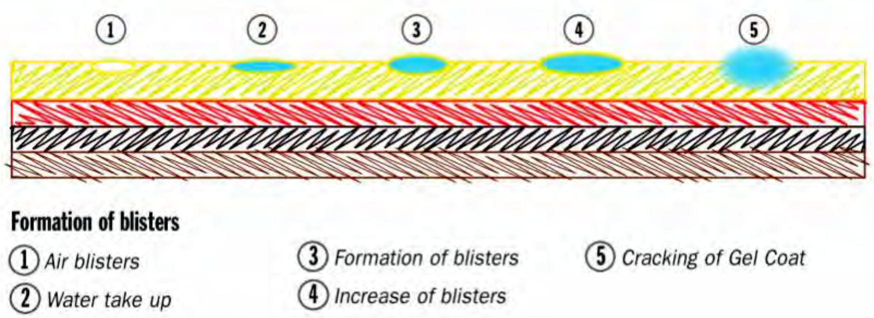

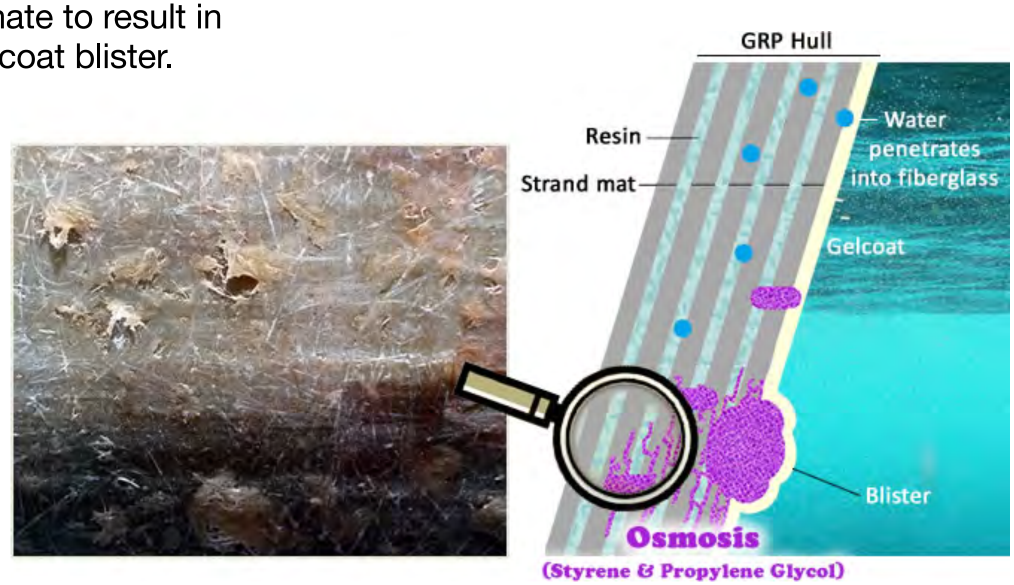

Blistered Hulls




Contamination Sources for Blister

Liquid Contaminate Sources During Spray-Up That Can Cause Blistering

Liquid	Common Source	Distinguishing Characteristics
Catalyst	Overspray, drips due to leaks of malfunctioning valves.	Usually when punctured, the blister has a vinegar-like odor; the area around it, if in the laminate, is browner or burnt color. If the part is less than 24 hours old, wet starch iodine test paper will turn blue.
Water	Air lines, improperly stored material, perspiration.	No real odor when punctured; area around blister is whitish or milky.
Solvents	Leaky solvent flush system, overspray, carried by wet rollers.	Odor; area sometimes white in color.
Oil	Compressor seals leaking.	Very little odor; fluid feels slick and will not evaporate.
Uncatalyzed Resin	Malfunctioning gun or ran out of catalyst.	Styrene odor and sticky.

Cook, Polycor Polyester Gel Coats and Resins

Galvanic Cathodic Blistering

A portion of a carbon fiber mast is shown with metal couplings attached to it

Schematic diagram of carbon/epoxy composite

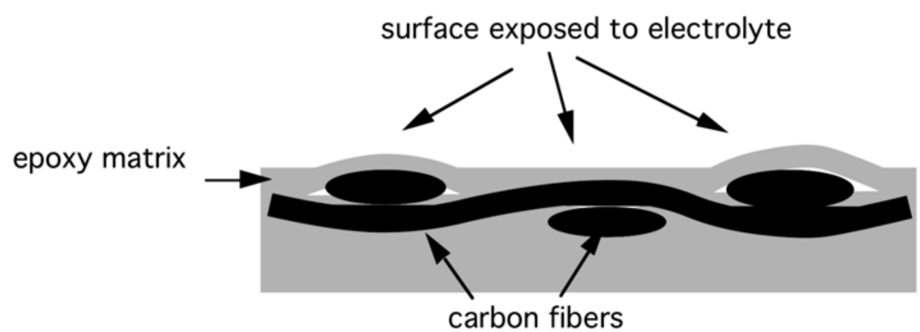

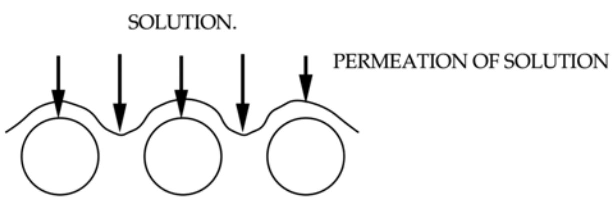

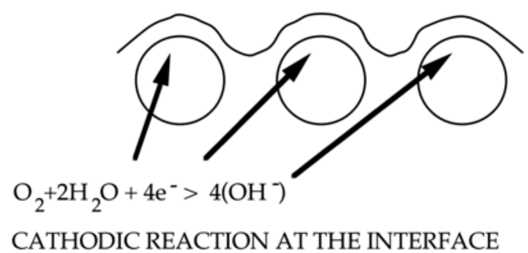

If the polymer layer over the location of osmotic pressure build up is thin, then the film will rupture. As a result, the solution will be directly exposed to carbon fibers with no intervening polymer layer. If the polymer layer is thick, The polymer can creep and slowly form a blister on the surface

Richard Brown, “Galvanic blistering in carbon fiber polymer composites,” University of Rhode Island, 2010.

Galvanic Activity

- Carbon fibers, unlike glass fibers, will conduct electricity. The carbon fiber's conductivity permits electrochemical activity - corrosion - to occur
- The cathodic activity at the carbon fibers can generate blistering
- Damage is usually limited to the surface, but this may initiate early fatigue failure and reduce impact resistance
- Long-term experience with large, carbon fiber marine structures is limited
- The phenomenon of galvanic blisters in carbon laminates has only recently been discovered
- Carbon fiber galvanic blisters require a microscope to observe - the problem is usually first observed in metal components that are in contact with the carbon fibers

Tucker & Brown, "Galvanic" Blisters in Carbon Fiber Composites, Professional Boatbuilder # 57

Galvanic Scale

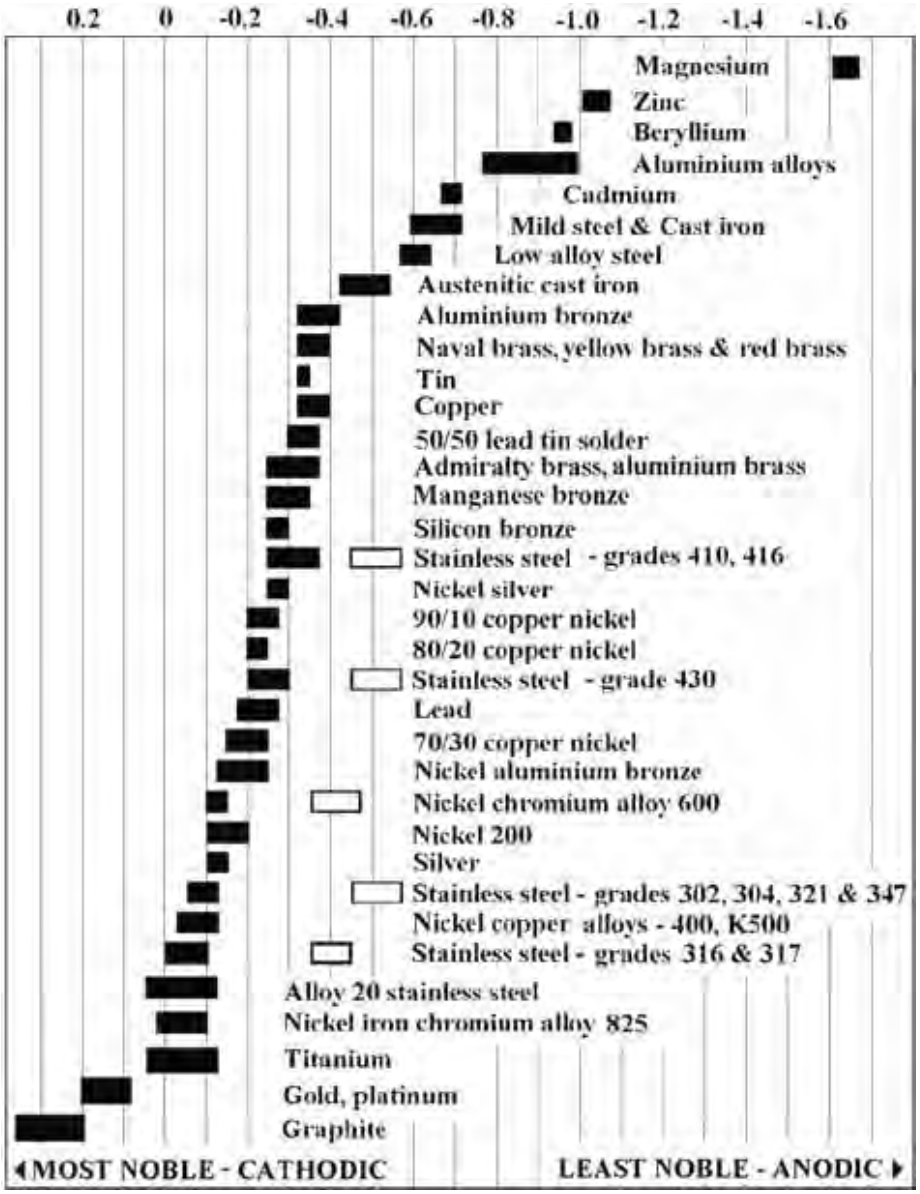

- The material that is closest to the anodic end of the galvanic scale will be corroded in preference to the one that is closest to the cathodic end of the scale.
- As the distance between materials on the galvanic scale increases, a corresponding rise occurs in the rate and the extent of the corrosion.
- Corrosion will increase the saltier the water is. Increasing temperature will also increase the conductivity of water and the resulting corrosion. The corrosion rate doubles with every 10 degrees Celsius (18 degrees Fahrenheit) increase in temperature.

Polymer Degradation

- Ultra Violet exposure – embrittles polymer, these days use clear coats which stop the process.
- Water uptake – polymers such as vinyl esters absorb 1.5% by weight of water.
- Water uptake can also cause polymer swelling and delamination.
- Dissolution – chemical attack, from imides in alkaline environment.

Richard Brown, "Degradation of Materials," University of Rhode Island, Nov. 2007

Ultra Violet Degradation

UV damaged (left) and restored gel coat (right)

Typical whitening of colored gel coat

Scott Bader Crystic marine gel-coat claims improved color stability and UV weather resistance

eric greene associates

Water Uptake

Water uptake curves for the vinyl ester-based composites

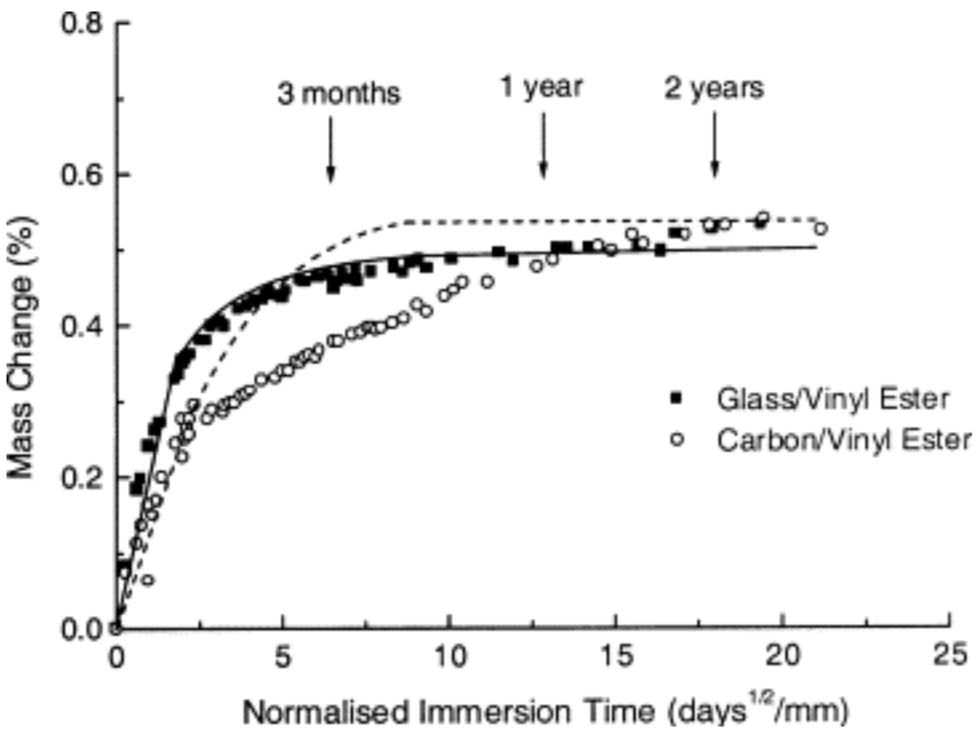

Effect of seawater immersion time on the normalized on flexural strength of the vinyl ester-based composites

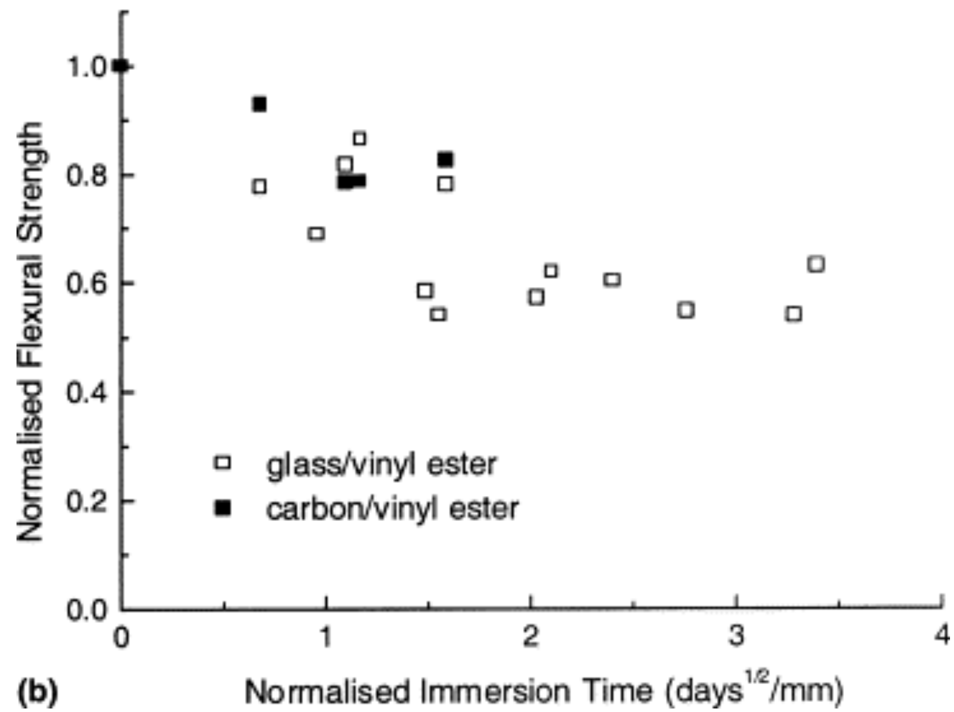

A. Kootsookos and A.P. Mouritz, "Seawater durability of glass- and carbon-polymer composites," *Composites Science and Technology*, Volume 64, August 2004.

Resistance to Chemical Attack

Petroleum Service Product Case Histories

APPLICATION	ENVIRONMENT	RESIN	SERVICE TEMP ºC	YEAR INSTALLED	FABRICATOR	SERVICE LOCATION	Comments
Tank Lining	Diesel Fuel	DION® 6631	Ambient	Various	Standard Oil	Standard Oil of California	Tank life 11-15 years
Tank Lining	Crude oil	DION® 6631	Ambient			Conoco/Standard Oil of California	
Tank lining	Heavy fuel oil	DION® 6694	-	1973		Standard Oil of California	
Steek tank overwrap	Motor fuels	DION® 6631	Ambient	1971	Plasteel International, inc licensees	International	Single wall and double wall UL listed tanks
Settling tank	Kerosene/5% Sodium hypochlorite	DION® 6694	-	1969	Standard Oil	Standard Oil of California	Mild caustic and kerosene separation. Replaced epoxy tank which failed
Storage tank	Naphtha, aromatics & H_2S	DION® 6694	50°C	1969	Standard Oil	Standard Oil of California	Removal and containment of aromatics entrained in hydrogen sulfate
Tank Lining	Perco sweeteners	DION® 6631	Ambient	1962	Standard Oil	Conoco/Standard Oil of California	Straight run gasoline percolated through 2m x 6.1 m steel FRP l columns Ned

DION® Polyester Resins, Reichold Chemical Company, Research Triangle Park, North Carolina, Sep 2010

Thermal Aging Affects

Schematic representation of composite structure scales

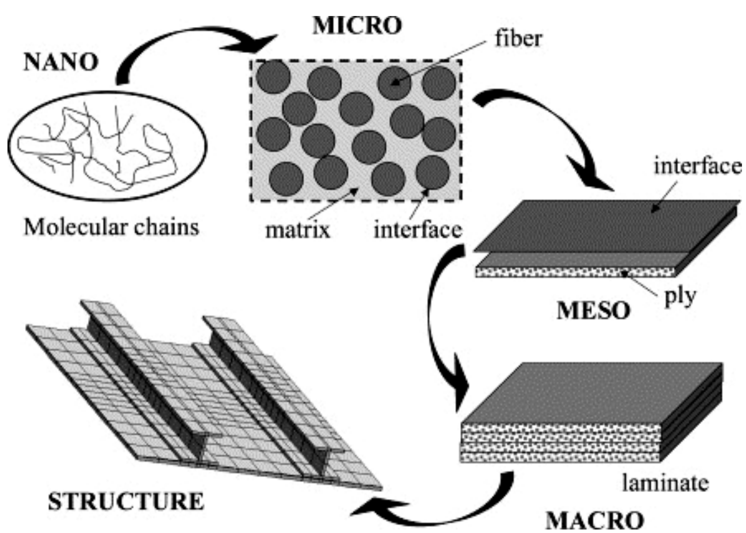

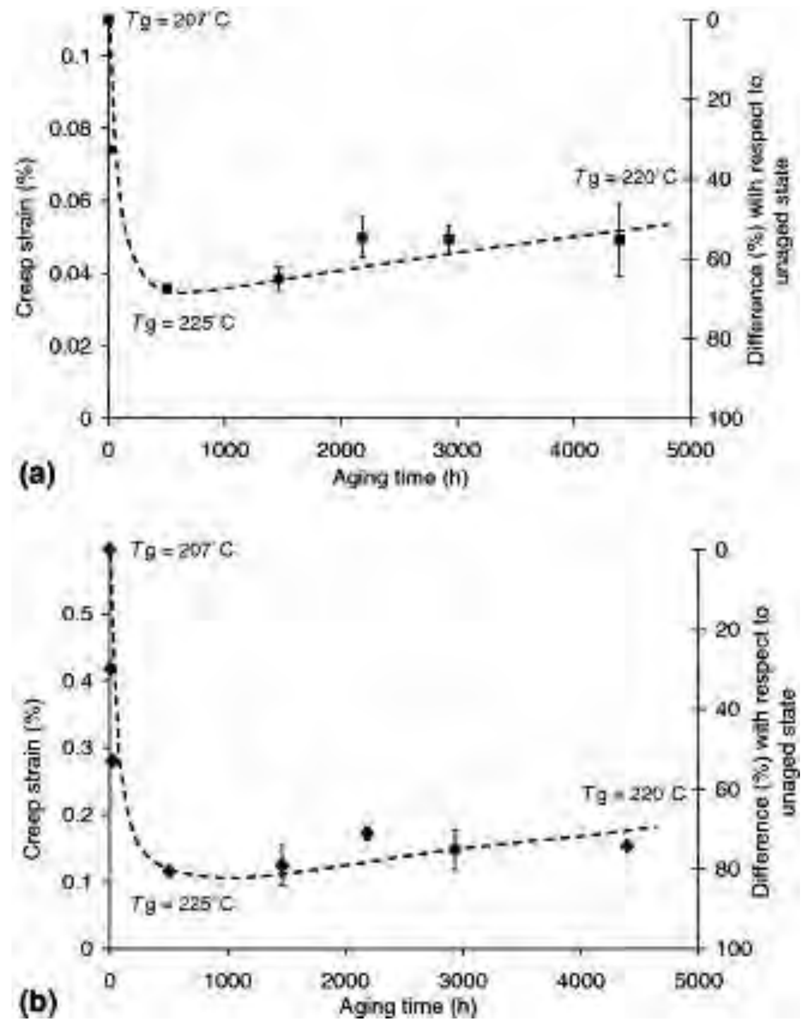

Creep tests on $[\pm45]_{4s}$ laminate: creep strain after 1000 s versus aging time at 180°C: (a) creep tests at 40 MPa; (b) creep tests at 60 MPa.

Viscoelastic behavior, thermo-mechanical damage and degrading resulting from physical and chemical aging can be analyzed in a multi-scale model.

David Lévêquea, Anne Schieffera, and Anne Mavela, Jean-François Maireb, "Analysis of how thermal aging affects the long-term mechanical behavior and strength of polymer–matrix composites," *Composites Science and Technology*, March 2005.

Long-Term Stiffness Degradation

Variation in Viscoelastic Modulus with Time [Structural Plastics Design Manual published by the American Society of Civil Engineers]

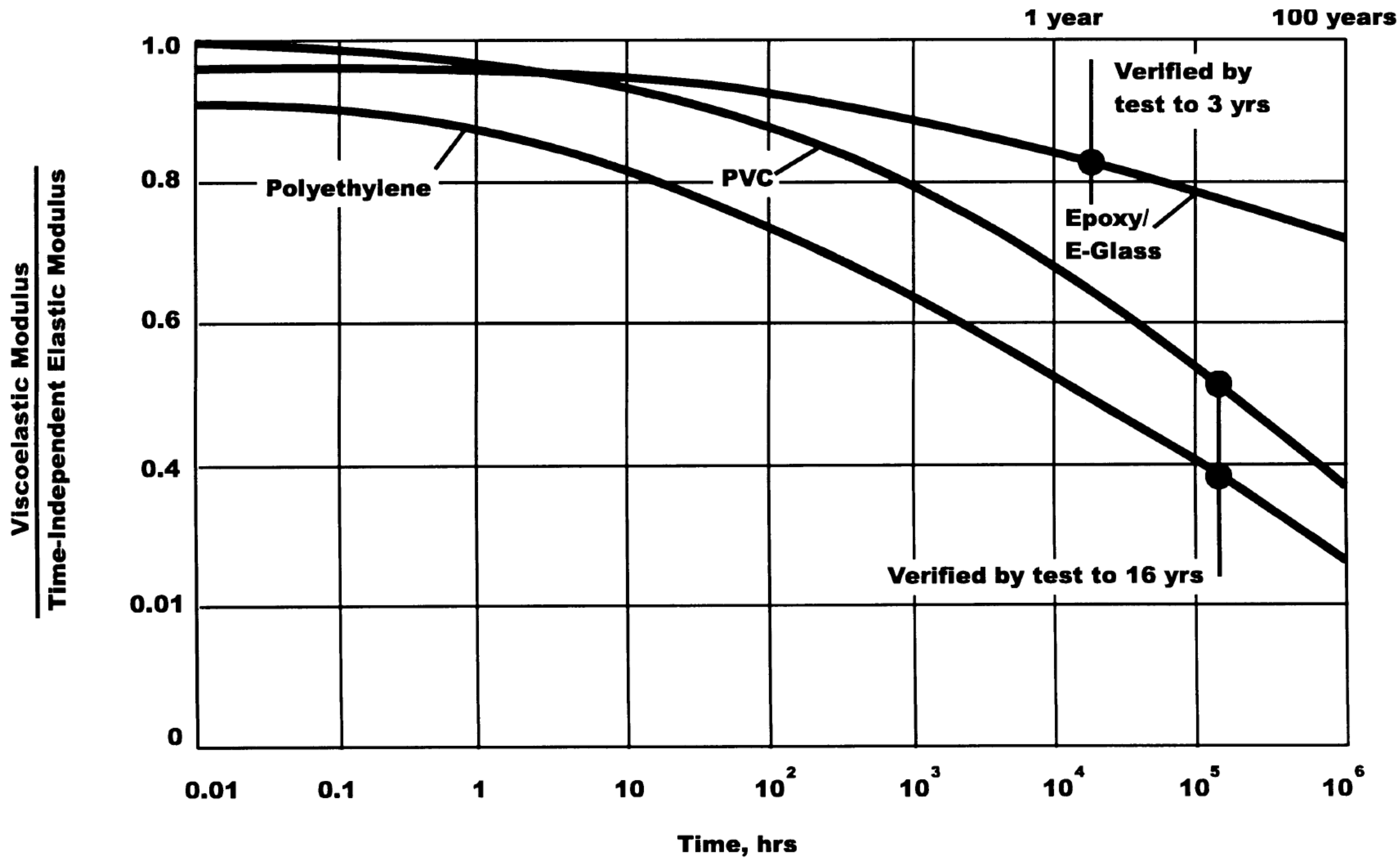

Lightning

Chances of boats being struck by lightning

Type	Chances per 1,000	$ Severity (10 = highest)
Multihull - Sail	9.1	10
Auxiliary Sail	4.5	6
Cruiser	.86	6
Sail Only	.73	3
Trawler	.18	5
Bass Boat	.18	1
Runabout	.12	2
Houseboat	.11	3
Pontoon	.03	8
Personal Watercraft	.003	1

BoatUS Marine Insurance Claim Files

Lightning and Sailboats

Lightning attachment to a sailboat

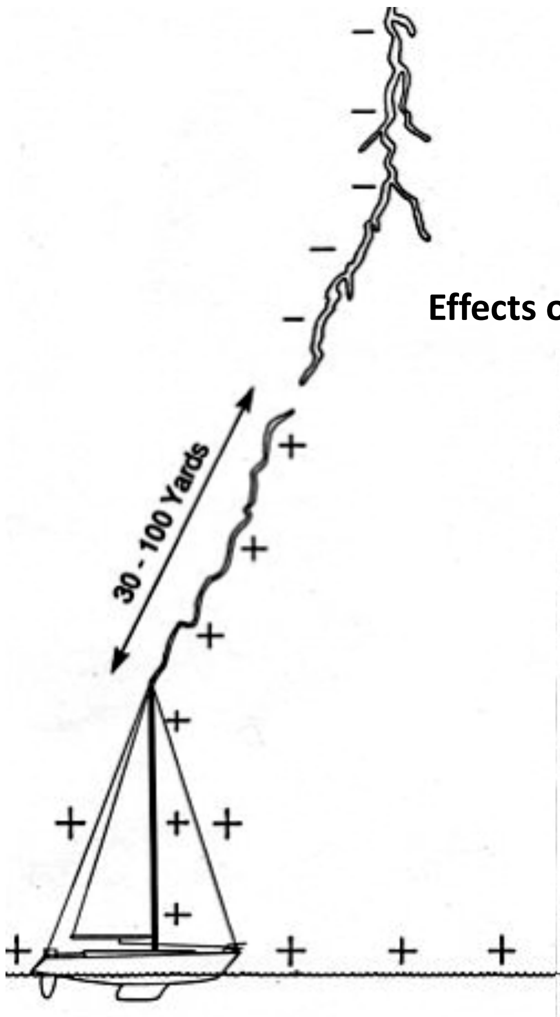

Effects of lightning strike to grounded boat

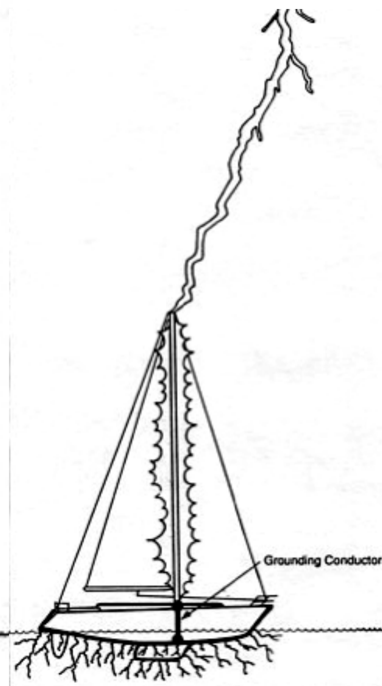

Proportion of boats struck by lightning suffering electronics damage of varying degrees

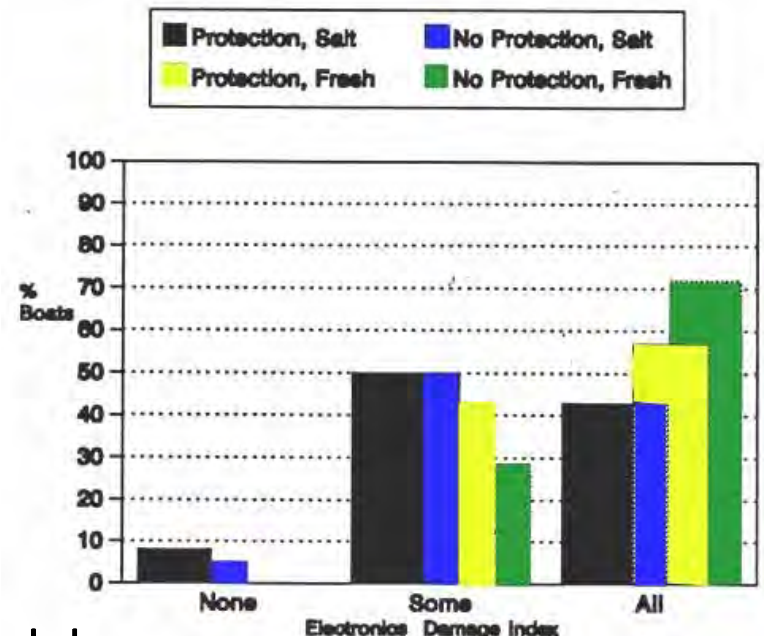

Effect to helmsman

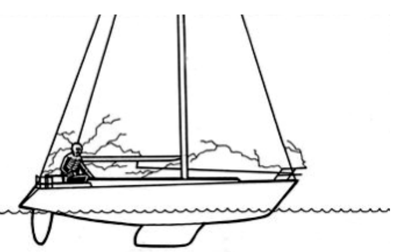

Ewen M Thompson, “Lightning and Boats,” University of Florida Sea Grant, 1992.

Typical Lightning Damage

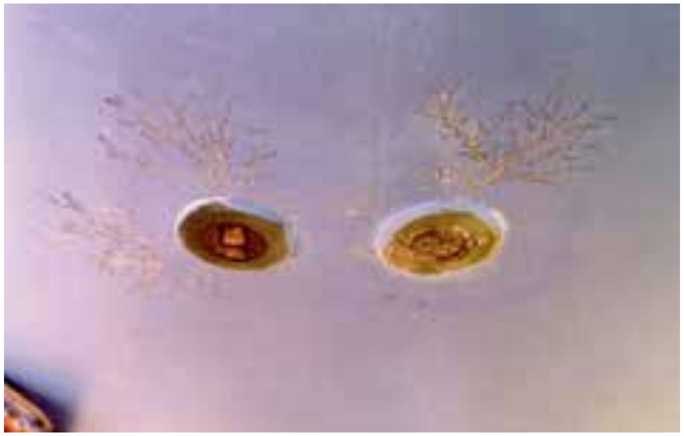

Eric Sponberg

HWH Electronics,
St Pete Beach, FL